Recycling of wind turbine blades in the form of glass fiber reinforced filaments for additive manufacturing

by

Amirmohammad Rahimizadeh

Department of Mechanical Engineering

McGill University

Montreal, Quebec, Canada

July 2020

A thesis submitted to McGill University in partial fulfillment of the requirements
for the degree of Doctor of Philosophy

Dedication

*To the loves of my life, **Hossein** and **Marezie**, my beloved parents, who gave me invaluable educational opportunities.*

Abstract

The wind energy industry represents one of the main application sectors for composites, where glass fiber reinforced materials are used to manufacture turbine blades. The dramatic growth of the wind industry over the past 20 years has resulted in an extensive amount of turbine waste, which includes manufacturing waste, in service waste and end-of-life waste. Turbine blades feature a life span of 20-25 years. Soon, it is predicted that the amount of end-of-life rotor blades will increase from 50,000 tonnes in 2020 to over 200,000 tonnes in 2034. Given the non-biodegradable nature of turbine blades, recent environmental legislation has increasingly demanded for the recycling and replacing of them.

This thesis presents a socially acceptable reuse and recycling method for the non-biodegradable materials in wind turbine blades. We propose to use fiberglass scrap from rotor blades as reinforcement in thermoplastic filaments for use in fused filament fabrication (FFF) 3D printing to achieve the following: addressing the challenging issue of wind turbine blade scrap that is increasingly growing every year; and improving mechanical properties of 3D printed parts using thermoplastics combined with recycled fibers.

A mechanical recycling scheme integrated with multiple classification operations are developed and used to obtain different grades of recycled glass fiber with various dimensional properties. On the first front, fibers featuring a length below the common nozzle size of the 3D printers are mixed with polylactic-acid (PLA) to produce recycled composite feedstock material for the FFF process. The developed feedstock is then used to fabricate tensile test samples with different fiber contents following ASTM D638. The results from tensile testing show an increasing and decreasing trend for the stiffness and strength of the samples, respectively. In addition, a comparative investigation is performed to assess the mechanical performance of the recycled parts relative to those made from virgin fibers, with results unveiling the higher tensile properties of the recycled parts.

On the second front, to better understand the mechanical behavior of the 3D printed recycled samples, micromechanical analysis including single fiber tensile and pull-out tests are performed to precisely characterize the properties of fibers recovered through mechanical and thermal recycling techniques. These characterizations, on one hand, prove the ability of the mechanically recycled fibers to form a stronger interface with PLA relative to pyrolyzed and virgin ones. On the other hand, the mechanical properties of single ground fibers determine their critical fiber length,

which is then used to properly optimize the recycling and manufacturing parameters. This optimization lead to the preservation of fibers longer than the critical length in the 3D printed composites and resolve the issue of strength degradation leading to structurally stronger and stiffer parts compared with those made from pure thermoplastic filaments. A numerical model that allows for the prediction of mechanical response of the parts made from recycled feedstock is also developed and validated through experimental measurements.

These experiments and analyses performed in this thesis suggest that the developed methodology can be used as a potential solution with high commercialization potential to mitigate the issue of overwhelming quantity of end-of-life wind turbine blades.

Résumé

L'industrie éolienne représente l'un des principaux secteurs d'application des composites, où des matériaux renforcés de fibres de verre sont utilisés pour fabriquer des pales de turbine. La croissance spectaculaire de l'industrie éolienne au cours des 20 dernières années a entraîné une grande quantité de déchets de turbines, qui comprend des déchets de fabrication, des déchets de service et des déchets en fin de vie. Les pales de turbine ont une durée de vie de 20 à 25 ans. Bientôt, il est prévu que la quantité de pales en fin de vie passera de 50 000 tonnes en 2020 à plus de 200 000 tonnes en 2034. Étant donné la nature non biodégradable des pales de turbine, les récentes législations environnementales vont de plus en plus exigé leur recyclage et leur remplacement.

Cette thèse présente une méthode de réutilisation et de recyclage socialement acceptable pour les matériaux non biodégradables dans les pales d'éoliennes. Nous proposons d'utiliser des déchets de fibre de verre provenant de pales de rotor comme renfort dans des filaments thermoplastiques pour une utilisation dans l'impression 3D de fabrication de filaments fondus (FFF) pour atteindre les objectifs suivants: résoudre le problème difficile des déchets de pales d'éoliennes qui augmente de plus en plus chaque année; et l'amélioration des propriétés mécaniques des pièces imprimées en 3D à l'aide de thermoplastiques combinés à des fibres recyclées. Un système de recyclage mécanique intégré à de multiples opérations de classification est développé et utilisé pour obtenir différentes qualités de fibres de verre recyclées avec différentes propriétés dimensionnelles. Sur le premier front, les fibres présentant une longueur inférieure à la taille de base commune des imprimantes 3D sont constituées d'acide polylactique mixte (PLA) pour produire une matière première composite recyclée pour le processus FFF. La matière première développée est ensuite utilisée pour fabriquer des échantillons d'essai de traction avec différents contenus en fibres conformément à la norme ASTM D638. Les résultats des essais de traction démontrent une tendance à la hausse et à la baisse pour la rigidité et la résistance des échantillons, respectivement. De plus, une enquête comparative est réalisée pour évaluer les performances mécaniques des pièces recyclées par rapport à celles en fibres vierges, les résultats dévoilant les propriétés de traction supérieures des pièces recyclées.

Sur le deuxième front, pour mieux comprendre le comportement mécanique des échantillons recyclés imprimés en 3D, une analyse micromécanique comprenant des tests de traction et

d'arrachement de fibre unique est effectuée pour caractériser avec précision les propriétés des fibres récupérées grâce aux techniques de recyclage mécanique et thermique. Ces caractérisations, d'une part, prouvent la capacité des fibres recyclées mécaniquement à former une interface plus solide avec le PLA par rapport aux fibres pyrolysées et vierge D'autre part, les propriétés mécaniques des fibres broyées simples déterminent la longueur critique de fibre, qui est ensuite utilisée pour optimiser correctement les paramètres de recyclage et de fabrication. Cette optimisation conduit à la préservation de fibres plus longues que la longueur critique dans les composites imprimés en 3D et résout le problème de la dégradation de la résistance conduisant à des pièces structurellement plus solides et plus rigides par rapport à celles fabriquées à partir de filaments thermoplastiques purs. Un modèle numérique permettant de prédire la réponse mécanique des pièces en matière première recyclée est également développé et validé par des mesures expérimentales.

Ces analyses et ces esssais expérimentales effectuées dans cette thèse suggèrent que la méthodologie développée peut être utilisée comme une solution potentielle à fort potentiel de commercialisation pour atténuer le problème de la quantité écrasante de pales d'éoliennes en fin de vie.

Acknowledgment

I would like to take this opportunity and thank all the people whose assistance was a milestone in the completion of this thesis. Foremost, I would like to thank my supervisor, Professor Larry Lessard, whose patient guidance, encouragement and advice throughout my time as his student were determinant for the accomplishment of work in this thesis. Indeed, his positive outlook and confidence in my research inspired me and gave me confidence.

I wish also to express my sincere appreciation to my co-supervisor, Professor Kazem Fayazbakhsh, who has the substance of a genius: he continually and convincingly guided and encouraged me to be professional and do the right thing even when the road got tough. Kazem was always available whenever I ran into a problem or issue. Without his persistent help, insightful comments and feedback, the goal of this project would not have been realized. It was an honour and privilege for me to be Kazem's first PhD student. Your advice on both research and my career have been invaluable for me in the future.

I have great pleasure in acknowledging my gratitude to my colleagues and friends from "Structure and Composite Materials Laboratory" and McGill University. I also would like to thank Mr. Jordan Kalman for all his hard work and help. I would feel amiss if I were to omit mentioning two of my dear friends **Sareh Taheri** and **Mohammad Tavallaeinejad**, who, in their own ways, kept me going on my path to success, helping me as per their abilities to ensure that good times keep flowing.

My deepest gratitude and thanks go to my family for their continuous and unparalleled love, help and support. Thank you for helping me to shape my life with positivity and passion. Without you I'd never be the person I am today. Thank you for everything.

Lastly, I would like to thank, the National Sciences and Engineering Research Council of Canada (NSERC), Research Center for High Performance Polymer and Composite Systems (CREPEC), Project Vision, the McGill Engineering Doctoral Award (MEDA) for their collaborative financial support for my study.

Table of Contents

List of Figures

List of Tables

Contributions of the author

This is a manuscript-based thesis consisting of four journal articles. The title of the articles, name of the authors, and their contributions are listed below:

1) Recycling of Fiberglass Wind Turbine Blades into Reinforced Filaments for use in Additive Manufacturing

Amirmohammad Rahimizadeh[a], Jordan Kalman[b], Kazem Fayazbakhsh[b,*], Larry Lessard[a]

[a] Department of Mechanical Engineering, McGill University, Montreal, QC H3A0C3, Canada

[b] Department of Aerospace Engineering, Ryerson University, Toronto, Ontario M5B2K3, Canada

[*]Corresponding author: kazem@ryerson.ca; Tel: (+1) 416-979-5000 ext. 6414; fax: (+1) 416-979-5056

Journal of Composites Part B: Engineering, 2019. 175: p. 107101

Author contributions:

A. Rahimizadeh: Performed the recycling and classification of the blades. Conducted the extrusion process. Performed all the thermal and mechanical analysis and post-processed the data. Wrote and edited the manuscript.

J. Kalman: Assisted A.R with the extrusion process. 3D printed the samples.

K. Fayazbakhsh: Supervised the whole research, gave substantial technical advice, and edited the manuscript.

L. Lessard: Supervised the whole research, gave substantial technical advice, and edited the manuscript.

2) Recycled glass fiber composites from wind turbine waste for 3D printing feedstock: effects of fiber content and interface on mechanical performance

Amirmohammad Rahimizadeh[1], Jordan Kalman[2], Rodolphe Henri[3], Kazem Fayazbakhsh[4,*], Larry Lessard[5]

[1] Department of Mechanical Engineering, McGill University, Montreal, QC H3A0C3, Canada; amirmohammad.rahimizadeh@mail.mcgill.ca

[2] Department of Aerospace Engineering, Ryerson University, Toronto, Ontario M5B2K3, Canada; jkalman@ryerson.ca

[3] Institute of Materials (IMX), Ecole Polytechnique Fédérale de Lausanne (EPFL), Lausanne CH-1015, Switzerland; rodolphe.henri@epfl.ch

[4] Department of Aerospace Engineering, Ryerson University, Toronto, Ontario M5B2K3, Canada; kazem@ryerson.ca

[5] Department of Mechanical Engineering, McGill University, Montreal, QC H3A0C3, Canada; larry.lessard@mcgill.ca

*Corresponding author: kazem@ryerson.ca; Tel: (+1) 416-979-5000 ext. 6414; fax: (+1) 416-979-5056

Journal of Materials, 12 (23), 3929

Author contributions:

A. Rahimizadeh: Performed all the experiments, conducted all the computational analysis, wrote and edited the manuscript.

J. Kalman: Assisted A.R with sample fabrication.

R. Henri: Assisted A.R with mechanical testing.

K. Fayazbakhsh: Supervised the whole research, gave substantial technical advice, and edited the manuscript.

L. Lessard: Supervised the whole research, gave substantial technical advice, and edited the manuscript.

3) Tensile properties and interfacial shear strength of recycled fibers from wind turbine waste

Amirmohammad Rahimizadeh[a], Mazin Tahir[a], Kazem Fayazbakhsh[b],*, Larry Lessard[a]

[a] Department of Mechanical Engineering, McGill University, Montreal, QC H3A0C3, Canada;

[b] Department of Aerospace Engineering, Ryerson University, Toronto, Ontario M5B2K3, Canada; kazem@ryerson.ca

*Corresponding author: kazem@ryerson.ca; Tel: (+1) 416-979-5000 ext. 6414; fax: (+1) 416-979-5056

Journal of Composites part A, 12 (23), 3929

Author contributions:

A. Rahimizadeh: Developed the methodology and performed all the experiments. Post-processed the data, wrote and edited the manuscript.

M. Tahir: Assisted A.R with sample preparation.

K. Fayazbakhsh: Supervised the whole research, gave substantial technical advice, and edited the manuscript.

L. Lessard: Supervised the whole research, gave substantial technical advice, and edited the manuscript.

4) Mechanical and thermal study of composite filaments from wind turbine waste for 3D printing

Amirmohammad Rahimizadeh[a], Jordan Kalman[b], Kazem Fayazbakhsh[b,*], Larry Lessard[a]

[a] Department of Mechanical Engineering, McGill University, Montreal, QC H3A0C3, Canada

[b] Department of Aerospace Engineering, Ryerson University, Toronto, Ontario M5B2K3, Canada

[*]Corresponding author: kazem@ryerson.ca; Tel: (+1) 416-979-5000 ext. 6414; fax: (+1) 416-979-5056

Article under review

Author contributions:

A. Rahimizadeh: Performed the recycling and classification of the recyclate. Performed the extrusion process, as well as all the thermal and mechanical analysis and post-processed the data. Conducted all the computational analysis. Wrote and edited the manuscript.

J. Kalman: Assisted A.R with the extrusion process. 3D printed the samples.

K. Fayazbakhsh: Supervised the whole research, gave substantial technical advice, and edited the manuscript.

L. Lessard: Supervised the whole research, gave substantial technical advice, and edited the manuscript.

Chapter 1

Introduction and literature review

1. Chapter 1: Introduction and literature review

1.1 Background and Motivation

The wind is a clean, free and readily available renewable energy source. This source of power generation plays an increasingly important role in the way we power our world. Wind energy offers numerous advantages, which have made it one of the fastest-growing energy sources worldwide over the past 20 years. The development of wind energy has the ability to free the world from the economic dependence on fossil fuels. In addition, it is one of the lowest-priced energy sources available today, costing between two and six cents per kilowatt-hour [1]. Certainly, wind energy is one of the frontrunners of the technological breakthroughs that might lead to more efficient and greener energy production.

According to the World Wind Energy Association, the total wind energy capacity has increased from 296,581 MW in 2013 to 539,291 MW in 2017, an increase that represents 82% growth over 4 years [2]. This development keeps continuing as wind energy is expected to contribute to 30% of the total world's energy resources by 2050 [3]. Canada is one of the countries endowed with exceptional wind resources. For over one decade, Canada has utilized wind energy as the main source for electricity production, which now contributes to around 6% of the total electricity demand. Since the year 2000, the total installed capacity of wind turbines in Canada has increased from 114 MW to 12816 MW.

As the wind industry grows, the size of the blades, as well as the amount of materials required to manufacture them increases. As shown in Figure 1-1, the rotor diameter has increased from 40 m in 1990 to 145 m in 2015, which corresponds to an increase of 260 % in the size of the blades [4]. This significant growth of wind turbine blade size has motivated the use of composite materials owing to their high strength-to-weight ratio, adequate corrosion resistance and high structural stiffness. A recent survey performed in late 2017 has revealed that approximately 13.41 % of the total produced composites in the world is used to manufacture wind turbine rotor blades, a value that is rapidly increasing every year.

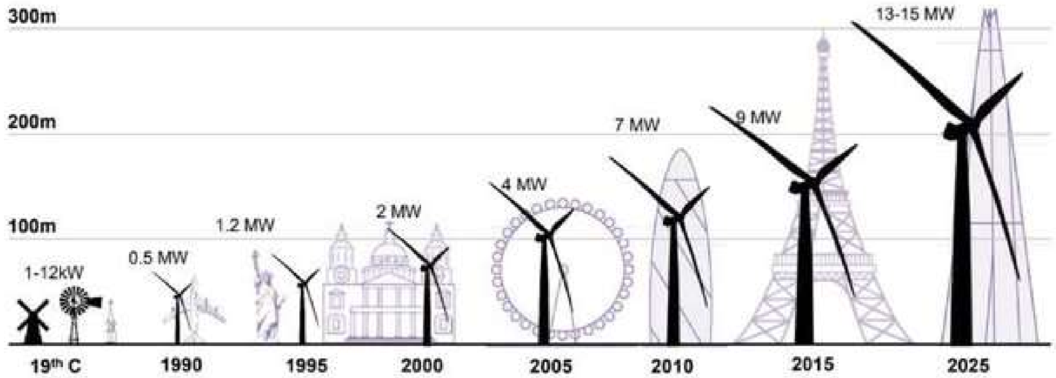

Figure 1-1: The size evolution of the wind turbine blades in terms of average rotor diameter [4].

Composite materials generally consist of two major components: a matrix and a reinforcement. While the matrix is mainly responsible for holding the constituents together, the reinforcement features high mechanical properties to resist against the applied loads. Besides the wind industry, recent insights in the manufacturing technologies and material processing of composite materials have led to extensive use of composites in many technical industries including automotive and aerospace. Among composite materials, the superior mechanical properties of glass fiber reinforced polymers (GFRP) combined with low cost, have made them an attractive alternative for solid materials, resulting in 90% use in all of the composites currently produced [5]. Aircraft, automotive parts, pipes, and sports equipment are some examples of application sectors for GFRPs [6, 7]. Recent developments in the wind energy industry have made it one of the major application sectors for these composites, where glass fiber reinforced polymers are used to manufacture wind turbine rotor blades. As illustrated in Figure 1-2, wind turbine blades are made of two shells joined together by weblinkings or box beams [8]. The blades are generally subjected to flapwise and edgewise loads, where the former arises from the wind pressure and the latter results from the gravitational forces and torque load. Internal spar box or webs are used to resist against the flapwise loads and the edgewise loads are taken by the edges of the cross section. Unidirectional composites are generally used at these regions to increase the load bearing capacity of blades against the flapwise and edgewise loads [9].

The UD composites used in wind turbine blades are typically made of E-glass fibers with 70% reinforcement weight ratio [9] (30% matrix). In addition to E-glass fibers, other classes of glass fibers, such as S-glass or R-glass have also been used in rotor blades with the aim of attaining higher mechanical properties with values up to 40% higher than those of E-glass fibers. Different types of reinforcement fibers such as carbon fibers have also been recently used in rotor blades. Nevertheless, despite their higher mechanical properties that could substantially reduce the size and weight of the blades, the high price and low damage tolerance of these reinforcement materials limit their extensive use in turbine blades [10, 11]. However, some companies such as Aarhus in Denmark or Zamudio in Spain still use carbon fibers in structural spar caps of large blades [10]. Besides synthetic fibers, natural fibers have been also used in some cases to manufacture small blades. Besides availability and environmental friendliness, natural fibers offer a wide availability, high strength and stiffness, which motivate the use of them in small blades. For instance, a group of scientists from Nepal, Denmark and Australia has investigated the applicability of wooden turbine blades from timbers with results showing high reliability and low-cost [12-15].

In terms of matrix material, thermoset resins including epoxies, polyesters and vinyl esters are typically used in wind blade composites, mainly due to their low cure temperature and viscosity [9]. While polyesters were initially used in small turbine blades, following the development of large and extra-large blades, epoxies replaced them. However, some recent studies have exploited a new class of polyesters with higher strength, faster cure time and higher durability, which meet all the requirements for large rotor blades and motivate the return to these matrix materials [9].

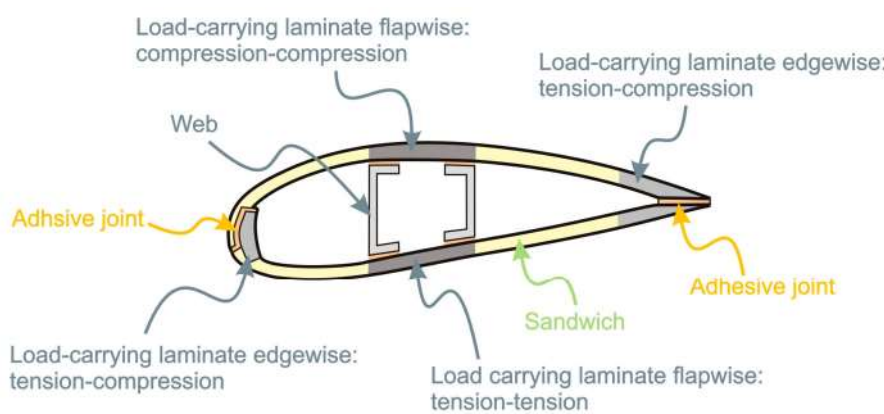

Figure 1-2: The cross section of a wind turbine blade [9].

The manufacturing technique used for wind turbine blades has undergone a noticeable evolution over the years. Traditionally, wet hand layup was the most commonly used technique to manufacture the shells of blades with small and medium lengths ranging between 35-55 m. With this manufacturing process, the composite shells were adhesively joined by the inner webs or spars. This process, however, was associated with a relatively high labor cost, low part quality and environmental impact. With the development of longer blades, the applicability of other manufacturing techniques, such as filament winding, prepreg and resin infusion was explored to overcome the issues associated with the conventional hand lay-up method [16]. Currently, resin infusion is the most widely used manufacturing technique for rotor blades, particularly for longer blades [9]. With this method, dry unidirectional fabrics of fibers are first layed down along the length of the blades, such that most of the plies are positioned near the root of the blades and partially around the tip. Polymer foams or balsa wood are typically used as core materials to form a sandwich structure. Then, a low viscosity resin is injected into the mold using pressure to fill up all the mold cavities. Finally, the component is cured at room temperature [17]. Figure 1-3 briefly illustrates the rotor blade manufacturing steps including assemblage and bonding of the shells and internal shear webs.

Although the introduction of resin infusion has significantly improved the manufacturing efficiency of rotor blades, it is associated with manufacturing defects including fabric slippage and wrinkles, which affect the final performance of the blades. As a result, a quality control operation is usually carried out following the manufacturing process to repair the possible defects.

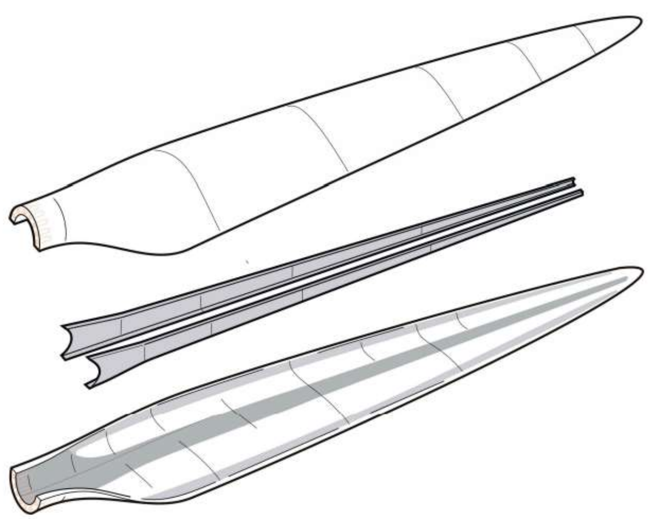

Figure 1-3: The schematic of the manufacturing of a wind turbine blade [9].

Despite the large volume of GFRPs used in the wind industry, the difficult recycling process for these materials has recently turned into a stumbling block, steering this industry for finding recycling solutions for end-of-life blades. The low price of virgin glass fibers coupled with inherent heterogenous nature of the matrix and the reinforcement have significantly reduced the economical profit of GFRPs recycling, such that most of the scrap glass reinforced parts are landfilled. However, recent strict environmental legislation has motivated the recycling and reusing of scrap composite parts [18, 19]. Despite some recent attempts at recycling of composites, two main bottlenecks are still recognized for the recycling process of wind turbine blades, cost efficiency and recycled product value. The problem of cost efficiency lies in the inexpensive cost of virgin glass fibers, which not only increases the use of these materials, but also lowers the commercial viability of any recycling system for them. Furthermore, the location of wind turbines in remote areas creates an expensive logistic problem for collecting end-of-life blades. In addition, the sensitivity of glass fibers to high temperatures along with their high brittleness remarkably reduce the mechanical properties of the recycled materials such that a value-added recycled product can not be achieved. Therefore, the motivation of this thesis is to address the critical challenge of growing composite waste from wind turbine blades through developing an optimum recycling scheme integrating mechanical recycling and 3D printing to achieve the following: improving the environmental sustainability of wind energy by recycling the rotor blades at the end-of-their life through a life cycle approach; and improving the mechanical properties of 3D printed parts using thermoplastics combined with recycled fibers.

This chapter first introduces the current state of art for the recycling techniques of composite materials. Then the fused filament fabrication (FFF) 3D printing process as a potential application sector for the recycled fibers from end-of-life rotor blades is discussed in order to define the design requirements for FFF feedstock. Based on these requirements, the thesis underlying principal and objectives are defined.

1.2 Recycling of Composites

The extensive disposal of composite products is leading to undesirable environmental impact due to their high organic content such as resin and wood [20, 21]. Recent reports have revealed that the total global production of composites has exceeded 10 million tons per year, which at end-of-life, will require over 5 million cubic meters for disposal [22]. While the thermoplastic wastes can be melted and remolded, the recycling process of thermoset composites is more arduous due to the crossed-linked molecular network of these polymers. So far, various technologies to recycle thermoset composite materials have been proposed and developed in the literature [21, 23, 24]. As shown in Figure 1-4, the current recycling solutions for thermoset composites can be categorized in two distinct groups, including those that involve mechanical comminution to resize the scarp and produce recyclates; and those that utilize thermal techniques at high temperatures to recover energy and materials.

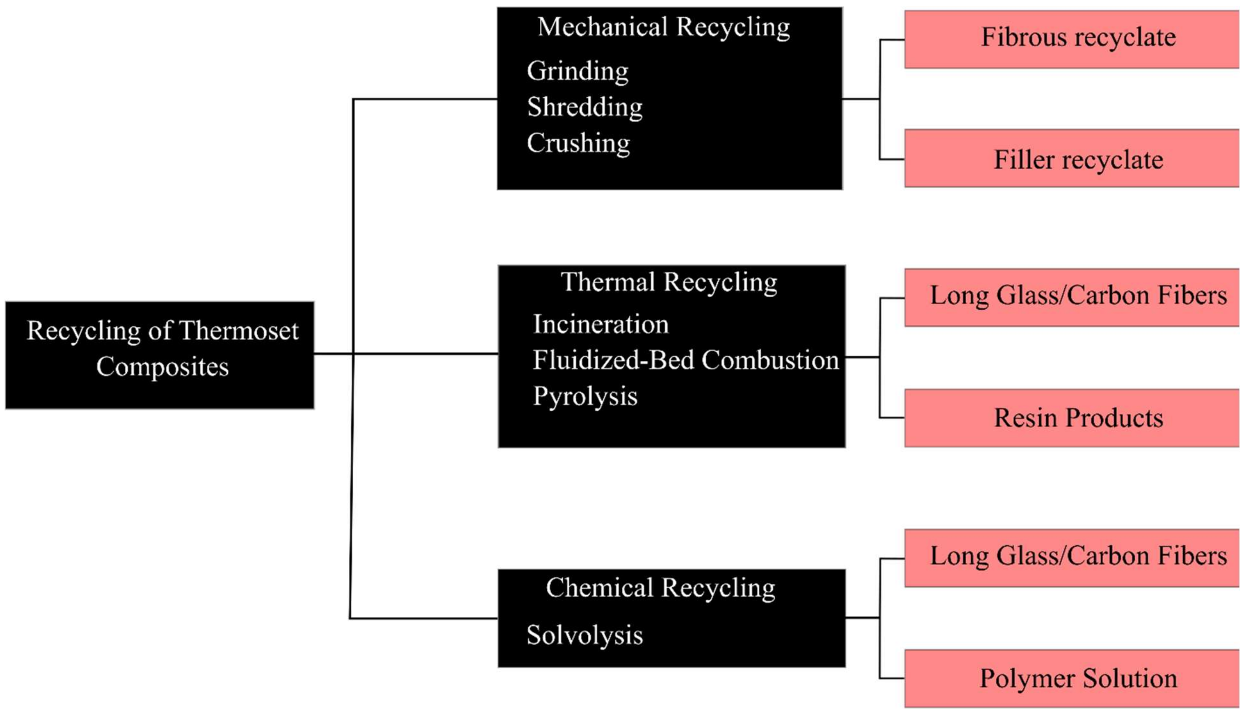

Figure 1-4: Recycling techniques for thermoset composite materials.

1.2.1 Mechanical recycling

This method was first introduced in the 1990s and Currently is considered as the only recycling technique with commercialization potential [25]. Mechanical recycling involves techniques that work for both glass and carbon fiber reinforced composites. The technique initiates with a suitable size reduction of the scrap by low speed cutting or crushing (50-100 mm) [25]. This facilitates the removal of metal and wood inserts, as well as the transportation of the waste to a recycling site. Following this initial size reduction, the size of the scrap is further reduced down to 0.05 mm to 10 mm through a hammer mill or other high-speed milling techniques for fine grinding. Finally, a classification process is performed such that fine particles of the waste are classified into fiber-rich (coarser) and matrix-rich (finer) fractions [23, 26]. Since mechanical grinding is not associated with any type of atmospheric pollution, this technique offers significant environmental and economical advantages over the other available recycling processes (see sections 1.2.2 and

1.2.3). In addition, this process benefits from the abrasive nature of glass fibers to efficiently reduce the size of GFRP composite waste [27]. The performance and functionality of this method has been the focus of a significant number of studies in the literature [26, 28]. For instance, Palmer et al. [29] used a TRIA screen-classifier type hammer mill to recover glass fibers from automotive front fenders. They validated the applicability of a novel zig-zag air separator method to obtain fine glass fibers featuring mechanical properties comparable to virgin fibers (Figure 1-5).

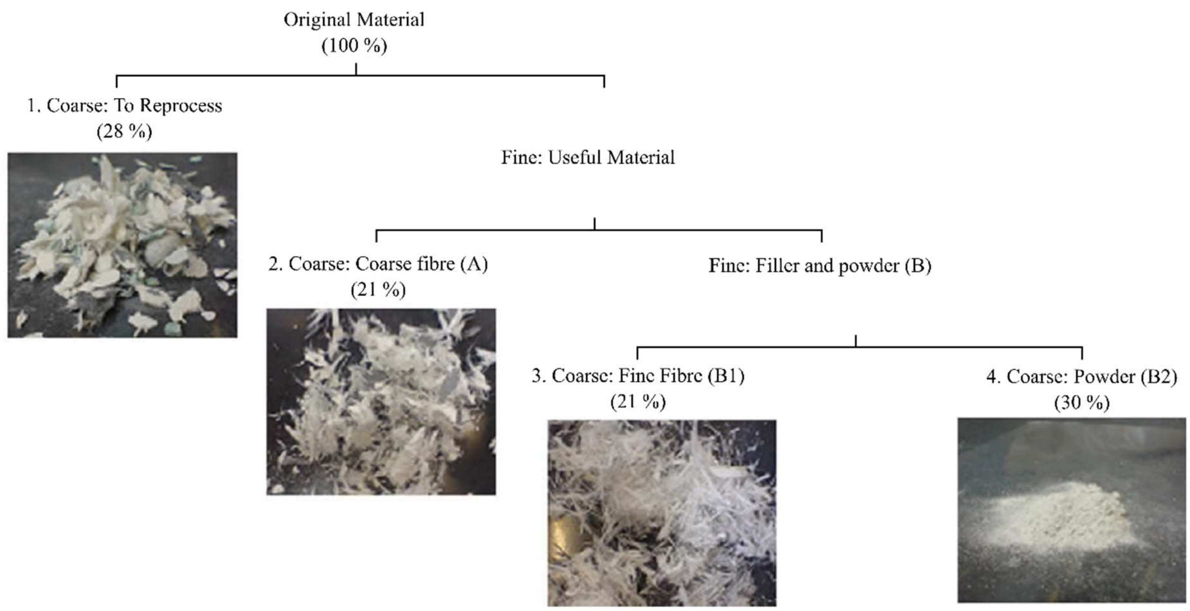

Figure 1-5: Different grades of recyclate obtained through air classification of mechanically recycled front fiberglass automotive fenders [25].

In another study, three grades of granulated recyclate from sheet moulding compound waste with different fiber sizes were obtained and used in bulk moulding compound (BMC) manufacturing to replace the virgin reinforcements [25]. The new BMC formulations showed reduced mechanical properties, particularly in flexural strength. This observation was ascribed to possible fiber damage, and poor interfacial bonding between the fibers and the new resin polymer. A number of companies have also investigated the potential of mechanical recycling at the industrial scale. Among them, ERCOM in Germany was established in 1990 and focused on the recycling of dismantled automotive parts into filler for new sheet moulding compounds (SMCs) [30, 31]. A mobile shredder was employed to perform the initial size reduction of the scrap into pieces of about 50 mm ×50 mm. Following this size reduction process, a hammer mill was used to further reduce the size of the waste and ease the classification of the recyclate into coarse and fine fractions. Phoenix Fiberglass in Canada was also founded in early 1990's with the aim of producing non-structural automotive components, such as corvette rear deck reinforcement, Econoline van engine cover, and Ram van interior trim package [32], out of SMC waste. The recycling technique of Phoenix was composed of a 2-stage shredding and pulverising process followed by grading of the recyclate through screens and air classifiers.

1.2.2 Thermal recycling

Thermal recycling refers to a recycling process where high thermal energy is utilized to decompose the polymer from scarp composites [33]. While this process mainly aims at recycling the reinforcement fibers, caloric energy stored in the chemical bonds of polymer composites can be also recovered through thermal recycling. The most common thermal recycling techniques are incineration, fluidised-bed combustion and pyrolysis.

1.2.2.1 Incineration

Incineration process focuses on the polymeric phase of the composites with the aim of releasing the calorific value stored in the chemical bonds of the polymer. Since most of the reinforcing fibers and fillers are incombustible, the calorific energy of composites highly depends on the proportion of polymer. Although the inorganic residues of composites after combustion have the potential to be used in the cement industry, incineration is not commonly classified as a recycling technology and is considered as one of the composite waste disposal methods [21]. Also, significant pollution results from this process.

1.2.2.2 Fluidised-bed combustion recycling process

Although incapable of recovering the valuable resin products, this technique is quite robust against mixes and contaminated materials. Initiating by a size reduction, the process is followed by resin decomposition at high temperatures ranging between 450-550 °C. Eventually, a separation operation is performed to pass the fiber and filler particles into a secondary combustion chamber for the fully oxidation of the polymer [34, 35] (Figure 1-6). This recycling process generally leads to fibers in fluffy form with surface condition similar to that of virgin fibers. Mechanical tests on recovered fibers have revealed degraded properties with values up to 25 % lower than those of virgin fibers [36, 37]. The short length of the recovered fibers along with the high property degradation associated with this method heavily reduce its economical viability for glass fiber composites, such that a minimum of about 10,000 tonnes/year of glass fiber composite scrap should be recycled via this method to be considered economical [36].

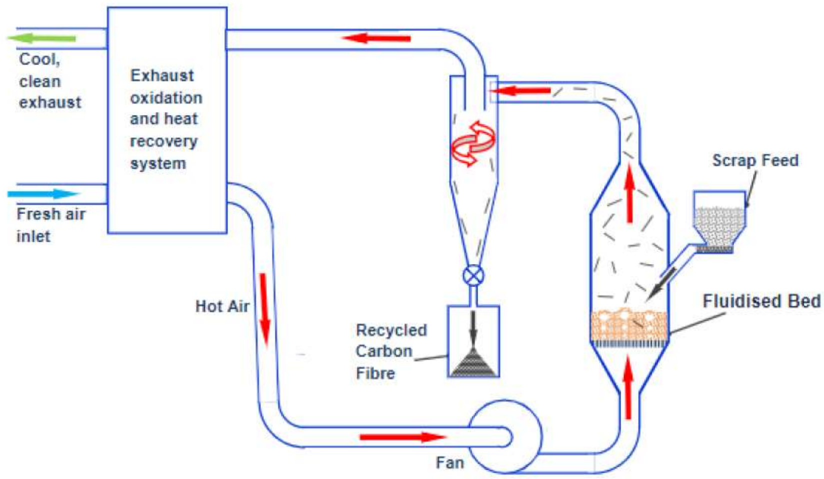

Figure 1-6: The recycling process used in fluidized-bed combustion [38].

1.2.2.3 Pyrolysis

Pyrolysis is a thermal decomposition of polymer that allows for the recovery of long, high modulus fibers, with the process operating at high temperatures ranging from 300-800°C in the absence of oxygen [39] (Figure 1-7). This technique has been successfully used for carbon fiber reinforced composites. One important advantage associated with pyrolysis of carbon fibers is the high mechanical properties of the recovered fibers, a fact that arises from the inert atmosphere used during the process. Gusao et al. used pyrolysis to recover carbon fibers from second generation aircraft composites, namely Boeing 787 [40]. They used a vacuum pyrolysis to limit the exposure of the reclaimed fibers to an oxidative environment so that the fibers retain their mechanical strength. With this technique, although a higher fiber purity was achieved, an ash layer was still covering the surface of the fibers resulting in low surface quality. Meyer et al. used a two-step pyrolysis method to extract fibers from carbon fiber composite waste [41]. In this study, the fibers were first recovered at 550 °C in the presence of nitrogen. Then, an oxidative operation at 550 °C was followed to fully remove the resin residue from the surface of the fibers. The recovered fibers retained 95 % of their tensile strength.

While partially successful, this thermal process has yet to be extended to accommodate glass fiber composites as previous studies have documented significant degradation associated with the pyrolysis of glass fibers [42, 43]. For examples, Cunliffe et al. have observed a reduction of approximately 40-50 % in the strength of E-glass fibers recovered from sheet molding compound using pyrolysis [44].

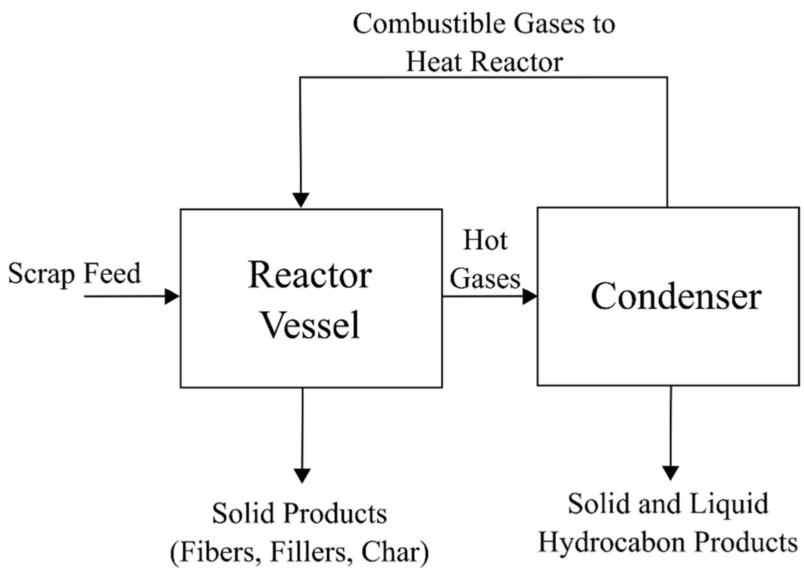

Figure 1-7: Pyrolysis process [24].

1.2.3 Chemical Recycling

The chemical recycling technique uses a dissolution reagent to breakdown the matrix polymer into high value oligomers so that the reinforcing fibers can be recovered [20, 45]. Diverse types of solvent have been identified in the literature such as water, glycols, alcohol and acids. The pressure and temperature required in the dissolution process highly depends on the type of the solvent [46, 47]. For instance, high temperature and pressure under either sub or supercritical conditions are generally required when water or alcohol are used as a solvent. This facilitates the depolymerization process and results in a faster dissolution and higher efficiency [48, 49]. Despite the satisfactory results of this technique, its high cost and inability to handle large quantities of waste have highly limited the applicability and commercialization of chemical technique in large scale. In addition, there is a chemical waste by-product created that represents another difficult environmental problem associated with this method.

1.3 Recycling of wind turbine blades

While clean and efficient, the enormous use of wind energy comes at the expense of widespread quantities of inorganic waste from the composite materials used in rotor blades.

Despite the recent advances in the composite industry, a mature recycling or reusing technology has yet to be developed for used rotor blades. As a consequence, a large portion of the blade waste currently produced, ends up in landfills, where leachates (a product obtained by leaching) from them can infiltrate the ground water and soil, a phenomenon associated with environmental impact and degradation. Apart from landfill, incineration is also used to dispose of the blades at the end of their life. However, recent studies have made it increasingly clear that the toxic substances present in the blades affect the living organisms, as well as the environment by getting adsorbed from the particulates generated during incineration of rotor blade materials [50-52]. The environmental concerns of composite wastes from the wind industry grows as the amount of composite material used in rotor blades has undergone a remarkable growth due to the increase in blades size and numbers of blades, as shown in Figure 1-8. Although many countries have recently imposed high environmental taxes on the landfill of organic materials, recent legislations, e.g. the EU directive on the landfill of waste, 1999/31/EC, prohibit the landfill of materials with more than 10% organic content. As a result, composite industries that are pioneering the use of organic materials, e.g. the wind turbine industry, are steered towards finding sustainable recycling solutions for their scrap composites.

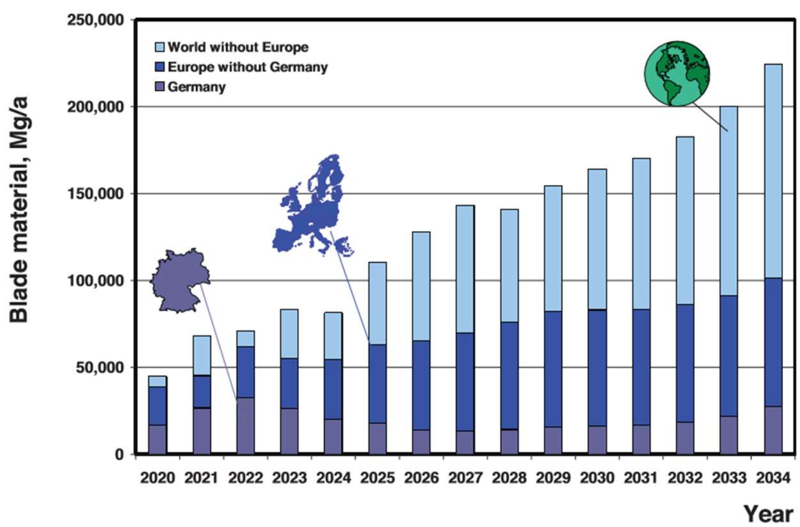

Figure 1-8: The prediction of required quantities of material used for turbine blades [3].

To overcome the overwhelming volume of end-of-life wind turbines blades, recently recycling of wind turbine blades has been significantly investigated in the literature [53-56]. KEMA and the Polish Industrial Chemistry Research Institute have studied the viability of mechanical recycling of turbine blades with the aim of reusing them in new composites. They have demonstrated that due to the poor mechanical properties of the recycled fibers, as well as their fiber size, the application of the recyclate is limited [3]. More recently, chemical and pyrolysis techniques have been utilized to recover glass fibers from end-of-life rotor blades. While pyrolysis led to significant property degradation in the recycled fibers, the chemical technique showed little promise in terms of commercialisation due to the use of hazardous chemicals and excessive cost. To this point, Larsen [3] has developed a pyrolysis process integrated with gasification to recover glass fibers and thermal energy from end-of-life wind turbine blades. In the proposed scheme, the blades are initially shredded into hand-sized chunks and then fed continuously into an oxygen-free rotating furnace at a temperature of 500°C. Once the resin is fully pyrolyzed, a combustion process in the presence of air is conducted to obtain clean fibers. Finally, the dust and ferrous metals are removed from the recyclate through magnets. ReFiber ApS has also developed and patented a pyrolysis-based recycling concept for wind turbine blades [57]. With this recycling technique, the gas obtained throughout the process is burned in CHP plants used in district heating for energy recovery. The recycled glass fibers are also processed for use in different basic applications such as wool for insulating purposes, short fibers for reinforcing casting compounds and plastic items. To mitigate the strength knock-down of the pyrolysis process, a two-step pyrolysis method has been recently developed and used to recycle wind turbine blades and recover reinforcement E-glass fibers [42]. The study resulted in an improved fiber quality, showing that the recovered fibers exhibited higher properties compared to those recovered via the traditional one-step pyrolysis process. However, this technique will incur an additional cost, which will adversely affect the commercialisation potential of thermal recycling for GFRPs. The feasibility of recycling glass fiber reinforced thermoplastic wind turbine blades was also exploited in a recent work by Cousins et al. [22]. Using a thermoplastic resin, a spar cap component for wind blades was manufactured and exposed to three different recycling methods including pyrolysis, dissolution and mechanical grinding. The results from this study demonstrated that dissolution process is capable of recovering the thermoplastic resin products and reinforcement fibers. In contrast, the pyrolysis process was only able to recover fibers featuring lower mechanical properties compared with virgin materials. In addition, mechanical grinding was unable to recover the valuable resin products. While interesting, this method can be only applied to thermoplastic reinforced blades, whereas the majority of the blades are composed of thermoset resins. Another recent research study investigated the feasibility of reusing the mechanically and thermally recovered fibers from wind turbines blades to reinforce polypropylene [19]. The results from this study have revealed that the mechanical properties of the recycled composite parts made using the shredded fibers are comparable to those using pyrolyzed fibers. They have also shown that, as opposed to pyrolyzed fibers, the shredded glass fibers retain the surface glass sizing, a characteristic that can influence the interfacial properties of the recovered fibers when mixed with a new polymer. As a result, mechanical grinding can be considered as a simple and straightforward solution to handle the glass fiber reinforced plastics.

Despite all these early studies, which have achieved partial success in recycling of wind turbine blades, a mature composite recycling landscape designed specifically for wind turbine blades with high commercialization capability is still lacking in the literature and in practice. In addition, the wind turbine industry is relatively young such that only a limited amount of practical experience on the recycling of turbines exists. As a result, a crucial need for a viable recycling solution that can turn the overwhelming composite wastes from wind industry to a value-added product exists.

1.4 Fused Filament Fabrication

With the shortcomings of the thermal and chemical recycling techniques for GFRPs, the choice of mechanical recycling could be an effective and straightforward recycling method for these materials. However, as it is often highlighted in the literature, the viability of this method relies on the carful separation of characterized fibers with lengths comparable to virgin fibers [25]. As a result, short fiber reinforced composites could be deemed as a superior potential application for mechanically recycled composites. One of the recent application sectors for short fiber composite materials, which is growing fast, is additive manufacturing (AM). AM provides an exciting opportunity to build objects from 3D models by joining materials layer upon layer [58]. AM technologies have enabled the fabrication of large and complex prototypes that are difficult to be manufactured through conventional methods. AM techniques include stereolithography apparatus (SLA) from photopolymer liquid [59], fused filament fabrication (FFF) from plastic filaments [60], laminated object manufacturing (LOM) from plastic laminations and selective laser melting [61]. Among all these techniques, FFF is the most widely used method to fabricate pure plastic parts with low cost, minimal wastage, and ease of material change [62]. As an emerging technology, many industries including automotive, medical, military and academic use FFF 3D printing as a rapid manufacturing tool. The widespread use of 3D printing has led to a significant increase in the value of the market for polymers used in FFF from $310 million in 2014 to $1.4 billion in 2019 [63].

Current feedstocks used in FFF are predominantly limited to thermoplastic filaments, including acrylonitrile butadiene styrene (ABS), polycarbonate (PC), polylactide (PLA), polyamide (PA), and the mixture of any two types of thermoplastic materials [60, 64]. The lack of mechanical properties in parts built from these thermoplastics is the major shortcoming of the FFF process, which restricts its applications to conceptual protypes rather than end-user functional products. As a result, it is critical to improve the FFF-fabricated pure thermoplastic parts, thus increasing their application and functionality. To overcome this issue, many efforts in the literature have attempted to improve the properties of FFF fabricated parts via introducing reinforcement materials such as glass fibers, into plastic materials to form composite reinforced 3D printing filaments [65-67]. Tekinalp et al. [64] and Ning et al. [62] exploited the feasibility of short fiber reinforced ABS composites as a feedstock for 3D-printing (Figure 1-9a). In an experimental study, Zhong et al. [68] studied the processability of three different types of glass reinforced filaments with an ABS matrix. The results showed that glass fibers are capable of improving the tensile strength and surface rigidity of the ABS filaments. In another study, Gray et al. [67] introduced a new class of filaments made of thermotropic liquid crystalline polymer (TLCP) fiber reinforced polypropylene composites. They observed that longer TLCP fibers compared to chopped fibers lead to larger tensile strength and improved functionality of the fabricated prototypes. Shofner et al. [69] used an ABS matrix to develop nano-fiber reinforced composites through FFF. The filaments were made of single-walled carbon nanotubes and ABS plastics. With these newly developed filaments, they observed, respectively, 40% and 60% increase in the tensile strength and Young's modulus of the 3D printed parts.

Papon et al. [70] reported the fracture properties of 3D printed short carbon fiber reinforced parts with different bead lay-up orientations. They reported that the composite parts with 0°/90° and 45°/-45° bead orientations featured a fracture toughness that was improved by, respectively, 42 % and 38 % as compared to neat PLA. Weng et al. [71] exploited the mechanical and thermal properties of parts made of organic montmorillonite (OMMT) reinforced ABS filament. Their experimental tests showed an intercalated structure formed in the 3D printed parts, which led to improved tensile and flexural properties proportional to the reinforcement content. As well, the composite parts showed a lower thermal expansion ratio when compared to pure ABS parts. It was also observed that adding OMMT can contribute to enhanced thermal decomposition and glass transition temperature as compared with pure ABS. In another experimental investigation, Dul et al. [72] characterized the mechanical properties of 3D printed ABS parts integrated with graphene (Figure 1-9c). Samples containing graphene with different weight fractions, namely 2, 4 and 8 wt% were printed and characterized. While an improvement in the tensile modulus of the samples was achieved, addition of graphene led to a reduction in the tensile strength, as well as the strain at break of the composite parts. In a more recent study, hemp hurd/PLA biocomposites were developed as feedstock for FFF (Figure 1-9b) [73]. The rheological tests showed that increasing the reinforcement content highly increases the viscosity of the filament. However, at high strain rates, the polymer shows shear thinning, which improves the melt flow and thus the processability of the filament. The mechanical tests demonstrated weaker properties for the FFF parts owing to their higher porosity. In addition, it was shown that increasing the hemp hurd content can negatively influence the flexural and tensile strength of the FFF parts by reducing the melt flow of the polymer and increasing the voids formed at the interface between the filler and polymer, as well as between the 3D printing layers.

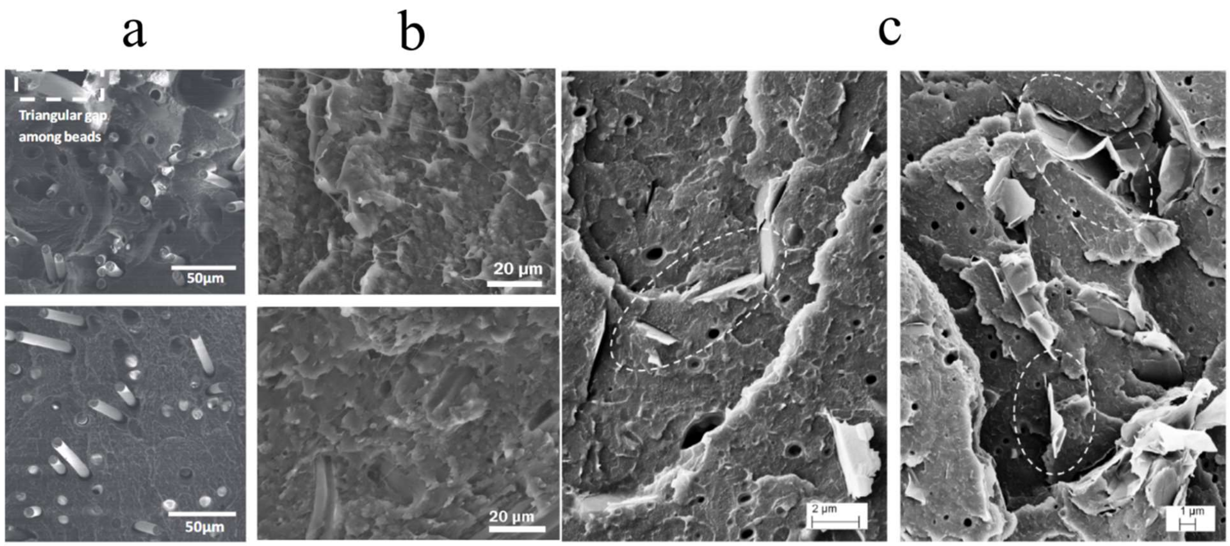

Figure 1-9: SEM micrographs from samples fabricated by reinforced FFF filaments: (a) carbon fiber reinforced ABS [64]; (b) hemp hurd reinforced PLA [73]; (c) graphene reinforced ABS [74].

The latest developments in the FFF process involves the incorporation of continuous fibers into polymer resins to 3D print continuous fiber reinforced composites. In this process, a double nozzle FFF 3D printer is used to separately extrude the polymer and reinforcement fiber. For example, in a study by Goh et al. [75], continuous glass and carbon fiber reinforced parts were successfully fabricated and tested. The results showed significantly improved properties for the glass fiber samples with values as high as 450 MPa and 7.2 GPa for the tensile strength and stiffness, respectively. As well, carbon fiber parts showed enhanced tensile strength and stiffness with values, respectively, 30 % and 80 % higher than those of glass fiber parts. In a more recent study, the tensile, fatigue and creep performance of 3D printed components made of three different types of reinforcement, namely carbon, glass and Kevlar fibers were assessed [76]. In this study, two sets of samples featuring a concentric and isotropic infill orientation were fabricated. The mechanical test results showed that components with isotropic infill orientation have the highest properties. This observation was attributed to the high fiber volume fraction, as well as the more aligned fibers in the isotropic samples. The SEM micrographs from the fractured surface of all the samples revealed fiber pull-out, delamination and fiber breakage as the most dominant failure modes.

All these aforementioned advances highlight the enormous potential in FFF 3D printing process to soon emerge as a prevalent technique and replace traditional manufacturing processes.

While the recent research trend on filament feedstock for FFF has only been focused on the use of virgin materials, the versatility of the technique to different materials introduces an exceptional opportunity for developing recycled composites via 3D printing. In particular, the increasingly growing application of the FFF process in many different industries, which translates to an extensive use of reinforced feedstock, opens up the possibility of accommodating a noticeable amount of composite wastes in this technology to produce a new class of filament feedstock reinforced with recycled materials.

1.5 Thesis rationale

In light of the critical need for recycling end-of-life wind turbine blades and the remarkable growth of FFF additive manufacturing technology, the main aim of this thesis is to develop and validate a recycling scheme for end-of-life scarp wind turbine blades via designing structurally efficient 3D printed composite component from recycled rotor blades (Figure 1-10). To achieve this goal, we propose a new class of FFF feedstock filament made of recycled fiber reinforced thermoplastics. An efficient and effective recycling route is developed to extract glass fibers from scrap blades. The recovered fibers are then characterized to obtain optimum process and design parameters to achieve efficient strengthening and stiffening from the recycled fibers in new composite systems. Lastly, the fibers are reincorporated into an optimized extrusion process to produce recycled fiber reinforced FFF feedstock, which is then used to fabricate composite parts.

One important aspect required to develop composite feedstock filament is the processability of the filament for the 3D printing process. To ensure the processability of the filament, multidisciplinary aspects including the physical properties, mechanical behaviour as well as the dimensional properties of the filament at micro and macro scales need to be accurately optimized. The specific objectives of the thesis are to:

1. Develop a cost-effective method for transforming large pieces of fiberglass wind turbine blades into fibers and particles that are suitable for the composite processing.
2. Characterize the tensile and interfacial properties of the recycled fibers to gain insight into the design parameters required to develop effective recycled composites.
3. Develop and validate optimum extrusion process parameters to successfully produce filaments with consistent diameter and properties as feedstock for FFF.

4. Mechanical and thermal characterization of 3D printed parts made from pure and fiber-reinforced thermoplastic filaments.
5. Develop a finite element model that enables a rapid assessment of the mechanical properties of 3D printed recycled parts.
6. Compare the performance and price of the newly developed filament to that of commercially available filament on the market to evaluate the viability of the proposed recycling scheme.

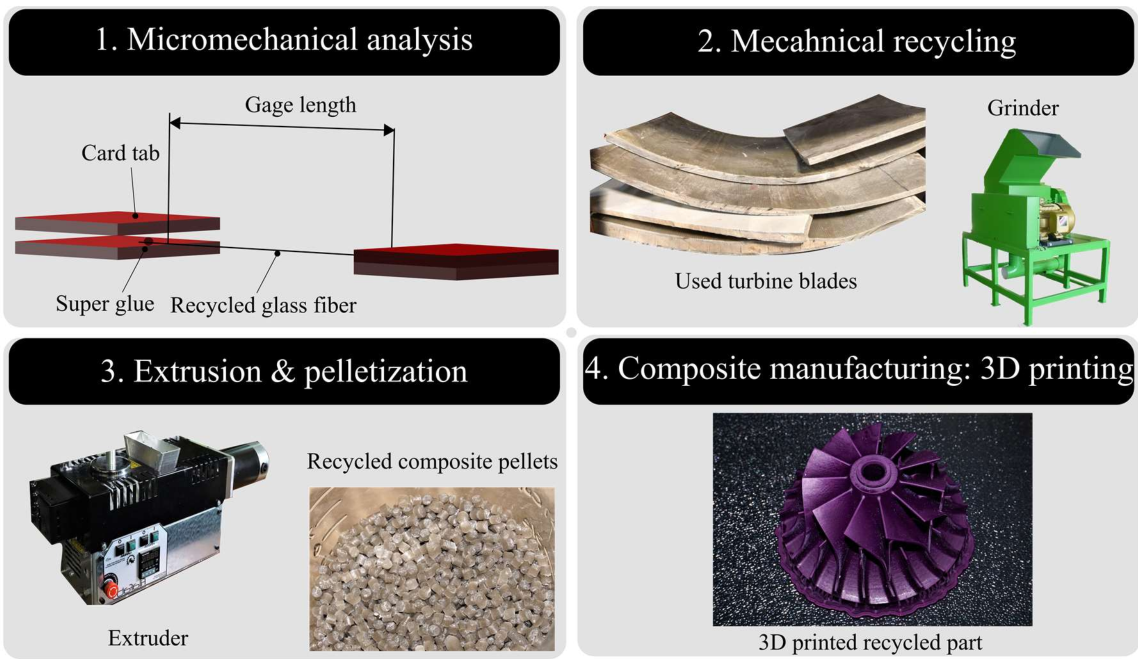

Figure 1-10: The proposed recycling solution for used wind turbine blades.

1.6 Structure of the thesis

This thesis is manuscript-based and is composed of six chapters. The current chapter (Chapter 1) briefly introduces the general background of wind turbine blades, followed by a literature review on the current recycling techniques for thermoset composites, including rotor blades. Additive manufacturing, particularly, fused filament fabrication as a potential market for recycled blades, is then extensively discussed and its merits and limitations are reviewed. At the end of Chapter 1, the overall objectives of this thesis are presented.

Chapter 2 proposes a recycling methodology integrating mechanical recycling and 3D printing to design and fabricate recycled 3D printed parts. FFF feedstock featuring 5 wt% fiber content are produced and used to manufacture tensile test coupons. The thermal and mechanical behavior of the newly developed filaments are studied and compared with commercially available pure PLA filament. In addition, the tensile properties of parts made from recycled fiber reinforced filament are assessed through tensile test on samples fabricated via FFF 3D printing.

Chapter 3 describes the effect of fiber content and recycled fibers surface morphology on the mechanical properties of 3D printed parts. Sample containing different fiber contents, including 5, 10, 15, 20 and 25 wt% are fabricated and evaluated through tensile testing. Following the tensile tests, an SEM investigation is carried out to study the fractured surface of the samples and characterize their void content. To study the effect of surface morphology of the recovered fibers on the interface properties of fabricated composites, 10 wt% tensile test coupons reinforced with virgin glass fibers featuring dimensional properties, e.g. average fiber length and fiber diameter, identical to those of recycled fibers are manufactured and characterized. The properties of samples made from virgin fibers are then compared with those made from recycled fibers to investigate the interface developed between the fibers and matrix.

Chapter 4 presents a systematic investigation on the mechanical and interfacial properties of fibers extracted from end-of-life wind turbine blades. Wind turbine blades are recycled through two different recycling schemes, namely thermal and mechanical, and single fibers from both recyclates are obtained and evaluated through single fiber tensile and pull-out tests. The mechanical properties of the recycled fibers, including the strength, stiffness and strain at failure are characterized and compared to those of virgin glass fibers. Using SEM and AFM investigations, the surface topography of the fibers is studied. Furthermore, the interfacial shear strength between the fibers and the new polymer system is measured and used along with the fibers properties to calculate the minimum critical fiber length required to achieve efficient strengthening and stiffening from the recycled fibers.

Chapter 5 combines the key elements of recycling and micromechanical analysis, obtained from chapter 2 through 4, to introduce recycled value-added products with superior mechanical properties. In particular, the recycling process is adjusted to preserve fibers with length above the critical length to achieve composites with effective strengthening and stiffening. Besides the experimental studies, this chapter also conducts a finite element (FE) modeling of the 3D printed recycled parts, which enables a rapid prediction of the tensile properties. While modeling of all the micromechanical features of a 3D printed part is complex, a homogenization technique is utilized to hierarchically evaluate the stiffness of the main building blocks of the microstructure of a 3D printed part. The results from the FE analysis are then compared with the experimental measurements to further evaluate the performance of the newly introduced 3D printing feedstock.

Finally, Chapter 6 highlights the main results and the main contributions of this thesis and concludes with a brief description of possible paths for future work.

1.7 References

[1] Neij L. Cost dynamics of wind power. Energy. 1999;24(5):375-89.

[2] WorldWind Energy Association. Available online: https://wwindeaorg/blog/2018/02/12/2017-statistics/.

[3] Larsen K. Recycling wind turbine blades. Renewable energy focus. 2009;9(7):70-3.

[4] O'Carroll A. Correlation of Mechanical Properties to Rain Erosion Resistance of Polymeric Materials 2018.

[5] Patel K, Gupta R, Garg M, Wang B, Dave U. Development of FRC Materials with Recycled Glass Fibers Recovered from Industrial GFRP-Acrylic Waste. Advances in Materials Science and Engineering. 2019;2019, 4149708.

[6] Dell'Anna R, Lionetto F, Montagna F, Maffezzoli A. Lay-Up and Consolidation of a Composite Pipe by In Situ Ultrasonic Welding of a Thermoplastic Matrix Composite Tape. Materials (Basel, Switzerland). 2018;11(5).

[7] Zhang L. The application of composite fiber materials in sports equipment. 2015 International Conference on Education, Management, Information and Medicine: Atlantis Press; 2015.

[8] Mølholt Jensen F, Branner K. 1 - Introduction to wind turbine blade design. In: Brøndsted P, Nijssen RPL, editors. Advances in Wind Turbine Blade Design and Materials: Woodhead Publishing; 2013. p. 3-28.

[9] Mishnaevsky L, Branner K, Petersen HN, Beauson J, McGugan M, Sorensen BF. Materials for Wind Turbine Blades: An Overview. Materials (Basel, Switzerland). 2017;10(11).

[10] Grande JA. Wind Power Blades Energize Composites Manufacturing. Plastics technology. 2008;54:68-75.

[11] Carbon Fiber vs. Fiberglass: A Comparison between the Two Materials Which Material Is Superior ? Available online: https://infogram/carbon-fiber-vs-fiberglass (accessed on 8 November 2017).

[12] Mishnaevsky L, Freere P, Sinha R, Acharya P, Shrestha R, Manandhar P. Small wind turbines with timber blades for developing countries: Materials choice, development, installation and experiences. Renewable Energy. 2011;36(8):2128-38.

[13] Sinha R, Acharya P, Freere P, Sharma R, Ghimire P, Mishnaevsky L. Selection of Nepalese Timber for Small Wind Turbine Blade Construction. Wind Engineering. 2010;34(3):263-76.

[14] Qing H, Mishnaevsky L. A 3D multilevel model of damage and strength of wood: Analysis of microstructural effects. Mechanics of Materials. 2011;43(9):487-95.

[15] Mishnaevsky Jr L, Sharma R, Qing H, Bech J, Sinha R, Evans R, et al. Strength and Reliability of Wood for the Components of Low-cost Wind Turbines: Computational and Experimental Analysis and Applications. Wind Engineering. 2009;33:183-96.

[16] Watson JC, Serrano JC. Composite Materials for Wind Blades. Wind Systems Magazine. 2010:46-51.

[17] Beckwith SW. Resin Infusion Technology. SAMPE Journal. 2007;43:66-70.

[18] Composites UK Trade Association. End of life options for composite materials.

[19] Group SM. Recycling of waste glass fiber reinforced plastic with microwave pyrolysis (LIFE07 ENV/S/000904). Stena recycling, Göteborg, Sweden2012.

[20] Pimenta S, Pinho ST. Recycling carbon fibre reinforced polymers for structural applications: technology review and market outlook. Waste management. 2011;31(2):378-92.

[21] Yang Y, Boom R, Irion B, van Heerden D-J, Kuiper P, de Wit H. Recycling of composite materials. Chemical Engineering and Processing: Process Intensification. 2012;51:53-68.

[22] Cousins DS, Suzuki Y, Murray RE, Samaniuk JR, Stebner AP. Recycling glass fiber thermoplastic composites from wind turbine blades. Journal of Cleaner Production. 2019;209:1252-63.

[23] Oliveux G, Dandy LO, Leeke GA. Current status of recycling of fibre reinforced polymers: Review of technologies, reuse and resulting properties. Progress in Materials Science. 2015;72:61-99.

[24] Pickering SJ. Recycling technologies for thermoset composite materials—current status. Composites Part A: Applied Science and Manufacturing. 2006;37(8):1206-15.

[25] Palmer J, Ghita O, Savage L, Evans K. Successful closed-loop recycling of thermoset composites. Composites Part A: Applied Science and Manufacturing. 2009;40(4):490-8.

[26] Schinner G, Brandt J, Richter H. Recycling carbon-fiber-reinforced thermoplastic composites. Journal of Thermoplastic Composite Materials. 1996;9(3):239-45.

[27] MARTIN SA. Comparison of hammermill and roller mill grinding and the effect of grain particle size on mixing and pelleting.: Master's thesis, Kansas State University; 1981.

[28] Roux M, Dransfeld C, Eguémann N, Giger L. Processing and recycling of thermoplastic composite fibre/PEEK aerospace part2014.

[29] Palmer J, Ghita OR, Savage L, Evans KE. Successful closed-loop recycling of thermoset composites. Composites Part A: Applied Science and Manufacturing. 2009;40(4):490-8.

[30] Composite recycling-raw material for the future. ERCOM composite recycling GmbH.

[31] Scheirs J. Polymer recycling: science, technology and applications. John! Wiley & Sons Ltd, Journals, Baffins Lane, Chichester, Sussex PO 19 1 UD, UK, 1998 591. 1998.

[32] Sims B, Booth C, Lakshmanam. Process for seperating fibers from composite materials. International Patent WO 93/05883, granted to Phoenix Fiberglass, Inc. 1993.

[33] Pickering SJ. 4 - Thermal methods for recycling waste composites. In: Goodship V, editor. Management, Recycling and Reuse of Waste Composites: Woodhead Publishing; 2010. p. 65-101.

[34] Jiang G, Pickering SJ, Lester EH, Turner T, Wong K, Warrior N. Characterisation of carbon fibres recycled from carbon fibre/epoxy resin composites using supercritical n-propanol. Composites Science and Technology. 2009;69(2):192-8.

[35] Jiang G, Pickering S, Walker G, Wong K, Rudd C. Surface characterisation of carbon fibre recycled using fluidised bed. Applied Surface Science. 2008;254(9):2588-93.

[36] Pickering S. Thermal methods for recycling waste composites. Management, recycling and reuse of waste composites: Management, Recycling and Reuse of Waste Composites; 2010. p. 65-101.

[37] Yip H, Pickering S, Rudd C. Characterisation of carbon fibres recycled from scrap composites using fluidised bed process. Plastics, rubber and composites. 2002;31(6):278-82.

[38] Meng F, McKechnie J, Turner TA, Pickering SJ. Energy and environmental assessment and reuse of fluidised bed recycled carbon fibres. Composites Part A: Applied Science and Manufacturing. 2017;100:206-14.

[39] Torres A, De Marco I, Caballero B, Laresgoiti M, Legarreta J, Cabrero M, et al. Recycling by pyrolysis of thermoset composites: characteristics of the liquid and gaseous fuels obtained. Fuel. 2000;79(8):897-902.

[40] Gosau J, Wesley T, Allred R. Carbon fiber reclamation from stateof-the-art 2nd generation aircraft composites. SAMPE'09 Conference SAMPE, Baltimore, MD, USA2009.

[41] Meyer L, Schulte K, Grove-Nielsen E. CFRP-recycling following a pyrolysis route: process optimization and potentials. Journal of Composite Materials. 2009;43(9):1121-32.

[42] Ginder RS, Ozcan S. Recycling of Commercial E-glass Reinforced Thermoset Composites via Two Temperature Step Pyrolysis to Improve Recovered Fiber Tensile Strength and Failure Strain. Recycling. 2019;4(2):24.

[43] Feih S, Manatpon K, Mathys Z, Gibson AG, Mouritz AP. Strength degradation of glass fibers at high temperatures. Journal of Materials Science. 2009;44(2):392-400.

[44] Cunliffe AM, Jones N, Williams PT. Pyrolysis of composite plastic waste. Environmental Technology. 2003;24(5):653-63.

[45] Liu Y, Liu J, Jiang Z, Tang T. Chemical recycling of carbon fibre reinforced epoxy resin composites in subcritical water: synergistic effect of phenol and KOH on the decomposition efficiency. Polymer degradation and stability. 2012;97(3):214-20.

[46] Piñero-Hernanz R, Dodds C, Hyde J, García-Serna J, Poliakoff M, Lester E, et al. Chemical recycling of carbon fibre reinforced composites in nearcritical and supercritical water. Composites Part A: Applied Science and Manufacturing. 2008;39(3):454-61.

[47] Piñero-Hernanz R, García-Serna J, Dodds C, Hyde J, Poliakoff M, Cocero MJ, et al. Chemical recycling of carbon fibre composites using alcohols under subcritical and supercritical conditions. The Journal of Supercritical Fluids. 2008;46(1):83-92.

[48] Hyde JR, Lester E, Kingman S, Pickering S, Wong KH. Supercritical propanol, a possible route to composite carbon fibre recovery: a viability study. Composites Part A: Applied Science and Manufacturing. 2006;37(11):2171-5.

[49] Morin C, Loppinet-Serani A, Cansell F, Aymonier C. Near-and supercritical solvolysis of carbon fibre reinforced polymers (CFRPs) for recycling carbon fibers as a valuable resource: State of the art. The journal of supercritical fluids. 2012;66:232-40.

[50] Gupta M. Combustion of Composite Material Assessment &d Quantification of Hazards, DRDO Science Spectrum, DESIDOC. India. 2009:27-30.

[51] Halim AA, Aziz HA, Johari MAM, Ariffin KS. Comparison study of ammonia and COD adsorption on zeolite, activated carbon and composite materials in landfill leachate treatment. Desalination. 2010;262(1-3):31-5.

[52] Misra V, Pandey S. Hazardous waste, impact on health and environment for development of better waste management strategies in future in India. Environment international. 2005;31(3):417-31.

[53] Cherrington R, Goodship V, Meredith J, Wood BM, Coles SR, Vuillaume A, et al. Producer responsibility: Defining the incentive for recycling composite wind turbine blades in Europe. Energy Policy. 2012;47:13-21.

[54] Åkesson D, Foltynowicz Z, Christéen J, Skrifvars M. Microwave pyrolysis as a method of recycling glass fibre from used blades of wind turbines. Journal of Reinforced Plastics and Composites. 2012;31(17):1136-42.

[55] Weinzettel J, Reenaas M, Solli C, Hertwich EG. Life cycle assessment of a floating offshore wind turbine. Renewable Energy. 2009;34(3):742-7.

[56] Merugula LA, Khanna V, Bakshi BR. Comparative life cycle assessment: Reinforcing wind turbine blades with carbon nanofibers. Sustainable Systems and Technology (ISSST), 2010 IEEE International Symposium on: IEEE; 2010. p. 1-6.

[57] http://www.refiber.com/technology.html.

[58] Rahim TNAT, Abdullah AM, Md Akil H. Recent Developments in Fused Deposition Modeling-Based 3D Printing of Polymers and Their Composites. Polymer Reviews. 2019;59(4):589-624.

[59] West AP, Sambu SP, Rosen DW. A process planning method for improving build performance in stereolithography. Computer-Aided Design. 2001;33(1):65-79.

[60] Dudek P. FDM 3D Printing Technology in Manufacturing Composite Elements. Archives of Metallurgy and Materials. 2013;58.

[61] Kruth JP. Lasers and materials in selective laser sintering. Assembly Automation. 2003;23(4):357-71.

[62] Ning F, Cong W, Qiu J, Wei J, Wang S. Additive manufacturing of carbon fiber reinforced thermoplastic composites using fused deposition modeling. Composites Part B: Engineering. 2015;80:369-78.

[63] Feasibility study: production of recycled 3d print filament. 2016.

[64] Tekinalp HL, Kunc V, Velez-Garcia GM, Duty CE, Love LJ, Naskar AK, et al. Highly oriented carbon fiber–polymer composites via additive manufacturing. Composites Science and Technology. 2014;105:144-50.

[65] Ning F, Cong W, Hu Z, Huang K. Additive manufacturing of thermoplastic matrix composites using fused deposition modeling: A comparison of two reinforcements. Journal of Composite Materials. 2017;51(27):3733-42.

[66] Yang C, Tian X, Liu T, Cao Y, Li D. 3D printing for continuous fiber reinforced thermoplastic composites: mechanism and performance. Rapid Prototyping Journal. 2017;23(1):209-15.

[67] Gray IV RW, Baird DG, Helge Bøhn J. Effects of processing conditions on short TLCP fiber reinforced FDM parts. Rapid Prototyping Journal. 1998;4(1):14-25.

[68] Zhong W, Li F, Zhang Z, Song L, Li Z. Short fiber reinforced composites for fused deposition modeling. Materials Science and Engineering: A. 2001;301(2):125-30.

[69] Shofner M, Lozano K, Rodríguez-Macías F, Barrera E. Nanofiber-reinforced polymers prepared by fused deposition modeling. Journal of applied polymer science. 2003;89(11):3081-90.

[70] Papon EA, Haque A. Fracture toughness of additively manufactured carbon fiber reinforced composites. Additive Manufacturing. 2019;26:41-52.

[71] Weng Z, Wang J, Senthil T, Wu L. Mechanical and thermal properties of ABS/montmorillonite nanocomposites for fused deposition modeling 3D printing. Materials & Design. 2016;102:276-83.

[72] Dul S, Pegoretti A. Fused deposition modeling with ABS-graphene nanocomposites. Composites Part A: Applied Science and Manufacturing. 2016;85:181-91.

[73] Xiao X, Chevali VS, Song P, He D, Wang H. Polylactide/hemp hurd biocomposites as sustainable 3D printing feedstock. Composites Science and Technology. 2019;184:107887.

[74] Dul S, Fambri L, Pegoretti A. Fused deposition modelling with ABS–graphene nanocomposites. Composites Part A: Applied Science and Manufacturing. 2016;85:181-91.

[75] Goh GD, Dikshit V, Nagalingam AP, Goh GL, Agarwala S, Sing SL, et al. Characterization of mechanical properties and fracture mode of additively manufactured carbon fiber and glass fiber reinforced thermoplastics. Materials & Design. 2018;137:79-89.

[76] Mohammadizadeh M, Imeri A, Fidan I, Elkelany M. 3D printed fiber reinforced polymer composites - Structural analysis. Composites Part B: Engineering. 2019;175:107112.

`

Chapter 2

Recycling of Fiberglass Wind Turbine Blades into Reinforced Filaments for use in Additive Manufacturing

2 Chapter 2: Recycling of Fiberglass Wind Turbine Blades into Reinforced Filaments for use in Additive Manufacturing

Amirmohammad Rahimizadeh[a], Jordan Kalman[b], Kazem Fayazbakhsh[b,*], Larry Lessard[a]

[a] Department of Mechanical Engineering, McGill University, Montreal, QC H3A0C3, Canada

[b] Department of Aerospace Engineering, Ryerson University, Toronto, Ontario M5B2K3, Canada

[*]Corresponding author: kazem@ryerson.ca; Tel: (+1) 416-979-5000 ext. 6414; fax: (+1) 416-979-5056

Journal of Composites Part B: Engineering, 2019. 175: p. 107101

2.1 Abstract

The wind energy industry is one of the fastest-growing application sectors of composites, where reinforcement fibers are used in the manufacturing of light rotor blades. Considering the limited lifetime of turbine blades, a growing number of wind turbines will start to be decommissioned. Turbine blades are generally landfilled at their end-of-life, which highly impacts the environment. This paper proposes a systematic scheme combining mechanical recycling and 3D printing to recycle the valuable constituents of the scrap blades and reuse them in a Fused Filament Fabrication (FFF) process with the aim of improving the mechanical performance of 3D printed components. Mechanical grinding integrated with a double sieving mechanism is utilized to recover the reinforcement fibers. Tensile test specimens with 5 wt% fiber content are fabricated from the recycled fibers and plastic pellets and their mechanical properties as well as internal microstructure are investigated. The results demonstrate an improvement of 16% and 10 % in the elastic modulus and ultimate strength of the reinforced composite filament as compared to the commercially available pure PLA filament. As well, a Young's modulus of 3.35 GPa was observed for the FFF fabricated samples, which is an 8% increase relative to pure PLA samples.

Keywords: A. Wind energy industry, E. Mechanical recycling, E. Fused filament fabrication, B. Mechanical properties

2.2 Introduction

The superior mechanical properties of composite materials provide an exiting opportunity to build structures that are lightweight and of high strength, characteristics that have led to many engineering applications for composites [1-4]. The wind energy industry represents one of the fastest growing application sectors of composites, where reinforcement fibers, such as fiberglass or carbon fibers, a plastic polymer, such as polyester or epoxy, and a core material are used to build strong and compliant rotor blades [5]. The dramatic growth of wind industry over the past 20 years has resulted in an extensive amount of end-of-life rotor blades. Current routes to dispose of turbine blades at their end-of-life involve landfill and incineration, methods that are associated with environmental impact [6, 7]. Given the non-biodegradable nature of turbine blades, recent environmental legislation has increasingly demanded for the recycling and replacing of turbine blades in the near future [5, 6, 8]. Recent research efforts in the area of wind energy have been focused on the development of sustainable methods for the recycling and reuse of rotor blades. To address this pivotal challenge, scientists have resorted to chemical and pyrolysis techniques to recover glass fibers from end-of-life turbine blades [6]. Despite the high mechanical properties of the recycled fibers, these techniques show little promise in terms of commercialisation due to the use of hazardous chemicals and/or excessive cost. Mechanical grinding is the only recycling technique, which has found its way to industrial application [9]. Compared to thermal and chemical techniques, this method offers a straightforward and economically feasible scheme for the recycling of composites, particularly glass fiber reinforced materials [10, 11]. A recent research study investigated the feasibility of reusing the mechanically recovered fibers from wind turbines blades to reinforce polypropylene [12]. The results have revealed that the mechanical properties of the recycled composite parts made of the shredded fibers are comparable to those observed for parts made of pyrolyzed fibers. They have also shown that as opposed to pyrolyzed fibers, the shredded glass fibers retain the glass sizing. As a result, mechanical grinding can be considered as a simple and straightforward solution to handle the glass fiber reinforced plastics.

Recent studies have shown that composite materials can be systematically designed and used to produce strong and stiff feedstocks for Additive Manufacturing (AM) processes [13-16]. AM represents a class of fabrication techniques where a layer-upon-layer method is used to build a part from a 3D model [17-19]. AM enables the fabrication of components with complex geometries, those that are unachievable using traditional manufacturing techniques [20]. Fused Filament Fabrication (FFF) is the most widely used 3D printing process due to its simplicity, low cost, and minimal wastage [21]. While extremely efficient, FFF parts are generally made of pure thermoplastic material, which results in low strength and stiffness, dominant factors in contributing to their limited structural performance [22-26]. The mechanical properties of the FFF manufactured parts depend upon a multiple of factors including the filament material, extrusion process of the filament, as well as the manufacturing process and design parameters. Recent advances in AM involve the integration of reinforcing materials with the thermoplastic polymers with the goal of enhancing their mechanical properties. This technique offers the possibility of manufacturing functional parts with strong and stiff microstructure.

Corcione et al. [27] incorporated NanoHydroxyApatite powder into polylactic acid (PLA) to produce b-tricalcium phosphate–based PLA composites as a feedstock material for FFF process. Differential Scanning Calorimetry (DSC) analysis showed promising results in terms of the glass transition temperature of the NanoHA/PLA filament, a crucial factor to the success of the 3D printing process. The newly introduced filament was successfully used to print bone allografts with higher compressive strength relative to those printed using pure PLA filaments. More recently, Kuo et al. [28] attempted to improve the thermomechanical properties of Acrylonitrile butadiene styrene (ABS) filaments using thermoplastic starches (TPS). ABS polymer and TPS agents were used to produce FFF feedstock filaments. In order to increase the processability of the filament, a plasticizer namely, glycerol/water was used. Mechanical and thermal tests performed on the filament showed an improved thermal resistance, heat distortion temperature, flexural modulus, impact strength, tensile strength, and flexural strength. Nikzad et al. [29] postulated that the addition of iron powder into ABS reduce the tensile strength of the filament when compared to pure ABS. Nevertheless, iron/ABS filament exhibited an improved thermal conductivity and heat capacity, which ensured thermally stable 3D printed parts with high dimensional accuracy.

Other strategies that deal with the improvement of FFF 3D printed parts involve the incorporation of reinforcement fibers e.g., carbon and glass fibers, into the polymeric filaments. In one interesting study, Shofner et al. [30] used ABS matrix to develop nano-fiber reinforced composites through FFF. The filament was made of single-walled carbon nanotubes and ABS plastic. With the newly developed filament, they observed 40% and 60% increase in the tensile strength and Young's modulus of the 3D printed parts, respectively. Zhong et al. [31] incorporated short glass fibers into ABS matrix to produce FFF filament. Their results showed that the parts made of glass fiber reinforced filament feature higher tensile strength relative to pure ABS. In a more recent study, Ning et al. [21] investigated the mechanical performance of FFF 3D printed parts made of virgin carbon fiber reinforced ABS filament. ASTM D638 standard was followed to prepare tensile test specimens with different fiber content, i.e. 3, 5, 7.5, 10, and 15 wt%. Compared with the pure ABS specimens, an improvement in the flexural and tensile strength was attained by increasing the fiber content from 3 to 5 wt%. However, a further increase in the fiber content from 5 wt% to 10 wt% resulted in a reduction of the tensile strength. This reduction in properties is attributed to the pores that develop during the extrusion and printing process of the filaments with high fiber content. Stoof et al. [32] exploited the possibility of natural fiber reinforced Poly-propylene composites as a feedstock for 3D-printing. Their work particularly investigated the effect of fibers on the strength and shrinkage of the printed samples. The results showed that the tensile strength and Young's modulus of both the filament and the 3D printed samples have increased by 70% and 210%, respectively. It was also observed that increasing the fiber content has the potential to mitigate the shrinkage of the 3D printed objects.

While all the studies mentioned so far focused on the use of virgin fibers, only recently have scrap materials been used to develop FFF feedstock. For example, in an experimental study, a novel FFF filament based on PLA and Lecce Stone (LS) scraps was successfully designed and developed [33]. Although no mechanical study was performed, the study showed that the thermal degradation of the newly developed filament is similar to that of the conventional pure PLA filament, thus ensuring a high processability of the LS/PLA filament. In another study, nylone6 industrial waste, Al_2O_3 and Al powder were used to achieve a filament featuring higher roughness and wear resistance relative to commercial FFF filament material [34].

The aim of this work is to use fiber glass scrap from wind turbine blades as reinforcement in thermoplastic filaments for 3D printing to achieve the following: addressing the challenging issue of wind turbine blade scrap that is increasingly growing every year; and improving mechanical properties of 3D printed thermoplastic parts without the need of adding high cost virgin fibers. In this paper, the ASTM D638 standard test method is followed to properly characterize tensile strength of 3D printed parts out of pure PLA and PLA reinforced with fiberglass. In the following sections, first, a systematic methodology is proposed integrating mechanical recycling and filament extrusion to manufacture PLA filaments reinforced with fiberglass. Then, specimen geometry, configuration, and testing procedure are described as per ASTM D638. Next, the specimen manufacturing, including 3D printing process and design parameters, is described extensively. Experimental testing is performed and the tensile strength for different filament materials is obtained. Finally, the performance of the 3D printed specimens with pure and reinforced PLA is discussed and recommendations for future research are presented.

2.3 Methodology

One of the causes of environmental pollution is landfill of wind turbine blades. This work proposes to recycle the turbine blades at their end-of-life and reincorporate them into thermoplastic FFF filaments. The cost analysis on the landfill of wind turbine blades has shown that it is presently the most economical feasible solution to dispose of the scrap blades. However, the EU directive on the landfill of waste, 1999/31/EC, prohibits the landfill of Glass Fiber Reinforced Plastics (GFRPs) and many countries are now imposing tax upon organic wastes, which are put into landfill [12]. Hence, despite the low cost of virgin glass fibers, the tighter environmental regulations that are sure to come, will enhance the economical long-term benefits for recycling GFRPs. The major aspects of the approach that are taken here rest on the integration of mechanical grinding and filament extrusion to transform the recycled glass fibers into commercial FFF feedstock material. Figure 2-1 depicts the current methodology, where the key steps are briefly described below:

1. A mechanical recycling method combining grinding and a double sieving process is performed to recover the glass fibers from the scrap blades. Since the diameter of the 3D printer nozzle used here is 0.4 mm, the double sieving operation ensures a supply of fibers with a length generally below 0.4 mm, a characteristic essential for filaments with high processability.
2. The mixture of the PLA pellets and the fibers are placed in a dehydrator machine for a drying process of 4 hours at 60ºC. This dehydrations process reduces the moisture content of the pellets that could generate voids during the extrusion process.

3. To generate the Recycled Glass Fiber Reinforced Filament (RGFRF) for FFF, the raw materials obtained in step 2 are first fed into a twin-screw extruder connected to a pelletizer to produce glass fiber reinforced pellets. Following the initial extrusion, the pellets are re-dried and fed into a single screw extruder to produce RGFRF. The extruder screw speed, the die temperature as well as the winder speed are tuned to attain a filament with consistent diameter of 1.75 mm. A laser micrometer with an accuracy of ±2 μm is used along with the extruder to monitor the filament diameter.
4. Tensile properties of a single filament made out of pure PLA, as a baseline, and reinforced filaments are compared. In addition, tensile coupons are manufactured as per ASTM D638 type I out of pure PLA filament and RGFRF. Tensile testing is performed on the coupons and the resulting mechanical properties are compared to evaluate the performance of the newly developed filament.

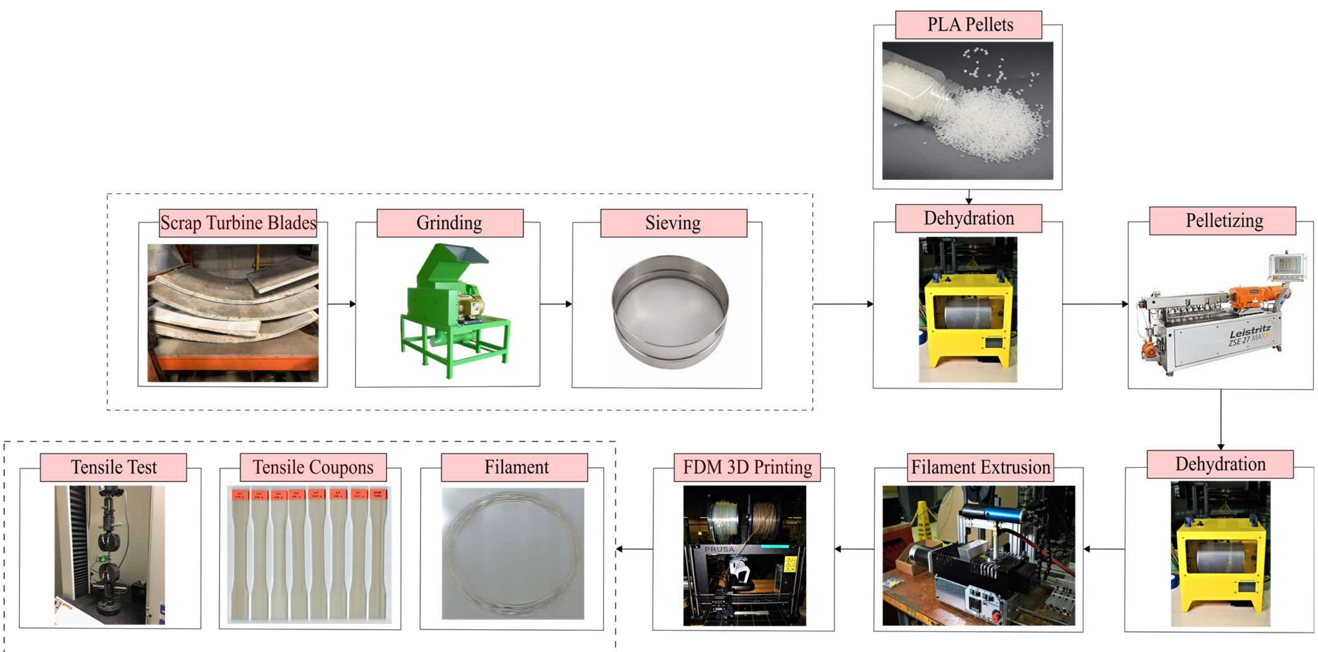

Figure 2-1: The proposed methodology for recycling of wind turbine blades.

2.3.1 Mechanical recycling

To avoid the consequences of landfill and incineration, one focus of this work is on the mechanical grinding of the rotor blades, a size reduction technique for a simple and fast recovery of the glass fibers from the scrap blades. Further, grinding with an impact and hammer mill has shown to be the most efficient way to reduce the size of glass fiber reinforced composites due to the abrasive nature of fiberglass [11]. In the present study, recycled glass fibers with an average length of 0.1-0.4 mm are obtained from grinding a turbine blade made of glass fiber reinforced epoxy composite. Since the nozzle diameter of the printer used in this investigation is 0.4 mm, this range of fiber length ensures a high processability for the proposed filament. Longer fiber lengths lead to the possibility of clogging the 3D printer output nozzle. As observed in Figure 2-2, a three-stage recycling procedure is used here to obtain the fibers for the filament extrusion: First, the blades are cut down into 20 × 20 cm pieces using a band saw and then fed into a grinder machine (ECO-WOLF, INC.) consisting of a hammer mill system and a classifier with a hole size of 3 mm. Following the first granulation process, visual inspection microscopy of the recycled materials demonstrates a mixture of resin powder and fibers, resulting in a fiber length range of 0.1-2.5 mm. To further classify the recycled materials, a double sieving mechanism is used and two grades of granulated material are obtained. The granulated blade obtained from the first grinding process is sieved through a stainless-steel screen with a hole size of 0.1 mm. The larger-sized recycled material is then re-fed in the sieve for the second sieving operation to extract more fine fibers that are in the desirable length range.

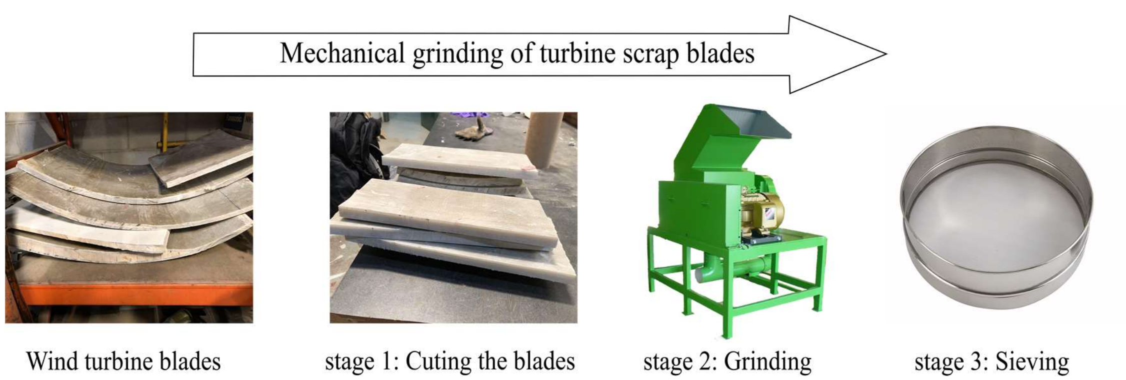

Figure 2-2: The proposed three-stage grinding methodology for the mechanical recycling of wind turbine blades.

2.3.2 Filament extrusion

The RGFRF was fabricated through a double melt extrusion process of PLA pellets (Ingeo 4043D, Natureworks LLC, Blair, Nebraska) and 5 wt% recycled glass fibers. PLA is a hygroscopic thermoplastic and readily absorbs moisture from the atmosphere. The presence of moisture will hydrolyze the biopolymer resulting in void generation during the extrusion process [35].

Furthermore, the presence of moisture on the surface of the fibers can form fiber clusters, which prevent a homogeneous distribution of fibers within the polymer. As a preventative measure, a dehydration process on the fibers and the PLA pellets is performed at 60 °C for 4 hours to dry the fibers and reduce the moisture content of the pellets to below 250 ppm. Once the fibers and the pellets are dried, we feed them into a twin-screw extruder (Leistritz ZSE18HP-40D, Nuremberg, Germany) with 8 subzones connected to a pelletizer to produce glass fiber reinforced pellets. This process ensures a homogeneous distribution of the fibers within the matrix, an essential factor to the dimensional accuracy of the filament, as well as the mechanical properties of the 3D printed components. The reinforced pellets are then re-dried and fed into a single screw extruder (FilaFab, D3D Innovations Limited, Bristol, UK) to produce RGFRF. To increase the dimensional accuracy of the filament, a spool winder machine is connected to the extruder, which allows for accurate control of the filament diameter. To consistently monitor the diameter of the filament, a laser micrometer with ±2 µm accuracy is used. The extrusion parameters including the screw speed, the speed of the winder as well as the die temperature are properly adjusted to achieve a 1.75 ± 0.05 mm filament, a suitable diameter and tolerance for the 3D printing process. The screw speed and the temperature of each zone during the initial and the second extrusion processes are reported in Table 2-1. Scanning Electron Microscopy (Hitachi UHR Cold-Emission FE-SEM SU8000) and optical microscopy (Nikon, Tokyo, Japan) are used to characterize the microstructural features of the RGFRF namely, the fiber distribution and fiber orientation. The filament is sectioned transversely and longitudinally, where the former is used to monitor the fiber distribution and the latter shows the fiber orientation. For the longitudinal cross section, the samples are potted in an epoxy resin, ground and polished in preparation for the microstructural analysis. Grinding is done using 120 grit, followed by 220 and 600 grit sandpaper, and polishing is performed using a 10 µm diamond slurry, then a 5 µm diamond slurry, and finished with a 0.3 µm alumina suspension.

Table 2-1: The single and twin-screw extruders parameters.

Twin screw pelletizer	Screw speed (rpm)	90
	Subzone 1-2 (Temp °C)	190
	Subzone 3(Temp °C)	185
	Subzone 4(Temp °C)	180
	Subzone 5(Temp °C)	175
	Subzone 6-8(Temp °C)	170
Single screw filament maker	Screw speed (rpm)	25
	Die temperature (Temp °C)	210
	Winder speed (rpm)	1

To study the effect of the recycled fibers on the physical properties of the filament, in particular, the glass transition temperature and the crystalline content, DSC analysis is performed on the RGFRF and the pure PLA filament. Samples weighing in the range of 6-10 mg are extracted from the filaments and loaded into the DSC instrument (DSC Q100, TA Instruments, USA). The thermal history of the samples induced during the filament preparation is first removed with a heating procedure. Following the initial heating ramp, the samples are cooled down to ambient temperature at a rate of 5 °C /min and then held isothermally for 3 minutes. After the removal of the thermal history, the temperature is then ramped at a rate of 5 °C/min up to 200 °C to capture the glass transition temperature, as well as the melting peak of the samples. The DSC analysis is performed at least three times for each sample to verify the accuracy of the results.

The mechanical properties of the RGFRF, as well as the interface between the recycled fibers and PLA are assessed by performing tensile tests on both the RGFRF and the pure PLA filaments. A set of lifting thimbles with an inside diameter of 7/8 inch is used to clamp the filaments in the tensile machine. To ensure the validity of the results, the test is repeated five times and the average results are reported.

2.3.3 Specimens design and manufacturing

ASTM D638-14 standard is followed here to characterize the tensile properties of 3D printed parts made of RGFRF and pure PLA. As per ASTM D638, five different types of tensile test specimen are suggested. Type I is the preferred specimen for a thickness of less than 7 mm. Hence, type I is selected here, and a 3D model is created in SolidWorks (Dassault Systems, Waltham, MA) as per the geometry and dimensions given in the standard. Although manufacturing process and design parameters such as nozzle temperature, bed temperature, layer thickness and infill percentage play a major role in the structural performance of FFF 3D printed parts, in this work the influence of the feedstock material is studied. To do so, the manufacturing process and design parameters are kept identical for all the specimens and a relative comparison is performed based on their tensile properties. As a result, five pure PLA and reinforced specimens with a total thickness of 3.36 mm and 0° raster orientation are prepared using a Prusa i3 Mk2S printer for the test. Manufacturing process and design parameters are summarized in Table 2-2. The mass value of the specimens is measured by a precision balance. Tensile tests on the 3D printed samples are conducted in a test machine (312 Q tensile machine, Testresources) with a 10 KN force transducer capacity and a 5 mm/min testing speed.

Table 2-2: Manufacturing and design parameters for specimen 3D printing.

Manufacturing parameter	Value	Manufacturing parameter	Value
Print direction	XYZ	Nozzle diameter (mm)	0.4
Raster angle	0	Nozzle temperature (°C)	215
Layer height (mm)	0.14	Cooling	No fan cooling
Bed temperature (°C)	60	Infill (%)	100
Print speed (mm/min)	2400	Filament diameter (mm)	1.75

2.4 Results and discussion

This section summarises the results from mechanical grinding, filament fabrication, and tensile testing of filaments and 3D printed specimens. Three sets of results are herein presented. The first describes the mechanical recycling of the scrap rotor blades. The second discusses the filament fabrication and its performance, namely tensile and physical properties. Finally, the third describes the mechanical properties of the 3D printed tensile coupons made of RGFRF, which are then compared to coupons made from the conventional pure PLA filament.

2.4.1 Mechanical grinding

The methodology described in Section 2.3 is applied here for the mechanical recycling of wind turbine blades. Approximately, 60 % of the ground recycled material has come out of the sieve and is usable for the 3D printing process. However, the remaining sieved residue could be either reground and used in the same recycling system or processed with larger nozzle diameters. Figure 2-3 illustrates the probability distribution of the fiber length evaluated by measuring the length of at least 300 fibers from each grade of granulated material. As seen, after the second sieve operation, most of the fibers feature lengths in the range of 0.15-0.18 mm, thus ensuring the processability of the fibers for the use in the FFF process. Although it is difficult to differentiate the fibers in terms of shape characteristics, it could be concluded from visual inspection that after the second sieve operation, fiber bundles are separated, and fibers are in a better refined state. Resin residue in the form of powder is also visible in the recyclate. In some sections of wind turbine blades, balsa wood is generally used as core to reduce the production costs. In the present study, only pure fiberglass sections of a rotor blade are used to recover the glass fibers. Therefore, no wood powder is present in the fiberglass compound and it includes only matrix powder and fiberglass. In particular, this work did not consider the effect of the wood powder on the properties of the 3D printing composite filament. In addition, the recovered fibers, featured a dimeter ranging between 16 – 20 µm, which represents the diameter of E-glass fiber, the most commonly type of glass fiber used in wind turbine blades.

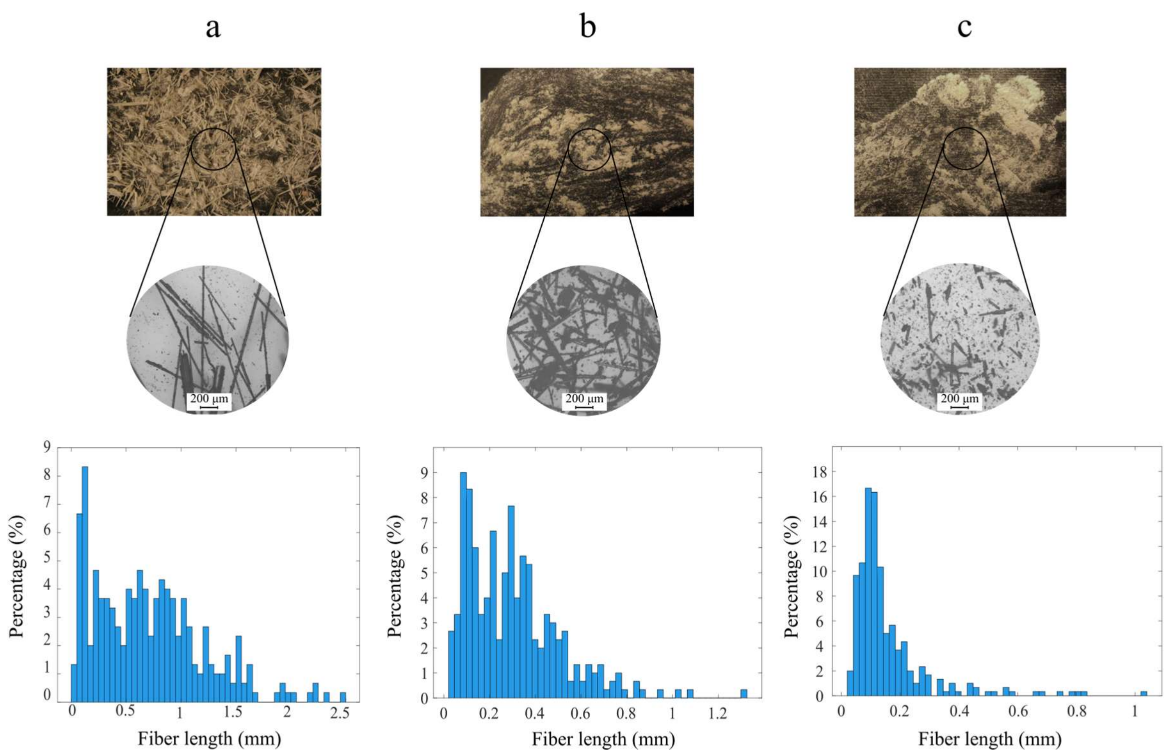

Figure 2-3: Probability distribution for fiber length of three grades of recycled fibers obtained from (a) grinding of blades; (b) first sieve operation; and (c) second sieve operation.

One of the main challenges that limits the use of the recycled fibers obtained from mechanical recycling, is traces of old resin, which might contribute to a weak interface between fibers and matrix. Wind turbine blades are generally made of glass fiber reinforced epoxy composites [36].

Figure 2-4 illustrates an example of the morphology of the recycled fibers. As seen, the epoxy residue still covers some parts of the surface of the fibers. The epoxy resin is characterised by the possession of more than one 1,2-epoxy groups per molecule, which are highly reactive with many substances, particularly those that are known as proton donors such as PLA [37]. This leads to the possibility of favorable interactions between functional groups of PLA and epoxy via hydrogen bonding. Such reactions allow for molecular chain extensions, which can improve the interfacial strength between the PLA and the recycled fibers without the need for expensive thermal or chemical treatment processes to remove the old resin. Further, the matrix residue on the surface of the fibers increases the fibers roughness, which could contribute to the mechanical interactions between the fibers and the PLA molecules.

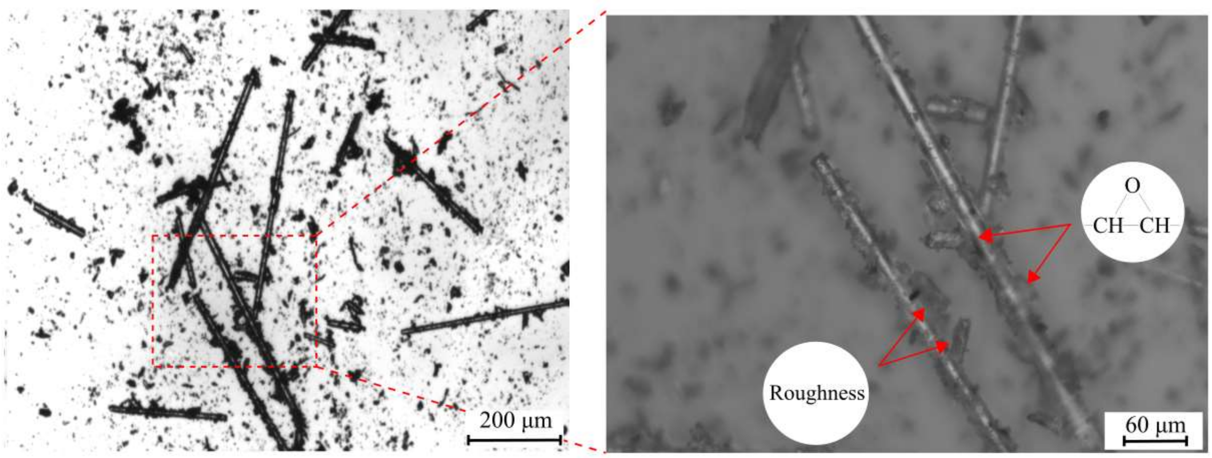

Figure 2-4: The residue of epoxy on the surface of the recycled fibers.

2.4.2 FFF 3D printing filaments

Figure 2-5 shows the pure PLA filament and RGFRF with 5% wt fiber content.

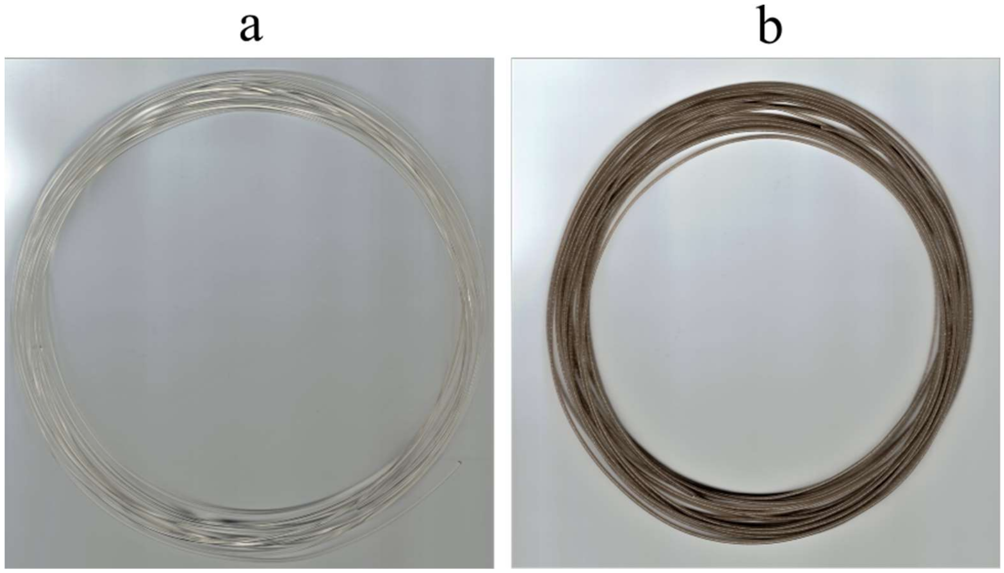

Figure 2-5: (a) The pure PLA filament; (b) the RGFRF with 5% fiber content.

A typical stress-strain curve for both the pure PLA filament and RGFRF, along with their tensile properties, are shown in Figure 2-6. The results demonstrate an increase of 10% in the Ultimate Tensile Strength (UTS) from 51.66 (σ = 0.58 and CV = 1.1%) to 56.63 (σ = 5.55 and CV = 9.8%) MPa and 16% in tensile modulus from 3.17 (σ = 0.1 and CV = 3.2%) to 3.6 (σ = 0.09 and CV = 2.5%) GPa for RGFRF relative to pure PLA filament. We recall that σ and CV represent the standard deviation and the coefficient of variation of the results, respectively. A larger variability is observed for the strength results of the reinforced composite filament, which could be ascribed to the diameter variations in the filament as well as, variations in the surface quality of the filament due to the presence of long fibers in the compound. On the other hand, the variability of the stiffness results for the composite filament is comparable to that of the pure PLA filament and all the samples showed higher stiffness relative to the pure PLA samples. The precise control of the filament diameter and carefully separating the fibers longer than the 3D printer nozzle diameter could result in lower variations in tensile strength.

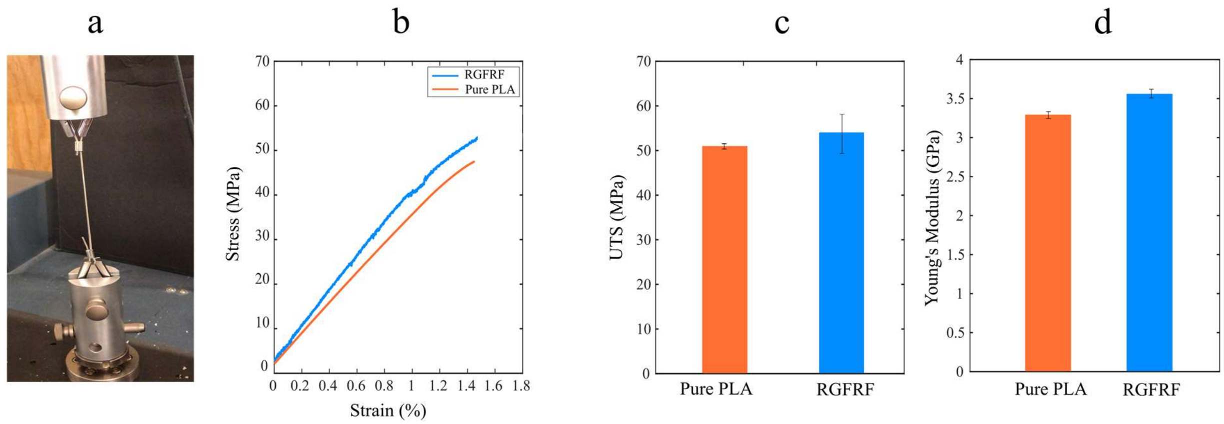

Figure 2-6: The tensile properties of the extruded pure PLA filament and reinforced filament: (a) test set-up; (b) stress-strain curve; (c) UTS; (d) Young's modulus.

The microstructures of the pure PLA filament and RGFRF along the transverse and longitudinal directions are shown in Figure 2-7. As it can be seen, the PLA filament shows smooth and round edges with no visible air bubbles, indicating the successful removal of the moisture content during the dehydration process. The RGFRF, on the other hand, contains relatively small internal voids that are distributed throughout the filament. The double extrusion process increases the likelihood of moisture absorption by the PLA and consequent air bubble formation probability during the extrusion process. As observed in the transverse cross section of RGFRF, glass fibers are visible in the reinforced filament and are well distributed throughout the cross section. The longitudinal cross section reveals that the fibers are generally well aligned in the directions of extrusion. This observation suggests that the RGFRF can be treated as a short glass fiber reinforced composite. Halpin-Tsai [38] has shown that the elastic modulus of short fiber reinforced composites along the fiber direction can be expressed as:

$$\frac{E_L}{E_m} = \frac{1 + (2l/d)\eta_L V_f}{1 - \eta_L V_f}, \tag{2-1}$$

$$\eta_L = \frac{E_f/E_m - 1}{\frac{E_f}{E_m} + 2(l/d)}, \tag{2-2}$$

where l represents fiber length, d is the fiber diameter, V_f is the volume fraction of the fibers, E_f is the elastic modulus of the fibers and E_m is the matrix modulus.

Based on the probability distribution analysis, the Young's modulus of RGFRF can be estimated assuming a uniform fiber length and fiber diameter of, respectively, 0.15 mm and 0.02 mm throughout the filament. The value of elastic stiffness for PLA and fiberglass is respectively 3.6 GPa and 72 GPa [39]. Therefore, the elastic stiffness of a short fiber reinforced composite with 5% wt fiber content can be predicted to be 4.3 GPa, which is larger than the average modulus observed for RGFRF. The discrepancy between the stiffness of RGFRF and the theoretical stiffness of short fiber reinforced composite can be attributed to the presence of voids, orientation of fibers within the filament structure, and variation in fiber length and filament diameter. The theoretical model of Halpin-Tsai indicates an elastic modulus 1.2 times greater than that of conventional PLA plastic. However, the average elastic modulus observed for the RGFRF is lower than the predicted stiffness, at approximately 1.14 times the average stiffness of the pure PLA filament.

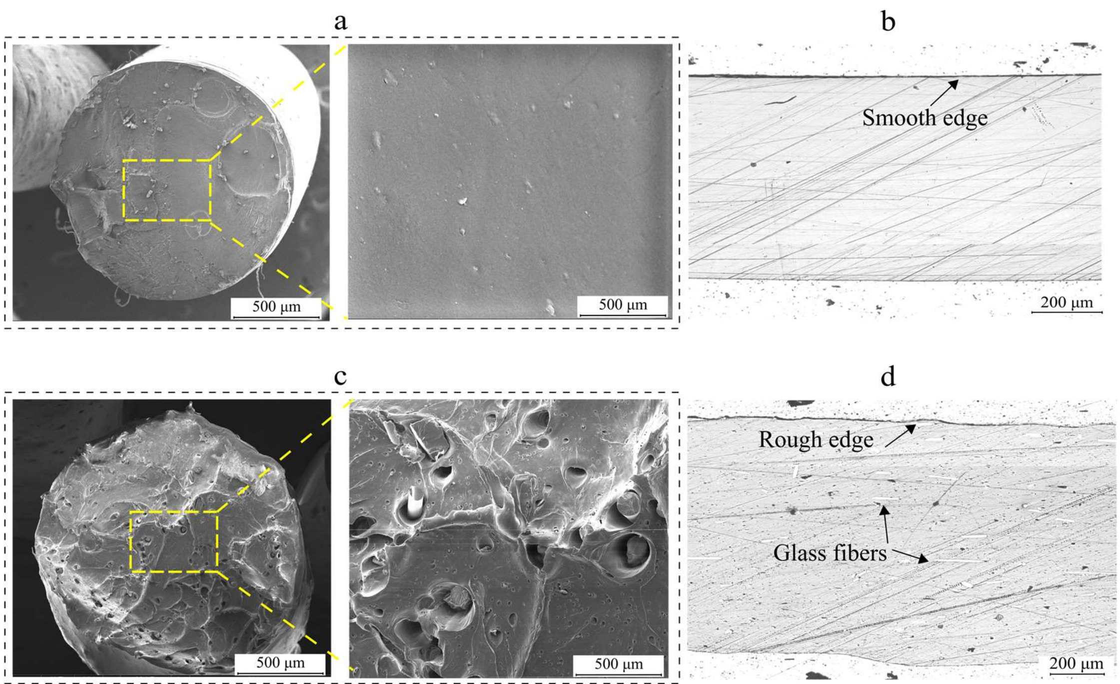

Figure 2-7: SEM images of pure PLA filament and RGFRF: (a) The transverse cross section of pure PLA filament; (b) the longitudinal cross section of pure PLA filament; (c) the transverse cross section of RGFRF; and (b) the longitudinal cross section of RGFRF.

The DSC curves shown in Figure 2-8 illustrate the heat flow versus the temperature scan of RGFRF and the pure PLA filament. The glass transition temperature of each filament is evaluated from the inflection point of the step transition using commercial software (TA Universal Analysis). The results are reported in Table 2-3. As seen, no significant change was observed in the glass transition temperature of RGFRF relative to the pure PLA baseline.

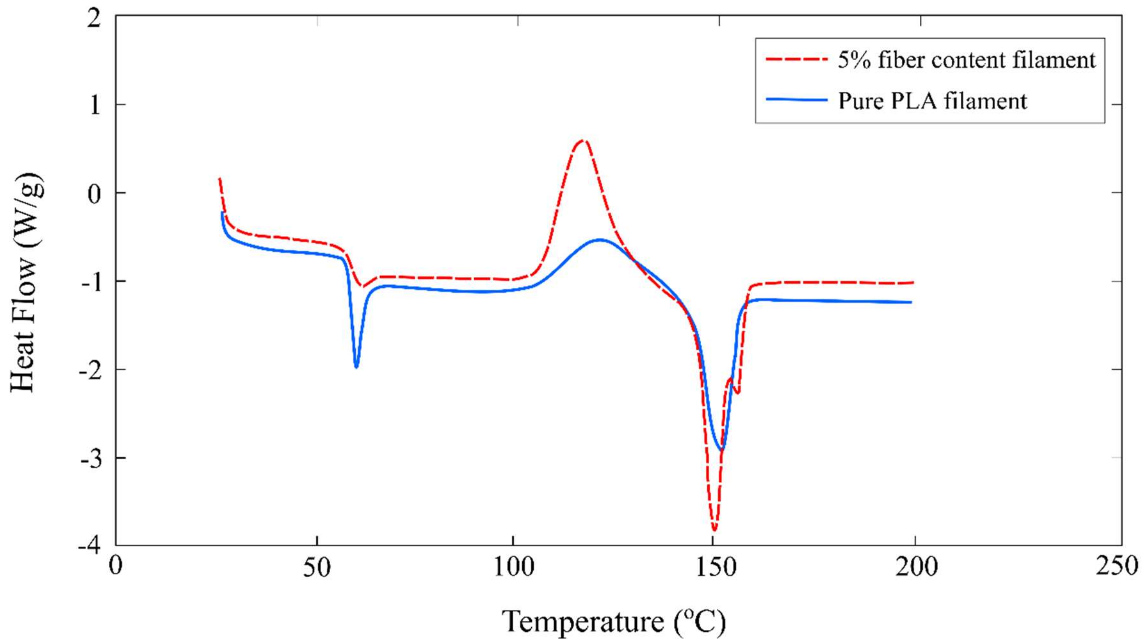

Figure 2-8: The DSC thermograms of the PLA filament and RGFRF.

To further investigate the effect of recycled glass fibers on the physical properties of the filament here introduced, we also computed its crystalline content and compared to that of the pure PLA baseline. The enthalpy of melt crystallisation represents the amount of crystalline content of a substance. As a result, the degree of crystallinity of a substance can be expressed as

$$\lambda_c = \frac{\Delta H_m - \Delta H_C}{\Delta H_f (1 - W_f)} \times 100, \tag{2-3}$$

where ΔH_m is the enthalpy of fusion, ΔH_C is the enthalpy of cold crystallisation, ΔH_f is the enthalpy of fusion of 100% crystalline PLA, which is selected to be 93.1 J/g [40], and W_f is the weight fraction of fibers in the polymer. Although low degree of crystallinity was observed for both samples, we observed that the reinforced filament is less amorphous as compared to pure PLA filament. The higher crystallinity of the reinforced filament could contribute to higher stiffness and lower degradation rate.

Table 2-3: The glass transition temperature and crystallinity of the pure PLA filament and RGFRF.

Specimen	T_g (°C)	T_m (°C)	$\Delta H_c\ (J/g)$	$\Delta H_m\ (J/g)$	λ_c (%)
Pure PLA	57.2	150.7	15.84	18.11	2.4
RGFRF	57.87	151.5	24.31	26.74	2.7

Another dominating property in the processability and performance of 3D printing filaments is the melt flow index, which is inversely proportional to viscosity. The viscosity of the RGFRF is evaluated by a rheometer (AR2000, TA instruments, USA) using a plate-plate configuration at 210 °C for shear rates ranging 0.01-10 1/s. The temperature used for the viscosity evaluation represents the temperature used in the 3D printing process. As illustrated in Figure 2-9, the results demonstrate a higher viscosity for the reinforced filament at low shear rates. However, as the shear rate increases, the links between the fibers and the PLA molecules break, leading to lower viscosity. This suggests that at the shear rates used in the 3D printing process, the effect of fiberglass on the rheological properties of the filament is minimal and negligible.

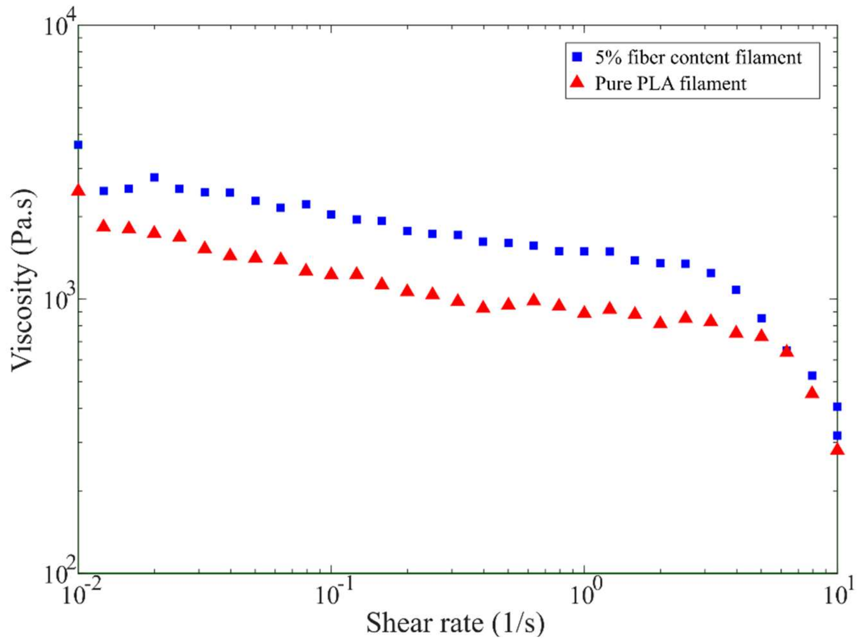

Figure 2-9: Rheological curves of the pure PLA filament and RGFRF.

2.4.3 FFF 3D printed coupons

The FFF 3D printed tensile test specimens are shown in Figure 2-10. The tensile test coupons are comprised of 24 layers with a unidirectional bead orientation.

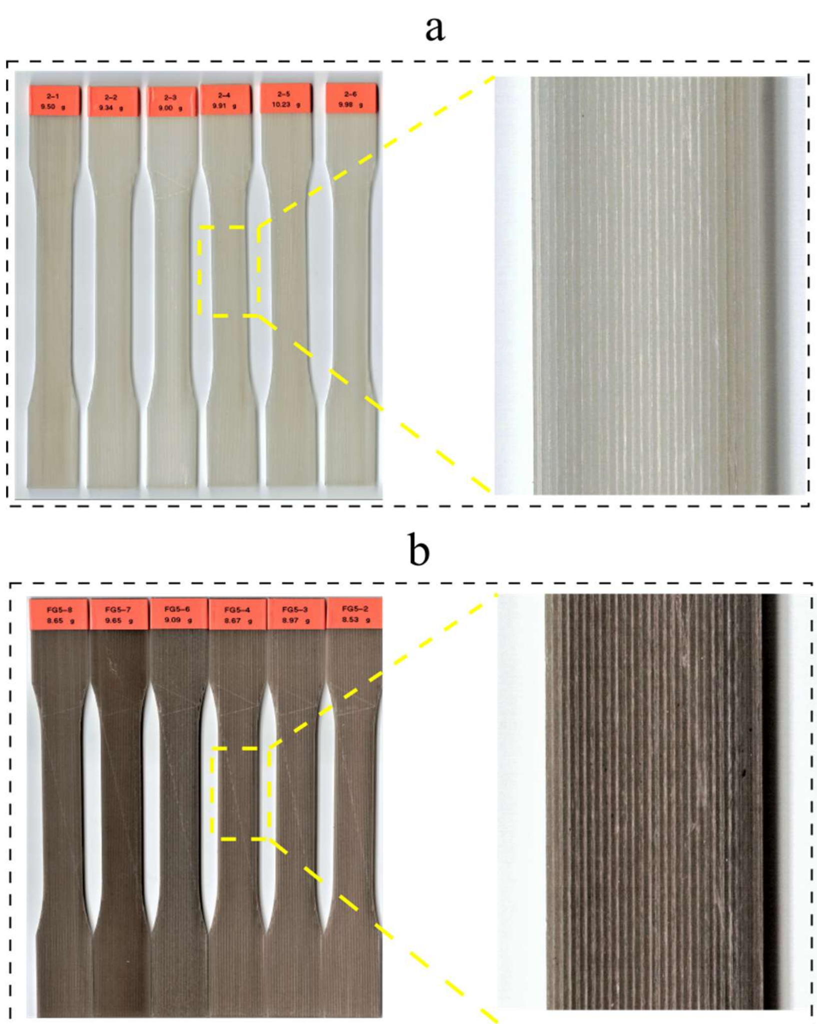

Figure 2-10: (a) the pure PLA tensile test coupons with unidirectional bead orientation; (b) the reinforced coupons with unidirectional bead orientation.

Figure 2-11 shows the representative engineering stress-strain curves for the tensile test samples. Due to diameter variations in the RGFRF, lower density values with respect to pure PLA samples were observed for the composite samples. To compensate for this, the UTS results of the composite samples are scaled-up with respect to the density of pure PLA specimens. It was observed that the 3D printed composite samples feature a Young's modulus enhanced by about 8% from 3.12 (σ = 0.15 and CV = 4.8%) to 3.35 (σ = 0.12 and CV = 3.6%) GPa compared with pure PLA specimens, while there was no meaningful increase in UTS. The elastic stiffness of the 3D printed specimens is slightly lower compared to the individual filaments, e.g. 1.5% and 7% reduction for pure PLA and composite coupons, respectively. The discrepancy between the filaments and the coupons could be attributed to the 3D printing process that introduces some defects and higher quantity of large voids, e.g. interlayer voids, within the samples [2, 41, 42]. As observed in Figure 2-12, while a brittle failure plane normal to the load axis was observed in pure PLA samples, the composite specimens failed due to interlayer delamination and debonding of adjacent beads. This could be due to the presence of voids distributed throughout the long axis of the reinforced coupons, which causes the failure to evolve with the propagation of cracks along the beads. Such porosity distribution may be the cause of the low ultimate strength for the composite specimens. Moreover, this type of failure highlights the fiber bridging phenomena, which directs the crack propagation in the longitudinal direction.

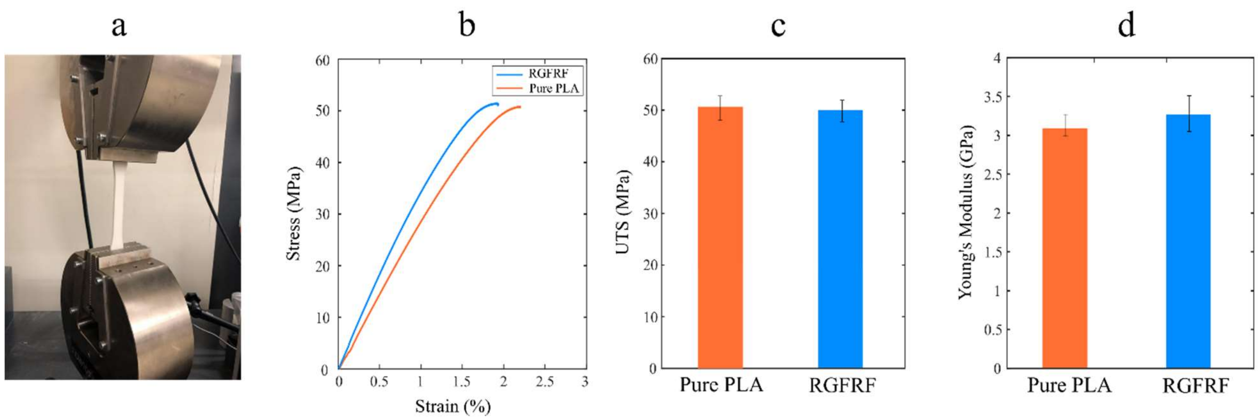

Figure 2-11: The tensile properties of the pure PLA and composite tensile test specimens: (a) test set-up; (b) stress-strain curve; (c) UTS; (d) Young's modulus.

To explore the porosity of the coupons, SEM images from the fracture surface of the pure PLA and reinforced specimens are examined. As seen in Figure 2-13, the reinforced samples feature larger internal voids, which are likely a result of nozzle clogging due to the presence of fibers with larger length compared to the nozzle diameter. The presence of ruptured fibers demonstrates an effective load transfer capacity between the PLA matrix and the recycled fibers. The SEM images show that some fibers have been pulled out of the PLA due to insufficient interfacial strength. This could be attributed to the variation of the epoxy residue on the fibers surface, which lowers the possibility of the molecular interactions and thus hydrogen bonding at the interface of the pulled-out fibers and PLA.

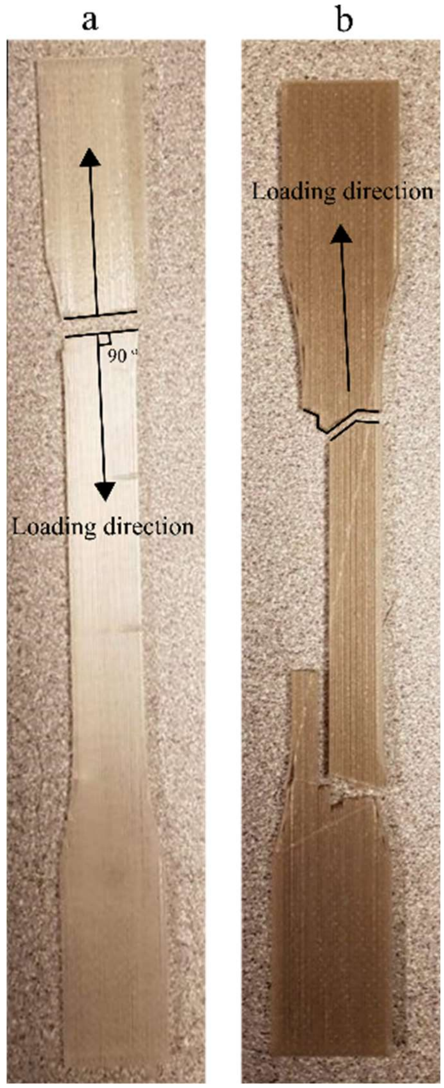

Figure 2-12: Failed samples: (a) pure PLA, and (b) recycled glass fiber reinforced PLA.

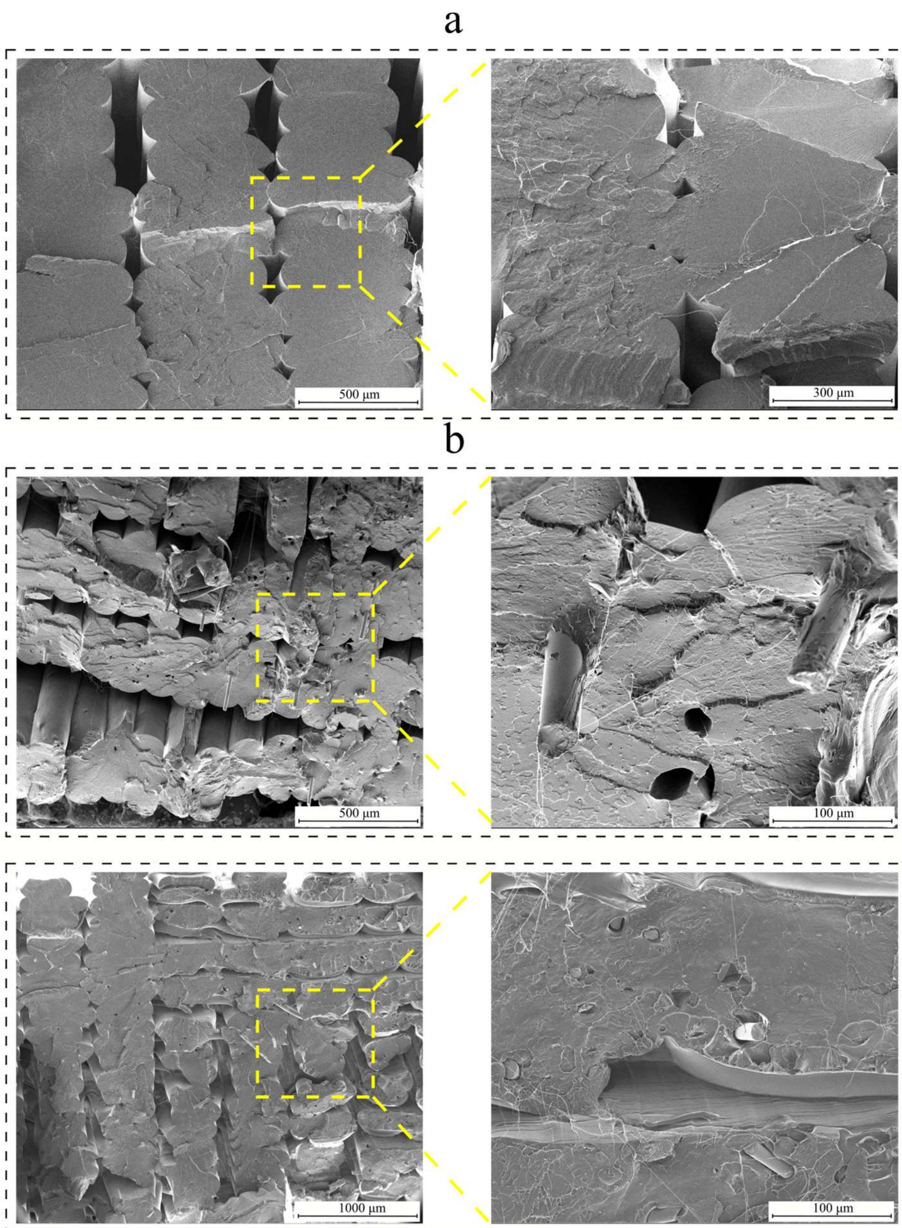

Figure 2-13: The fracture surface SEM of the 3D printed specimens: (a) pure PLA; and (b) with recycled glass fibers.

2.5 Conclusion

This study describes and validates a methodology integrating mechanical recycling and FFF 3D printing as a potential solution to the problem of composite waste from wind turbine blades. The scrap turbine blades are first ground and sieved to obtain processable recycled glass fibers for application in 3D printing. The ground fibers are then mixed with PLA, a biodegradable polymer, to extrude glass fiber reinforced filament. To demonstrate the mechanical performance of the newly developed filament, tensile test specimens with 5 wt% fiber content are fabricated and the effect on tensile properties, namely Young's modulus and tensile strength, are studied. The reinforced filament features a glass transition temperature comparable to that of pure PLA filament. However, a slight increase in the crystallinity of the reinforced filament is observed with respect to pure PLA filament. The results show that the addition of 5 wt% recycled fibers leads to an increase of 16% and 10% in the Young's modulus and strength of the pure PLA filament, respectively. Considering variability in tensile strength results, further experimental studies and larger sample sizes are required to validate potential improvements in strength.

Mechanical tests on FFF fabricated coupons demonstrate an increase of 8% in the Young's modulus relative to pure PLA samples, while there is no significant improvement in tensile strength. This level of performance would translate in the potential of application of recycled glass fibers from wind turbine blades into the 3D printing industry. SEM micrographs from the fracture surface of FFF composite samples show the presence of ruptured fibers confirming an effective load transfer between the PLA matrix and the recycled fibers. To better understand the interfacial strength between the recycled fibers and the thermoplastic matrix, further study is required to compare the interface of PLA with virgin and recycled fibers. Another aspect that requires further investigation is the effect of fiber content on the interfacial bonding and the mechanical properties of the 3D printed samples.

2.6 Acknowledgements

The authors would like to acknowledge the financial support provided by the following: Research Center for High Performance Polymer and Composite Systems (CREPEC), Projet Vision; and The Natural Sciences and Engineering Research Council of Canada (NSERC), RGPIN-2018-04144. We also would like to acknowledge Dr. Ebrahim Jalili and Professor Abdellah Ajji at Ecole Polytechnique de Montreal, for their consultation and technical support.

2.7 References

[1] Yang Y, Boom R, Irion B, van Heerden D-J, Kuiper P, de Wit H. Recycling of composite materials. Chemical Engineering and Processing: Process Intensification. 2012;51:53-68.

[2] Tian X, Liu T, Yang C, Wang Q, Li D. Interface and performance of 3D printed continuous carbon fiber reinforced PLA composites. Composites Part A: Applied Science and Manufacturing. 2016;88:198-205.

[3] Advani S, Hsiao K-T. Introduction to composites and manufacturing processes. Manufacturing Techniques for Polymer Matrix Composites (PMCs): Elsevier; 2012. p. 1-12.

[4] Campbell Jr FC. Manufacturing processes for advanced composites: Elsevier; 2003.

[5] Albers H, Greiner S, Seifert H, Kühne U. Recycling of wind turbine rotor blades–fact or fiction. DEWI Mag. 2009;34:32-41.

[6] Larsen K. Recycling wind turbine blades. Renewable energy focus. 2009;9(7):70-3.

[7] Job S. Recycling glass fibre reinforced composites–history and progress. Reinforced Plastics. 2013;57(5):19-23.

[8] Cherrington R, Goodship V, Meredith J, Wood BM, Coles SR, Vuillaume A, et al. Producer responsibility: Defining the incentive for recycling composite wind turbine blades in Europe. Energy Policy. 2012;47:13-21.

[9] Palmer J, Ghita OR, Savage L, Evans KE. Successful closed-loop recycling of thermoset composites. Composites Part A: Applied Science and Manufacturing. 2009;40(4):490-8.

[10] Oliveux G, Dandy LO, Leeke GA. Current status of recycling of fibre reinforced polymers: Review of technologies, reuse and resulting properties. Progress in Materials Science. 2015;72:61-99.

[11] MARTIN SA. Comparison of hammermill and roller mill grinding and the effect of grain particle size on mixing and pelleting.: Master's thesis, Kansas State University; 1981.

[12] Group SM. Recycling of waste glass fiber reinforced plastic with microwave pyrolysis (LIFE07 ENV/S/000904). Stena recycling, Göteborg, Sweden2012.

[13] Yang C, Tian X, Liu T, Cao Y, Li D. 3D printing for continuous fiber reinforced thermoplastic composites: mechanism and performance. Rapid Prototyping Journal. 2017;23(1):209-15.

[14] Greco A, Maffezzoli A. Rotational molding of biodegradable composites obtained with PLA reinforced by the wooden backbone of opuntia ficus indica cladodes. Journal of Applied Polymer Science. 2015;132(48).

[15] Gray IV RW, Baird DG, Helge Bøhn J. Effects of processing conditions on short TLCP fiber reinforced FDM parts. Rapid Prototyping Journal. 1998;4(1):14-25.

[16] Gray IV RW, Baird DG, Bøhn JH. Thermoplastic composites reinforced with long fiber thermotropic liquid crystalline polymers for fused deposition modeling. Polymer composites. 1998;19(4):383-94.

[17] Mueller B. Additive manufacturing technologies–Rapid prototyping to direct digital manufacturing. Assembly Automation. 2012;32(2).

[18] Wong KV, Hernandez A. A review of additive manufacturing. ISRN Mechanical Engineering. 2012;2012, 208760.

[19] Stampfl J, Hatzenbichler M. Additive manufacturing technologies. CIRP Encyclopedia of Production Engineering: Springer; 2014. p. 20-7.

[20] Horn TJ, Harrysson OL. Overview of current additive manufacturing technologies and selected applications. Science progress. 2012;95(3):255-82.

[21] Ning F, Cong W, Qiu J, Wei J, Wang S. Additive manufacturing of carbon fiber reinforced thermoplastic composites using fused deposition modeling. Composites Part B: Engineering. 2015;80:369-78.

[22] Dudek P. FDM 3D printing technology in manufacturing composite elements. Archives of Metallurgy and Materials. 2013;58(4):1415-8.

[23] Tekinalp HL, Kunc V, Velez-Garcia GM, Duty CE, Love LJ, Naskar AK, et al. Highly oriented carbon fiber–polymer composites via additive manufacturing. Composites Science and Technology. 2014;105:144-50.

[24] Novakova-Marcincinova L, Novak-Marcincin J, Barna J, Torok J. Special materials used in FDM rapid prototyping technology application. Intelligent Engineering Systems (INES), 2012 IEEE 16th International Conference on: IEEE; 2012. p. 73-6.

[25] Turner BN, Gold SA. A review of melt extrusion additive manufacturing processes: II. Materials, dimensional accuracy, and surface roughness. Rapid Prototyping Journal. 2015;21(3):250-61.

[26] N. Turner B, Strong R, A. Gold S. A review of melt extrusion additive manufacturing processes: I. Process design and modeling. Rapid Prototyping Journal. 2014;20(3):192-204.

[27] Esposito Corcione C, Gervaso F, Scalera F, Montagna F, Sannino A, Maffezzoli A. The feasibility of printing polylactic acid–nanohydroxyapatite composites using a low-cost fused deposition modeling 3D printer. Journal of Applied Polymer Science. 2017;134(13).

[28] Kuo C-C, Liu L-C, Teng W-F, Chang H-Y, Chien F-M, Liao S-J, et al. Preparation of starch/acrylonitrile-butadiene-styrene copolymers (ABS) biomass alloys and their feasible evaluation for 3D printing applications. Composites Part B: Engineering. 2016;86:36-9.

[29] Nikzad M, Masood S, Sbarski I. Thermo-mechanical properties of a highly filled polymeric composites for fused deposition modeling. Materials & Design. 2011;32(6):3448-56.

[30] Shofner M, Lozano K, Rodríguez-Macías F, Barrera E. Nanofiber-reinforced polymers prepared by fused deposition modeling. Journal of applied polymer science. 2003;89(11):3081-90.

[31] Zhong W, Li F, Zhang Z, Song L, Li Z. Short fiber reinforced composites for fused deposition modeling. Materials Science and Engineering: A. 2001;301(2):125-30.

[32] Stoof D, Pickering K. Sustainable composite fused deposition modelling filament using recycled pre-consumer polypropylene. Composites Part B: Engineering. 2018;135:110-8.

[33] Corcione CE, Palumbo E, Masciullo A, Montagna F, Torricelli MC. Fused Deposition Modeling (FDM): An innovative technique aimed at reusing Lecce stone waste for industrial design and building applications. Construction and Building Materials. 2018;158:276-84.

[34] Singh S, Singh R. Experimental investigations for use of nylon6 industrial waste as FDM feedstock filament for investment casting applications. 2016.

[35] NatureWorks. Crystallizing and Drying Ingeo Biopolymer.

[36] Mishnaevsky L, Branner K, Petersen HN, Beauson J, McGugan M, Sorensen BF. Materials for Wind Turbine Blades: An Overview. Materials (Basel, Switzerland). 2017;10(11).

[37] Brydson JA. 26 - Epoxide Resins. In: Brydson JA, editor. Plastics Materials (Seventh Edition). Oxford: Butterworth-Heinemann; 1999. p. 744-77.

[38] Sung N. Analysis and performance of fiber composites, Second Ed., by Bhagwan D. Agarwal and Lawrence J. Broutman, Wiley, New York, 1990, 449 pp. Price: $59.95. Journal of Polymer Science Part A: Polymer Chemistry. 1991;29(12):1835-.

[39] NatureWorks. Ingeo™ Biopolymer 4043D Technical Data Sheet, 3D Printing Monofilament – General Purpose Grade.

[40] Ivey M, Melenka GW, Carey JP, Ayranci C. Characterizing short-fiber-reinforced composites produced using additive manufacturing. Advanced Manufacturing: Polymer & Composites Science. 2017;3(3):81-91.

[41] Gunaydin K, S. Türkmen H. Common FDM 3D Printing Defects2018.

[42] Calvert P. Freeform Fabrication. In: Buschow KHJ, Cahn RW, Flemings MC, Ilschner B, Kramer EJ, Mahajan S, et al., editors. Encyclopedia of Materials: Science and Technology. Oxford: Elsevier; 2001. p. 3340-7.

Link between Chapter 2 and Chapter 3

The previous chapter examined the viability of using recovered glass fibers from used wind turbine blades in FFF feedstock. Filaments with one specific fiber content, namely 5 wt% was manufactured. The thermal, as well as the mechanical performance of the newly developed filament was examined. In the next chapter, the effect of fiber content on the mechanical behavior of additively manufactured recycled parts will be studied. Therein, the interface developed between the recycled fibers and the new polymer will be also investigated and compared with virgin glass fibers.

Chapter 3

Recycled glass fiber composites from wind turbine waste for 3D printing feedstock: effects of fiber content and interface on mechanical performance

3 Chapter 3: Recycled glass fiber composites from wind turbine waste for 3D printing feedstock: effects of fiber content and interface on mechanical performance

Amirmohammad Rahimizadeh[1], Jordan Kalman[2], Rodolphe Henri[3], Kazem Fayazbakhsh[4,*], Larry Lessard[5]

[1] Department of Mechanical Engineering, McGill University, Montreal, QC H3A0C3, Canada; amirmohammad.rahimizadeh@mail.mcgill.ca

[2] Department of Aerospace Engineering, Ryerson University, Toronto, Ontario M5B2K3, Canada; jkalman@ryerson.ca

[3] Institute of Materials (IMX), Ecole Polytechnique Fédérale de Lausanne (EPFL), Lausanne CH-1015, Switzerland; rodolphe.henri@epfl.ch

[4] Department of Aerospace Engineering, Ryerson University, Toronto, Ontario M5B2K3, Canada; kazem@ryerson.ca

[5] Department of Mechanical Engineering, McGill University, Montreal, QC H3A0C3, Canada; larry.lessard@mcgill.ca

*Corresponding author: kazem@ryerson.ca; Tel: (+1) 416-979-5000 ext. 6414; fax: (+1) 416-979-5056

Journal of Materials, 12 (23), 3929

3.1 Abstract

This research validates the viability of a recycling and reusing process for end-of-life glass fiber reinforced wind turbine blades. Short glass fibers from scrap turbine blades are reclaimed and mixed with polylactic acid (PLA) through a double extrusion process to produce composite feedstock with recycled glass fibers for fused filament fabrication (FFF) 3D printing. Reinforced filaments with different fiber contents, as high as 25% by weight, are extruded and used to 3D print tensile specimens per ASTM D638-14. For 25 wt% reinforcement, the samples showed up to 74% increase in specific stiffness compared to pure PLA samples, while there was a reduction of 42 % and 65 % in specific tensile strength and failure strain, respectively. To capture the level of impregnation of the non-pyrolyzed recycled fibers and PLA, samples made from reinforced filaments with virgin and recycled fibers are fabricated and assessed in terms of mechanical properties and interface. For the composite specimens out of reinforced PLA with recycled glass fibers, it was found that the specific modulus and tensile strength are respectively 18% and 19% higher than those of samples reinforced with virgin glass fibers. The cause for this observation is mainly attributed to the fact that the surface of recycled fibers is partially covered with epoxy particles, a phenomenon that allows for favorable interactions between the molecules of PLA and epoxy, thus improving the interface bonding between the fibers and PLA.

Keywords: Wind turbine blades; Polylactic acid; Glass fiber; Fused filament fabrication; 3D printing.

3.2 Introduction

The extensive disposal of composite products is leading to undesirable environmental impacts due to their high organic content such as resin and wood [1, 2]. Recent reports have revealed that the total global production of composites has exceeded 10 million tones per year, which at end of life, will require over 5 million cubic meters for disposal [3]. Among composite materials, the superior mechanical properties of glass fiber reinforced polymers (GFRP) combined with low cost, have made them an attractive alternative for solid materials, resulting in 90% use in all of composites currently produced [4]. Aircraft, automotive parts, pipes, and sports equipment are some examples of application sectors for GFRPs [5, 6]. Among GFRP products, wind turbine rotor blades serve as one of the major application sectors of GFRPs, which has undergone a significant growth since the year 2000 [7-9]. A wind turbine blade generally consists of two glass fiber composite shells, which are adhesively bonded together. Also, they typically contain a core material, e.g. balsa wood or foam, which is used in some sections of the blade with the aim of reducing the production cost. The accelerating growth of wind energy, which translates to a production of 6 million tons of GFRP over the coming decade, has highlighted the issue of composite recycling. Although current disposal methods such as incineration or landfill offer simple and low-cost solutions for the blade waste disposal, the rapidly increasing cost, imminent recycling legislation, as well as the lower availability of landfill sites, have made such disposal techniques economically and socially unacceptable [10-13]. Many countries are now increasing landfill taxes to steer the industry into finding new solutions [14]. Nevertheless, several thermal and chemical techniques are offered in the literature for the recycling of thermoset GFRPs [2, 15]. However, these methods are generally associated with a substantial loss in the mechanical properties of the recovered fibers as compared to virgin first-pass materials [16, 17]. In addition, their inability to handle large quantities of waste highly limits their applicability.

Currently, mechanical grinding is considered as the only recycling technique with commercialization potential [18]. This method was first introduced in 1990s and involves the breakdown of composites by shredding, milling, grinding or other size reduction processes. The aim of this technique is to reduce the size of the scrap composites and reincorporate them as reinforcement or filler into new composite structures. Since mechanical grinding is not associated with any atmospheric pollution, this technique offers significant environmental and economical advantages over the other available recycling processes. In addition, this process benefits from the abrasive nature of glass fibers to efficiently reduce the size of GFRP composite wastes [19]. The performance and functionality of this method has been the focus of a significant number of studies in the literature [20, 21]. For instance, Palmer et al. [22] used a TRIA screen-classifier type hammer mill to recover glass fibers from automotive front fenders. They validated the applicability of a novel zig-zag air separator method to obtain fine glass fibers featuring mechanical properties comparable to virgin fibers. In another study, three grades of granulated recyclate from sheet moulding compound waste with different fiber sizes were obtained and used in bulk moulding compound (BMC) manufacturing to replace the virgin reinforcements [18]. The new BMC formulations showed reduced mechanical properties, particularly in flexural strength. This observation was ascribed to possible fiber damage, and poor interfacial bonding between the fibers and the new resin polymer.

While mechanical grinding has been known as an effective and efficient recycling technique, it is strictly highlighted in the literature that the viability of this method relies on the careful separation of characterized fibers with length comparable to virgin fibers [18]. As a result, short fiber reinforced composites could be deemed as a superior potential application for mechanically recycled composites. One of the recent application sectors for short fiber composite materials, which is growing fast, is additive manufacturing (AM). Benefiting from a layer upon layer manufacturing technique, AM provides an exciting opportunity for rapid fabrication of parts with complex geometry [23-25]. Recently, a new class of 3D printing filaments integrating reinforcement materials namely, short and continuous fibers, with pure thermoplastic polymers to improve their mechanical performance, has been introduced [26-30]. Zhong et al. [27] exploited the effect of short glass fibers on the mechanical properties of acrylonitrile butadiene styrene (ABS) fabricated parts. They presented composite filaments with three distinct fiber contents, which could enhance the surface rigidity and tensile strength of the traditional pure ABS filaments. Papon et al. [31] showed that the addition of short carbon fibers into neat PLA can improve the fracture properties of 3D printed parts. In another study, continuous carbon fiber bundles were used to reinforce 3D printed polycarbonate parts. The results from this study demonstrated a substantial increase of, respectively, 77 % and 85 % in the tensile yield strength and modulus of elasticity of parts printed with three fiber bundles [30]. The latest advances in the AM technology include efforts to improve the sustainability of this widespread manufacturing process via the use of recycled materials. For instance, an optimized fused particle fabrication method has been recently developed, which allows for reusing recycled polymers to manufacture 3D printed parts with properties comparable to those of virgin components [32, 33]. More recently, Rahimizadeh et al. [34] validated a recycling process to reclaim short glass fibers from scrap rotor blades for use in 3D printing. The results from this study showed that the stiffness and strength of the reinforced filament are improved by 16 % and 8 %, respectively. As well, an improvement of 8 % was reported for the stiffness of the composite samples made of recovered fibers. While interesting, in this study, the effect of the resin residue on the interface bonding developed between the recycled fibers and the new resin system, as well as the influence of fiber content on the properties of the recycled composites were not studied.

The aim of the current investigation is twofold: (i) to experimentally examine the effect of the recycled fibers extracted from rotor blades wastes on the tensile properties of FFF fabricated specimens. Filaments with varying fiber content are extruded and used to fabricate tensile test specimens as per ASTM D638-14. The effect of the fiber content on the mechanical properties and porosity of the FFF 3D printed samples is evaluated (ii) to investigate the impregnation of the recycled fibers and PLA. 3D printing filaments containing recycled glass fibers and virgin glass fibers with silane coating are produced and used to fabricate tensile test specimens. Fracture interface of these are then observed using scanning electron microscopy (SEM) to analyze the interfacial strength between the fibers and resin. At the end, the closing remarks and routes for future studies are discussed.

3.3 Materials and Methods

In section 3.3.1, we first explain the recycling and manufacturing process developed to obtain recycled glass fiber reinforced filament. The steps include mechanical recycling, pelletizing and filament extrusion. Section 3.3.2 details the fabrication process of additively manufactured recycled tensile test specimens as per ASTM D638.

3.3.1 Recycling and Extrusion Procedure

Figure 3-1 shows the recycling scheme, which is used to extract the glass fibers from wind turbine blades. Mechanical grinding of the end of life turbine blades is used to extract the reinforcement fibers from the blades. In this process, the scrap blades are first cut into 20×20 cm pieces and fed into a hammer mill grinder (ECO-WOLF, INC.) equipped with a 3 mm classifier screen. As can be observed in Figure 3-1b, only sections made of pure fiberglass composites are used in this study. As a result, the recyclate compound obtained after the grinding process is not isolated glass fibers, rather a mixture of glass fibers and particles of resin.

Since the presence of fibers longer than the 3D printer nozzle diameter can lead to nozzle clogging and jamming, we resort to a double sieving operation to separate off the fibers with length above 0.4 mm. As a result, the recycled materials are classified through an 8" ASTM stainless-steel sieve with a mesh size of 140. Following this process, the sieved material is further classified through another sieving operation to obtain better refined fibers in the desirable length range. Although efficient and simple, sieving mechanism is generally associated with the possibility of contamination with longer fibers as the high aspect ratio fibers might fall through the sieve meshes.

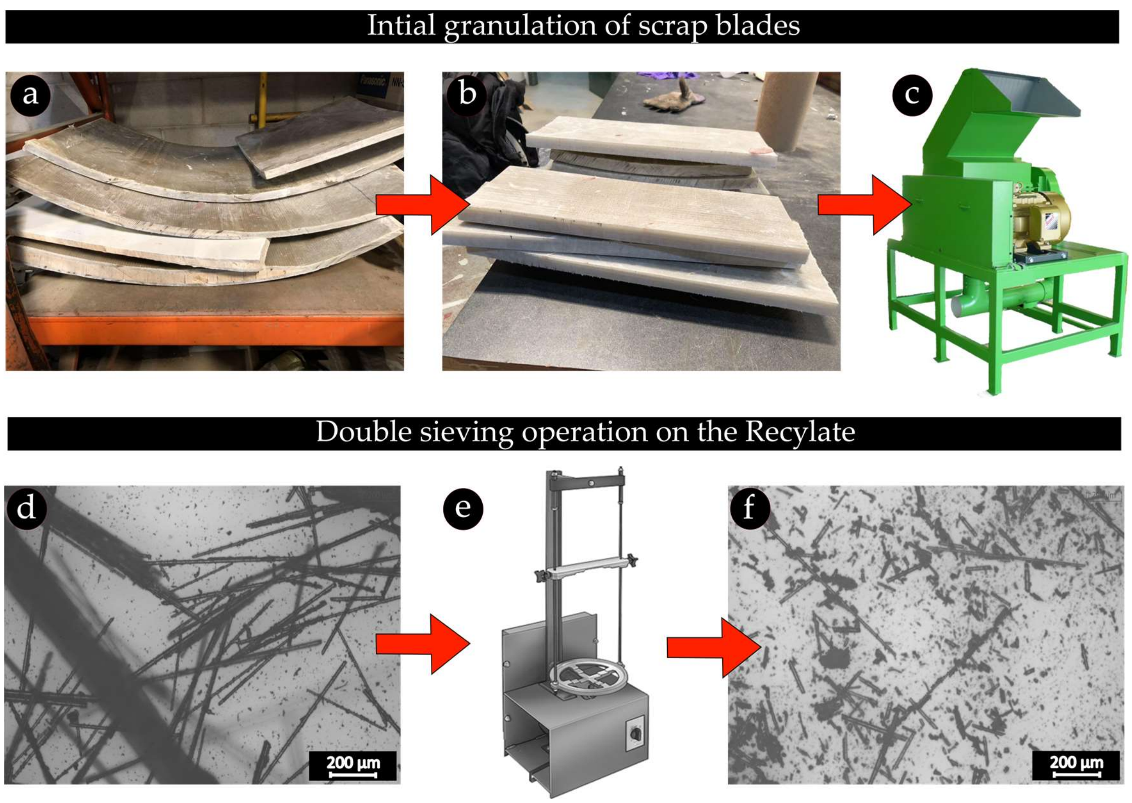

Figure 3-1: The recycling process to obtain glass fibers processable for FFF 3D printing: (a) scrap wind turbine blades; (b) 20 × 20 cm pieces of the scrap blades; (c) hammer mill grinder used to grind the pieces; (d) ground recyclate obtained after the initial granulation of the blade pieces; (e) double sieving operation on the ground recycled materials; (f) the last grade of the recyclate obtained after the second sieve operation.

To characterize the recycled materials, in particular the epoxy residue content, thermogravimetric analysis (TGA) is performed. TGA is conducted in order to assess the amount of retained matrix residue inside the recyclate. Samples weighing 7 mg are extracted from the initial and last grade of the recyclate and loaded into a TGA System (Q500, TA Instruments, USA). A heating program in the range of 20–800 °C with a heating rate of 10 °C/min is then used to decompose the resin powder. The TGA is performed in the presence of nitrogen followed by an oxidative stage such that no ash content is left on the surface of the fibers. One crucial factor contributing to the performance and processability of short fiber reinforced 3D printing filaments, is the fiber distribution. To homogeneously distribute the fibers within PLA, as shown in Figure 3-2, we resort to a double extrusion process where the recycled materials are first mixed with virgin PLA pellets (Ingeo 4043D, Natureworks LLC, Blair, Nebraska) and fed into a twin-screw extruder (Leistritz ZSE18HP-40D, Nuremberg, Germany) with 8 subzones. Using a pelletizer, the produced composite filament is then chopped up into small pellets featuring different fiber contents including 5 wt%, 10 wt%, 15 wt%, 20 wt% and 25 wt%. It should be recalled that the reclaimed recyclate materials with *no prior pyrolysis* are directly used in this pelletization process.

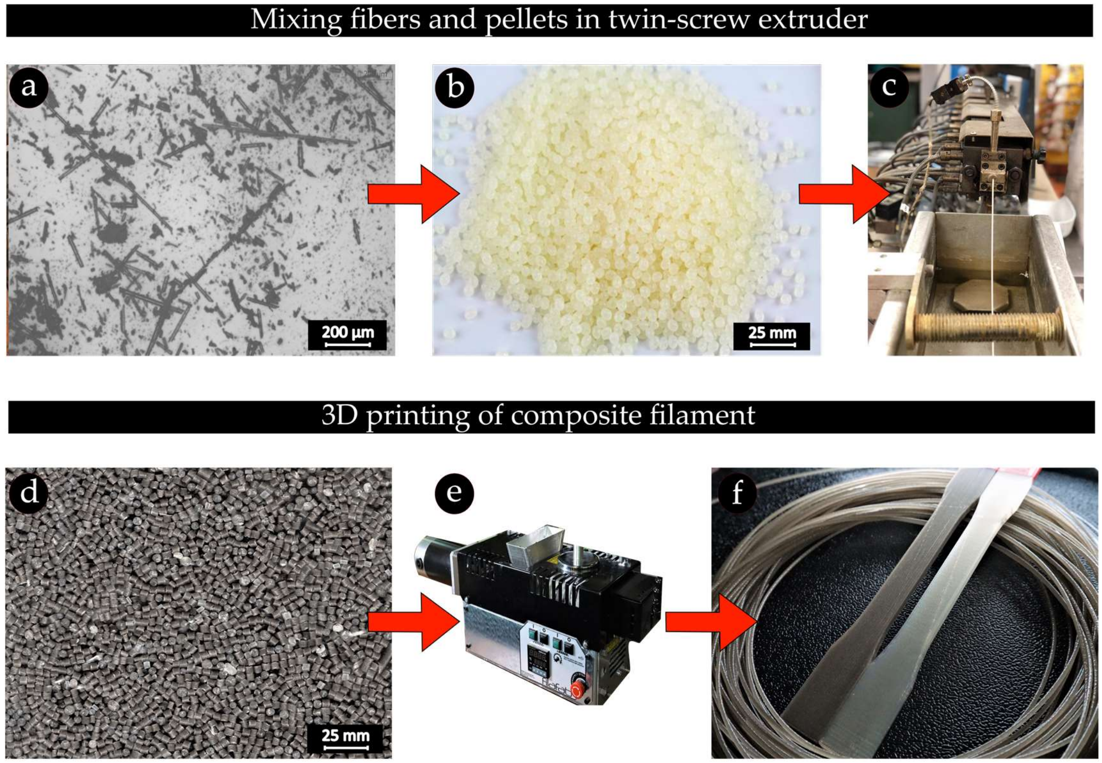

Figure 3-2: The double extrusion process to obtain 3D printing composite filament: (a) the last grade of the recyclate; (b) PLA pellets; (c) palettization process with a twin-screw extruder; (d) the glass fiber reinforced pellets; (e) single screw filament extruder; (f) the recycled glass fiber reinforced filaments and composite tensile test specimens.

Subsequently, the composite pellets are fed into a single screw extruder (FilaFab, D3D Innovations Limited, Bristol, UK) to obtain composite filaments with different fiber contents. Using an air-cooling system, the filament is cooled down immediately after the extrusion and its diameter is consistently monitored through a laser micrometer with ±2 µm accuracy. To minimize the possible diameter variations throughout the filament, a spool winder machine is utilized and the extrusion parameters including the die temperature, speed of the winder, as well as the screw speed are well adjusted to attain a 1.75 ± 0.05 mm filament. This range of variation represents an acceptable tolerance and diameter for the FFF process. The temperature profiles used in the extrusion processes are obtained through a trial and error method on the standard parameters recommended by the material supplier. These parameters are optimized to produce filaments with acceptable surface quality and no degradation in the polymer [35]. Table 3-1 shows all the process parameters used during the first and the second extrusion.

Table 3-1: The extrusion parameters for the single-screw and twin-screw extruders.

Initial extrusion	Screw speed (rpm)	90
	Subzone 1-2 (Temp °C)	190
	Subzone 3 (Temp °C)	185
	Subzone 4 (Temp °C)	180
	Subzone 5 (Temp °C)	175
	Subzone 6-8 (Temp °C)	170
Second extrusion	Screw speed (rpm)	25
	Die temperature (Temp °C)	210
	Winder speed (rpm)	1

3.3.2 Characterization of Material Properties

Tensile test samples in accordance with the ASTM D638 Type I specimen geometry and dimensions are manufactured and used to evaluate the mechanical performance of the recycled composite parts. Samples with a total thickness of 3.36 mm and a stacking sequence of $[0]_{24}$ are manufactured using a Prusa i3 Mk2S printer. Seven specimens for each fiber content (0 wt% or pure PLA, 5 wt%, 10 wt%, 15 wt%, 20 wt% and 25 wt%) are manufactured, for a total of 42 specimens. Then, the samples are weighed using a precision balance with an accuracy of 0.01 g. Design and manufacturing parameters for the FFF process are reported in Table 3-2. These parameters were optimized in a research study to manufacture specimens with high surface quality and dimensional accuracy [36]. A 313Q tensile machine from Testresources with a 50 kN load cell is used for tensile testing at a 5 mm/min displacement rate. The fracture interface of the specimens is evaluated using scanning electron microscopy (Hitachi UHR Cold-Emission FE-SEM SU8000). To examine the role of fiber surface coating on the impregnation level of the recycled fibers and PLA and compare to that of virgin glass fibers, representative virgin fiber reinforced filaments with 10 wt% fiber content are produced and used to manufacture test specimens. The stacking sequence and thickness of these samples are identical to those of the recycled glass fiber specimens. The virgin glass fibers (MEF-11-100, Shenzhen Taida Technology Co., Ltd, China) are coated with silane sizing and feature an average diameter of 0.017 mm and a fiber length of 0.007-0.4 mm, dimensional properties similar to those of recycled fibers. Therefore, the interface developed between the two different composite systems, namely recycled fibers/PLA and virgin fibers/PLA, can be surmised to contribute to the relative mechanical performance of theses composites.

Table 3-2: Manufacturing and design parameters for specimen 3D printing.

Manufacturing parameter	Value	Manufacturing parameter	Value
Print direction	XYZ	Nozzle diameter (mm)	0.4
Raster angle	0	Nozzle temperature (°C)	215
Layer height (mm)	0.14	Cooling	No fan cooling
Bed temperature (°C)	60	Infill (%)	100
Print speed (mm/min)	2400	Filament diameter (mm)	1.75

3.4 Results

This section presents results for the proposed mechanical recycling scheme, which is used to fabricate and evaluate FFF samples out of recycled composite filament and pure PLA filament, a commercially available baseline. Also, the interfacial bonding between the recycled fibers and PLA is evaluated using the approach described in Section 3.3.2.

3.4.1 Mechanical Grinding

The recycling system presented in Section 3.3.1 resulted in the recyclate compound shown in Figure 3-3a. In order to characterize the length of the fibers, a group of at least 300 fibers from the last grade of the sieved recycled compound was sized. Figure 3-3d plots the distribution of data versus the fiber length. The yellow rectangles show the experimental measurements, and the solid line is the Gaussian curve of the best fit. As seen, most of the fibers feature a length of below 0.4 mm, a critical characteristic to the processability of the fiber reinforced filaments for the FFF 3D printing process. The average fiber length is around 0.19 mm. Although fibers with length of above 0.4 mm are visible in the recycled materials, the final grade of the recyclate appears to have suitable fiber length distribution. In addition, the double sieving operation has yielded recyclate compound consisting of individual refined fibers with no fiber bundles.

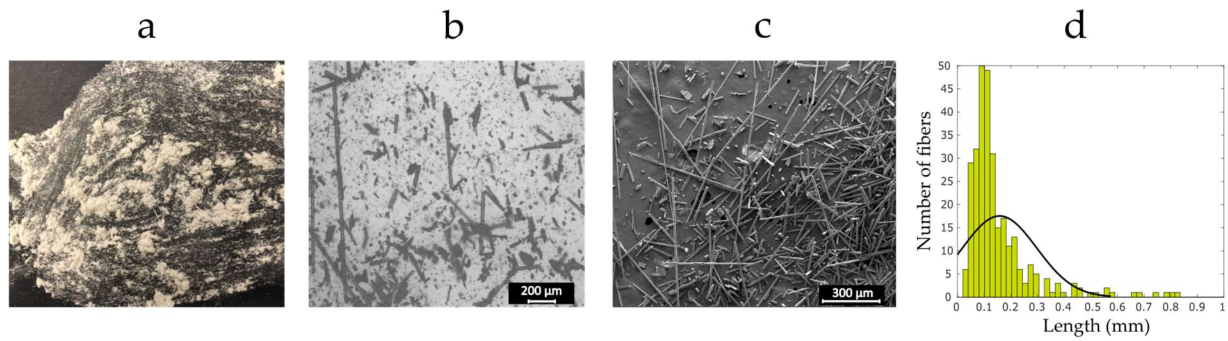

Figure 3-3: Recycled fibers: (a) the final grade recyclate; (b) an optical microscopy image from the recycled compound; (c) a SEM micrograph from the recycled compound; and (d) probability distribution for fiber length of the last grade of ground fibers.

Figure 3-4 illustrates the structural morphology of the recycled and virgin glass fibers. The SEM micrographs show that the recycled fibers retained a significant amount of epoxy residue on the surface, while the virgin fibers have a thin and uniform silane coating layer. Powdered epoxy particles are also visible in the recycled materials. On one hand, the epoxy residue powder decreases the surface quality of the fibers, which could lead to local stress concentration and thus, lower strength. On the other hand, it could increase the fiber surface roughness enabling mechanical interactions between the PLA molecules and the fibers. In addition, it is demonstrated in the literature that epoxy has the potential to form hydrogen bonding with PLA, which could also further enhance the impregnation level of the recycled fibers and PLA [37].

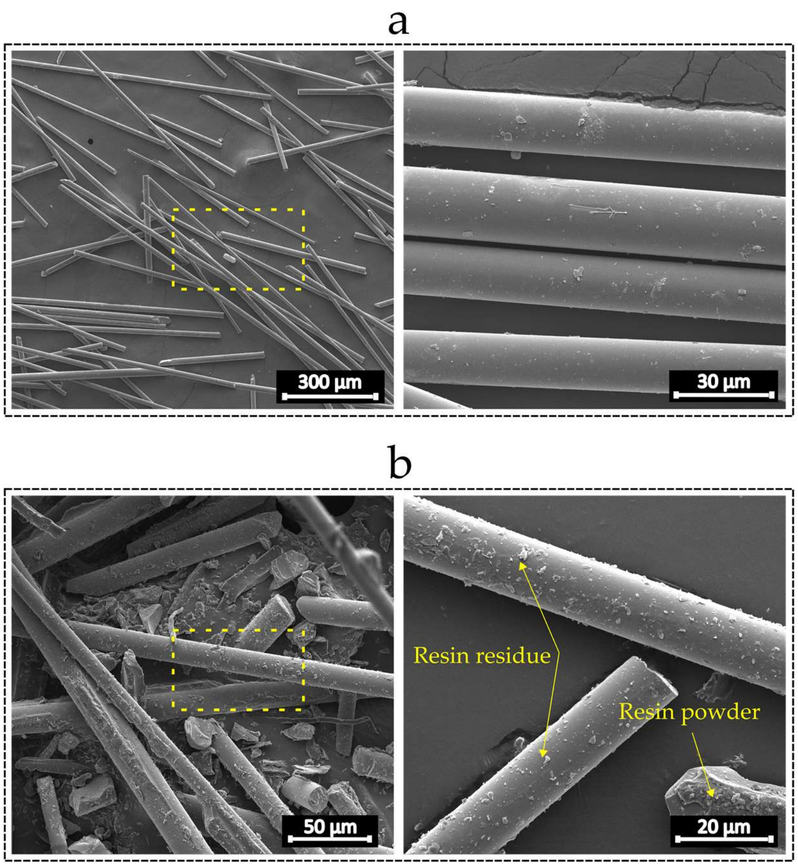

Figure 3-4: SEM micrographs: (a) virgin glass fibers; and (b) recycled glass fibers.

An important factor in defining the added value of recycled materials is the resulting enhancement in mechanical performance when used in new material system. This occurs when maximum amount of reinforcing glass fibers is preserved during the sieving of the ground recycled materials. The level of the reclaimed fibers is here evaluated by performing TGA on the recyclate obtained after the initial granulation and the second sieving mechanism. As it can be observed in Figure 3-5, while the ground recycled materials approximately contain 44% of the resin residue, the second sieving operation enabled a proper separation of the powder particles such that almost 77 % of the fibers are retained. This indicates that the last grade of the recyclate can provide a better reinforcement as compared to the initial ground materials.

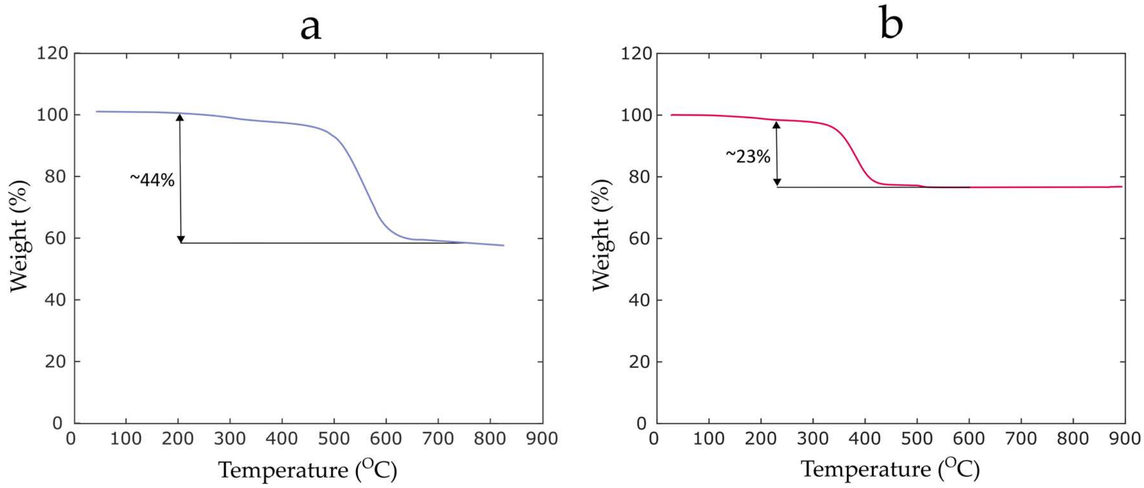

Figure 3-5: The thermogravimetry thermograms of the recyclate materials: (a) ground recyclate ; (b) last grade of the recyclate obtained after the second sieve operation.

3.4.2 Recycled Composite 3D printing Filaments

The microstructure of the pure PLA filament and the reinforced ones with different recycled fiber contents is displayed in Figure 3-6. As seen, the pure PLA filament features a solid cross section with no visible voids. However, the addition of the recycled glass fibers leads to visible porosities in the filament, which get increasingly larger as the fiber content increases. In addition, non-impregnated resin particles with sharp corners appear in the composite filaments. Apart from potential stress concentration regions, relatively small pores are formed around these particles, which could affect the properties by generating the possibility of micro crack formation.

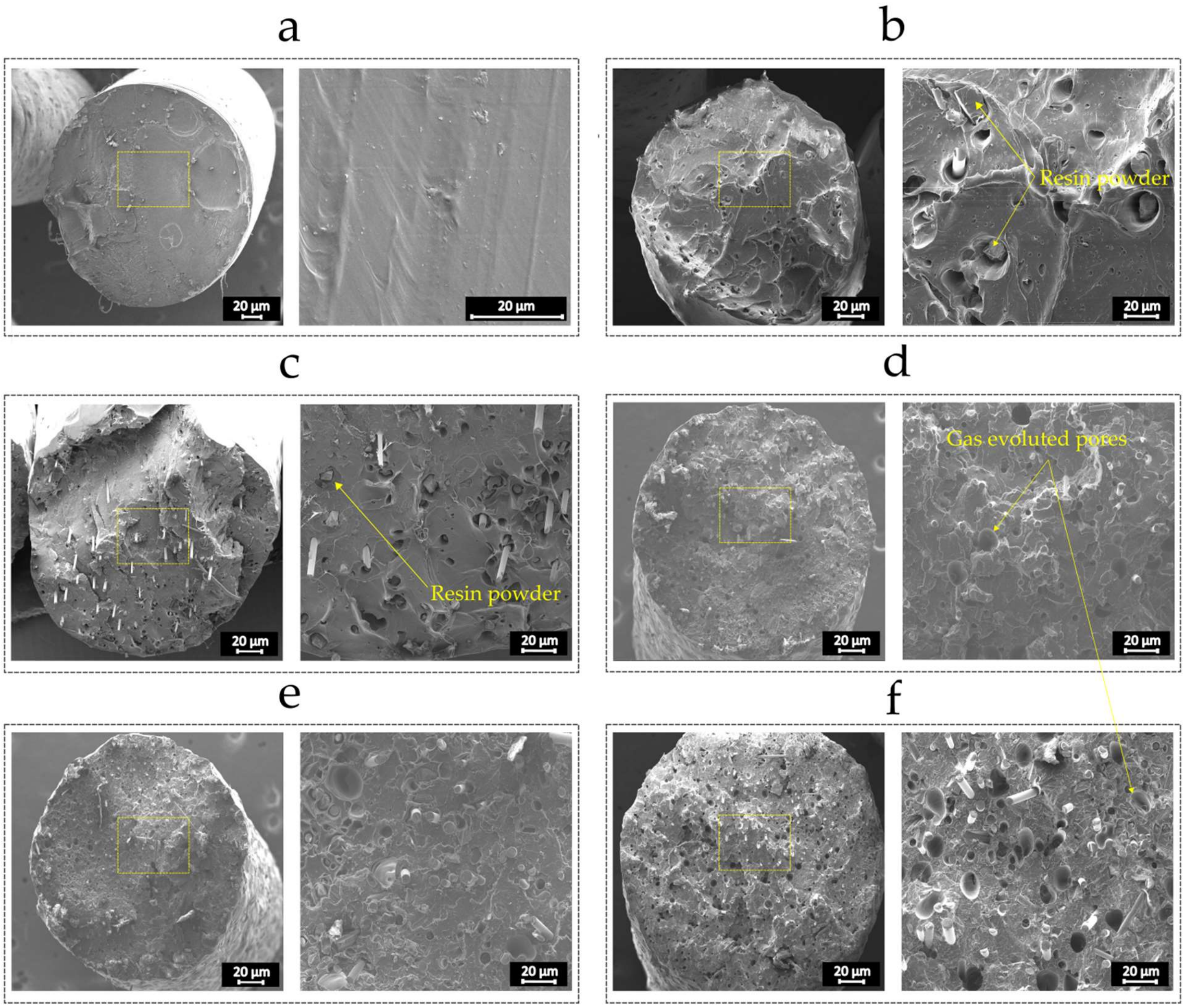

Figure 3-6: Microstructures of FFF 3D printing filament with different fiber content: (a) 0 wt% ; (b) 5 wt% ; (c) 10 wt% ; (d) 15 wt% ; (e) 20 wt% ; and (f) 25 wt%.

3.4.3 Mechanical Characterization of the FFF 3D Printed Tensile Specimens

Figure 3-7 shows one 3D printed specimen per each fiber content. The unidirectional bead orientation can be seen in all samples. A comparison of the typical stress vs. strain curves of the specimens is shown in Figure 3-8. The curves are selected from the results of seven specimens.

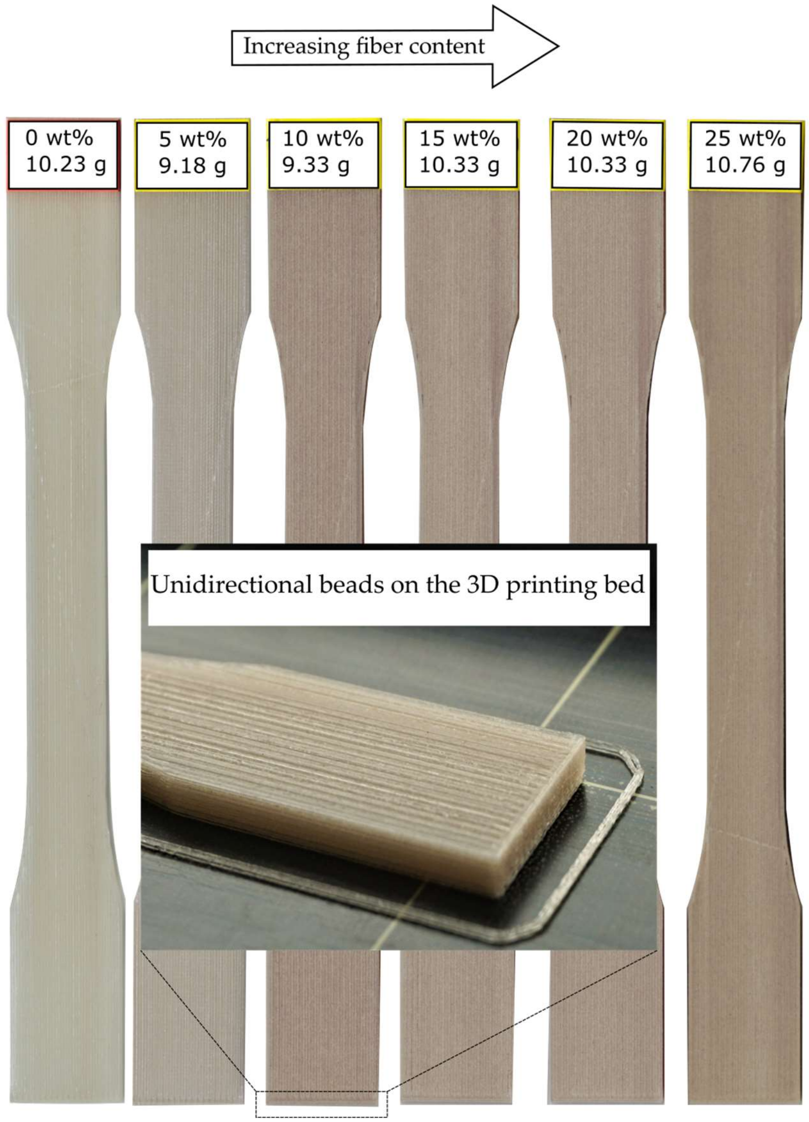

Figure 3-7: The FFF 3D printed coupons with unidirectional bead orientation and different fiber content.

Figure 3-9a and 3-9b illustrate the specific tensile strength and stiffness of the 3D printed coupons. Due to some minor variations in the weight of the samples, the normalized specific properties are reported. The results indicate that as the fiber content increases, the mean specific tensile stiffness of the samples improves, leading to structurally stiff components. A significant increase in specific tensile modulus occurs from 5 wt% to 10 wt%. The maximum specific stiffness is observed for the 25 wt% coupons with an improvement of 74% (2.56 GP.cm^3/gr to 4.45 GP.cm^3/gr). The error bars in the figures show the standard deviation (SD) of multiple tests. SD values can be mainly ascribed to the variation of the fiber length, resin powder, as well as the discrepancy between the fibers surface roughness, which arises from the epoxy particles remained on the surface of the ground fibers. As per the specific strength, lower values are measured for the composite samples. The results show that as the fiber content increases, the specific tensile strength of the samples reduces, such that a reduction of 42% is observed for the 25 wt% coupons.

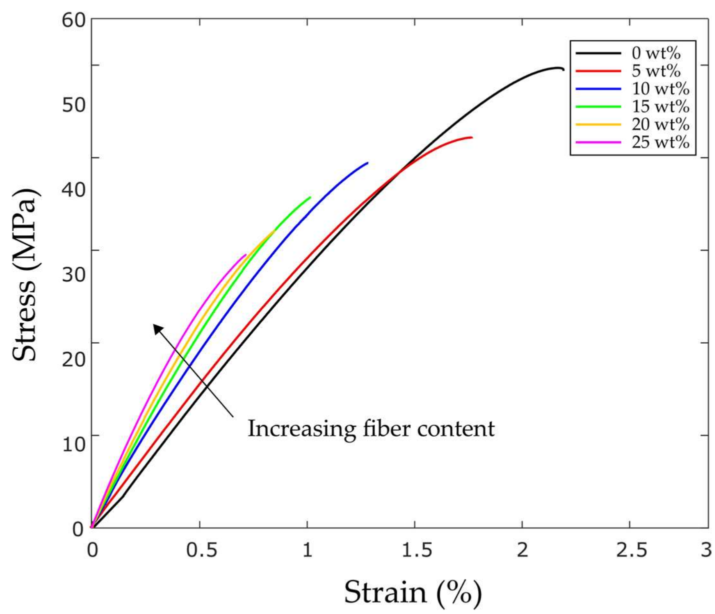

Figure 3-8: Stress-strain curves of pure PLA and recycled glass fiber reinforced specimens.

As shown in Figure 3-9c, the ductility of the 3D printed samples also reduces with the increase of the fiber content. The pure PLA samples show the largest failure strain of 2 %. On the other hand, the composite samples with 25 wt% recycled fibers lead to the smallest mean failure strain of about 0.7 %, which suggests a reduction of about 65%.

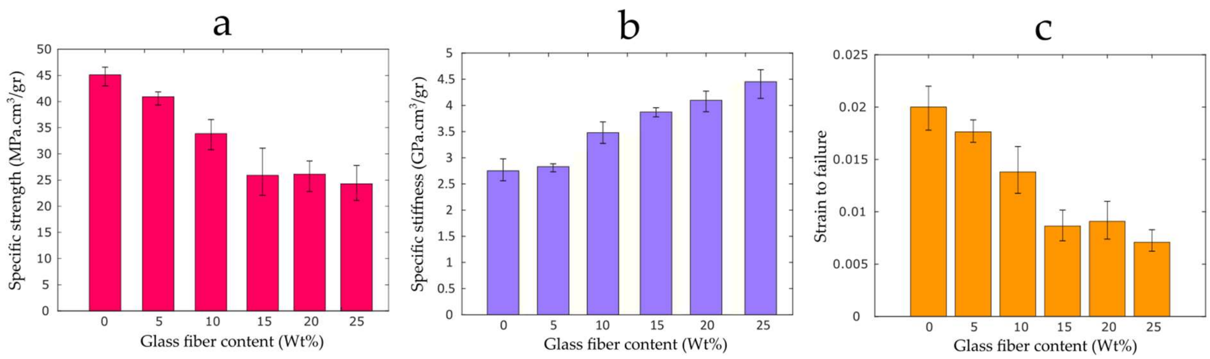

Figure 3-9: Tensile properties of glass fiber reinforced specimens with different fiber content: (a) Specific stiffness; (b) specific strength; and (c) failure strain.

Different established analytical models including Mori-Tanaka, shear lag, and Halpin-Tsai are used to predict and compare the elastic stiffness of short glass fiber composites to that of the 3D printed parts [38, 39]. The theories are briefly described in Table 3-3. In these equations, E_f, E_m, v and l/d denote the fiber stiffness, matrix stiffness, fiber volume fraction, and fiber aspect ratio, respectively. Also, S, C_c, C_m and C_i represent the Eshebly tensor, and stiffness tensor of the composite, matrix, and fiber, respectively. As displayed in Figure 3-10, the theoretical models showed a similar trend as the experimental results and they agree well, particularly at low weight fractions. However, the high viscosity of the polymer at high weight fractions coupled with nozzle clogging increased the porosity of the 3D printed parts leading to larger difference between the experimental results and the analytical models.

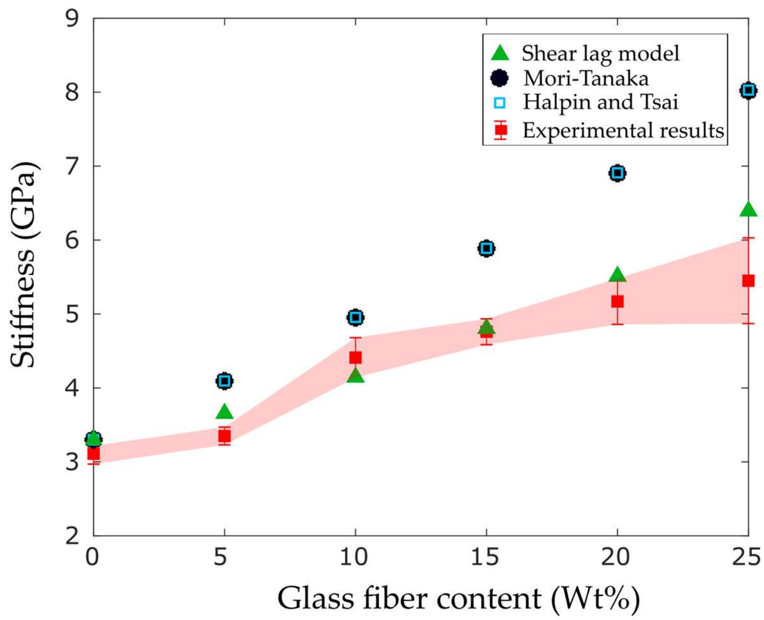

Figure 3-10: Experimental and analytical stiffness results of short fiber composites versus fiber content.

Table 3-3: Analytical models for short fiber composites.

Theory	Expression
Shear lag model	$E_c = \lambda E_f v + E_f(1-v)$ $\lambda = 1 - \frac{tanh\eta l/2}{\eta l/2}$ $\eta = \sqrt{\frac{2G_m}{E_f {r_f}^2 \ln(\frac{R}{r_f})}}$
Mori-Tanaka	$C_c = \langle (C_i - C_m)B_i \rangle [(1-v)I + v\langle B_i \rangle]^{-1} + C_m$ $B_i = [S(C_m)^{-1}(C_i - C_m) + I]^{-1}$
Halpin-Tsai	$E_c = \frac{1+2(l/d)\eta_L v}{1-\eta_L v} E_m$ $\eta_L = \frac{\frac{E_f}{E_m} - 1}{\frac{E_f}{E_m} + 2(l/d)}$

To further investigate the reasons behind the mechanical behavior of the composite 3D printed specimens, their microstructure at the fracture surface is studied. Figure 3-11 shows the scanning electron micrographs of representative samples from the top and front views. As can be seen, the addition of the recycled fibers substantially reduced the surface quality of the coupons. It was observed that the surface quality of the coupons is consistent with the fiber content. The lower the fiber content, the better surface quality. As the fiber content of the filament increases, the distribution of the fibers within the beads aggravates such that some of the fibers are not deposited properly and are not embedded within PLA. This phenomenon generates local stress concentration regions, which could be one reason for the low strength of the composite samples. Another cause for the lower strength of the composite samples could be the presence of resin particles and fibers with ineffective length in the critical zones, which boost the possibility of microcrack formation. The nonuniform distribution of resin particles on the surface of fibers, particularly at fiber ends, could be another culprit for the reduction in ultimate strength of the composite samples. Moreover, the composite samples with higher fiber content contained a higher quantity of pores. This observation could be ascribed to the presence of large pores in the composite filaments and also the incidence of nozzle clogging when printing with higher fiber content filaments. Previous works showed a similarity in the strength and stiffness trend for 3D printed composite parts [40, 41]. For example, in a recent study on hemp hurd/PLA filament, while an increase in the volume fraction of the fiber improved the part stiffness, it was associated with a larger quantity of voids, which led to lower tensile and flexural strength for the 3D printed samples [42]. In another study, 3D printed graphene-based ABS parts featured lower tensile strength and ductility as compared to virgin ABS samples [43]. Two main possible reasons for this property degradation were identified as high viscosity of the polymer, as well as the local stress concentration induced by graphene nanoplates. This observation confirms the stress raiser effect of the epoxy particles dispersed in the recycled glass fiber composite parts.

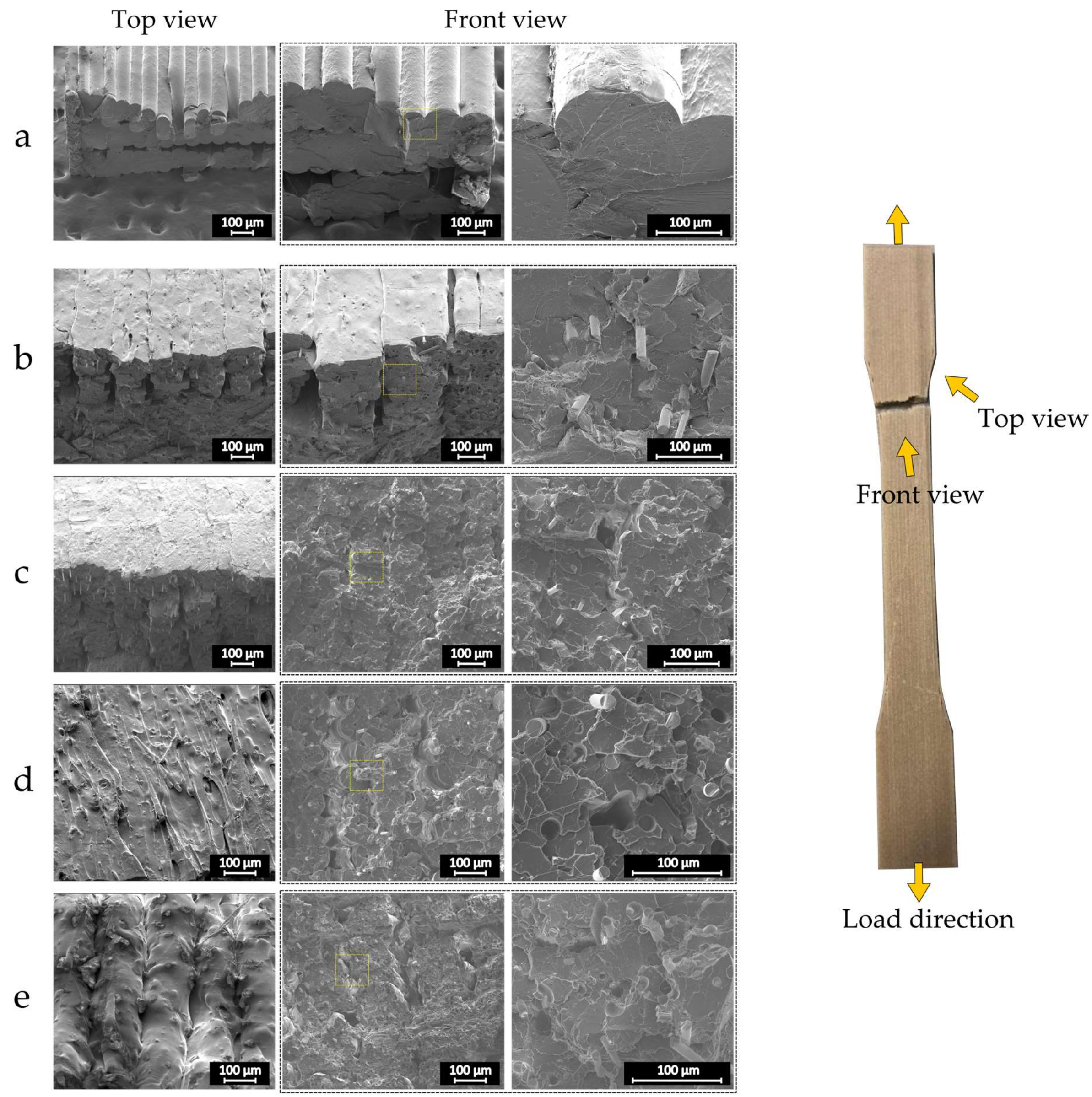

Figure 3-11: Representative SEM micrographs of the composite samples with (a) 0 wt%; (b) 10 wt%; (c) 15 wt%; (d) 20 wt%; (e) 25 wt% fiber content.

3.5 Interfacial Bonding Strength

To examine the bonding strength at the interface between the PLA and the ground fibers, a relative study is performed between tensile test specimens reinforced with virgin glass fibers and samples made out of recycled fibers. To do so, representative samples with 10 wt% virgin and recycled glass fibers are manufactured and tested. Figure 3-12b and 3-12c show, respectively, a microscopic and a SEM image of the virgin fibers, illustrating isolated glass fibers with varying length. As seen, the length distribution of the virgin fibers is similar to that of recycled fibers. Furthermore, they feature an average fiber length of approximately 0.19 mm, a dimensional characteristic identical to that of recycled fibers. This ensures that any difference in the samples properties is only due to the interfacial strength between the fibers and the resin.

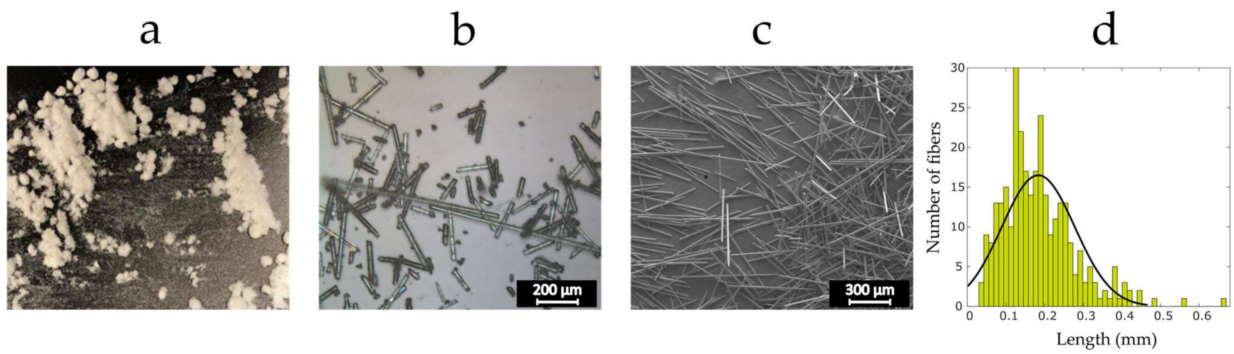

Figure 3-12: Virgin fibers: (a) the reinforcement fiber compound; (b) an optical microscopy image from the virgin fibers; (c) a SEM micrograph from the virgin fibers; and (d) probability distribution for the fiber length of the virgin fibers.

The mechanical properties of the samples with both the virgin and recycled fibers are shown in Figure 3-13. Noticeably, the samples with recycled fiber glass showed higher specific strength and stiffness, with values 19% and 8 % higher than those of specimens reinforced with virgin fibers. However, slightly higher failure strain with value as high as 5% was observed for the virgin samples. This value of failure strain pertains to the lower stiffness of the virgin samples.

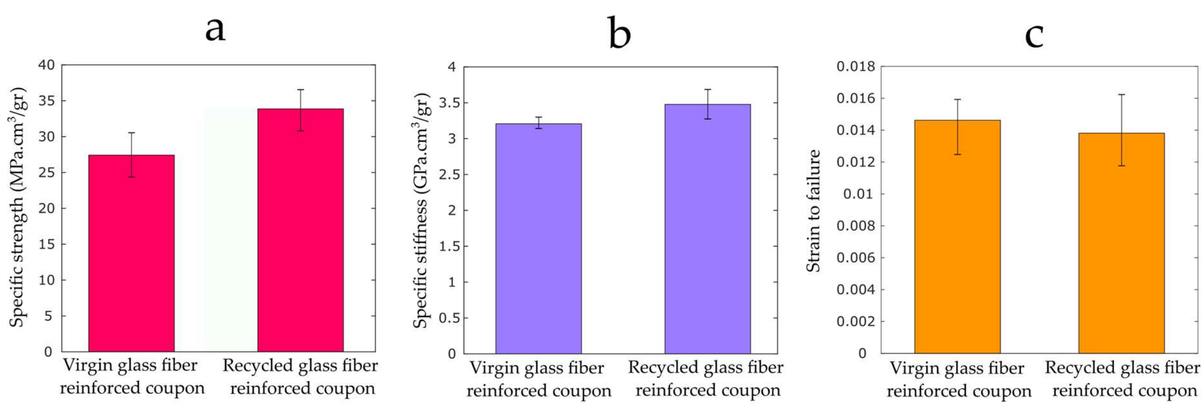

Figure 3-13: Tensile properties of specimens reinforced with recycled and virgin fiber glass with 10 wt% fiber content: (a) The specific strength; (b) the specific stiffness; and (c) strain to failure.

As shown in Figure 3-14, the SEM images from the fracture surface of the samples with virgin and recycled fibers reveal a better impregnation of the recycled fibers and PLA as compared to virgin glass fibers. Although pulled out fibers can be detected on the fracture surface of the recycled samples, most of the recycled fibers are broken and embedded within PLA. On the other hand, many holes on the fracture surface of the specimen reinforced with virgin fibers appear, which show fully pulled out fibers. The presence of epoxy residues on the surface of fibers can contribute to the interfacial strength by providing the possibility of mechanical and chemical interactions between PLA and fibers, where the former results from fiber surface roughness and the latter arises from hydrogen bonding [37]. This indicates an excellent opportunity to fabricate structurally stiff and light weight components with the use of ground fibers from scrap rotor blades.

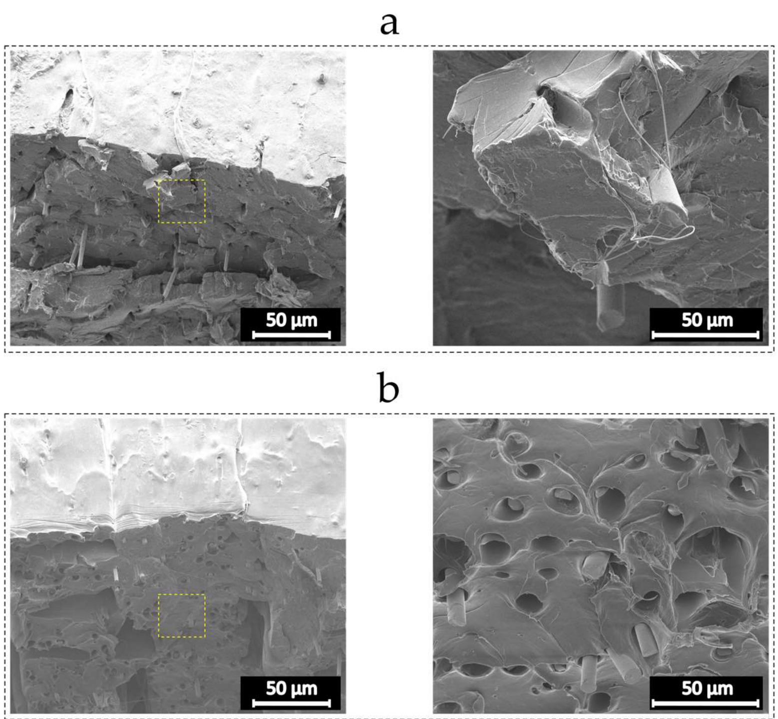

Figure 3-14: SEM micrographs from the fracture surface of tensile specimens: (a) recycled glass fiber reinforced specimen; and (b) virgin glass fiber reinforced specimen.

Previous studies reported structural performance of 3D printed samples reinforced with virgin fibers [44, 45]. Mechanical properties obtained for PLA specimens reinforced with recycled glass fibers in this study can be compared with values from the literature. As shown in Table 3-4, the strength and stiffness of 3D printed specimens in the current study are, respectively, 14% and 108% higher than those of virgin carbon fiber reinforced ABS parts with identical fiber content. On the other hand, for virgin carbon fiber reinforced PLA, the mean value of the strength and stiffness are, respectively, 38 % and 18% higher than those of recycled glass fiber reinforced PLA. Besides using virgin fibers, this discrepancy arises from higher mechanical properties of carbon fibers with respect to recycled glass fibers. Nevertheless, given the low price of PLA and free access to composite wastes from rotor blades, the results of this work offer the opportunity to replace the existing composite filaments with an inexpensive material featuring comparable properties.

Table 3-4: Comparison of the mechanical properties for the recycled glass fiber reinforced parts and conventional reinforced 3D printed parts.

Authors	Material	Fiber content (%)	Strength (MPa)	Stiffness (GPa)
Ning et al. [45]	Carbon fiber/ABS	15	35	2.3
Ivey et al. [44]	Carbon fiber/PLA	15	55.2	5.68
Present work	Glass fiber/PLA	15	40	4.8

3.6 Economic and Environmental Advancement

Interest in recycling of composites is rapidly increasing as the composite material industry strives to become more environmentally friendly. It is significant to be at the forefront of recycling technology to reduce the carbon footprint of composites. Considering the limited lifespan of wind turbine blades, which is between 20-25 years, the first generation of blades will be decommissioned in near future. Disposing of these blades will be a major issue as it is not feasible to merely cut up the blades and put them in a landfill. According to economic analysis, the landfilling cost for a material flow of 10000 Mg/Y of turbine blades is about 837 K USD, which is the most economical feasible solution, presently available [46]. However, the environmental legislations in many countries restrict the landfill of materials with more than 10% organic materials, including turbine rotor blades.

The main contribution of this work relies on a sustainable cost-effective way using an efficient grinder to convert the processed fiberglass into manageable short fibers. This approach will avoid the need for high-energy conversion processes, such as pyrolysis, for recycling. A recent study on the recycling of wind turbine blades has highlighted that the primary energy requirement for mechanical, thermal, and chemical recycling of glass fiber thermoplastic reinforced blades are, respectively, 0.29 MJ/Kg, 1 MJ/Kg, and 4 MJ/Kg, values which indicate the high efficiency of the grinding process for glass fiber composites [3]. One major obstacle hindering the use of mechanical recycling, is the loss of high aspect ratio fibers. That being said, the results of this investigation have shown that short fiberglass-reinforced polymers can lead to stiffer 3D printed components with added value for the end users. Using a sustainable and biodegradable polymer, the proposed process will be sustainable since the 3D printed parts made by fiberglass reinforced polymer filaments could also be reused and re-cycled back into the same system, making the entire process waste free, as shown in Figure 3-15. One critical factor contributing to the applicability of the proposed recycling scheme, is the length of the fibers in the recycled compound. Weight statistics investigation shows that approximately 55-60 % of the ground recyclate comes out of the sieve after the second sieve operation and the remaining recycled material is not processable. However, the non-sieved residue could be either further ground and reused in the same recycling system or processed using 3D printers with larger nozzle diameters.

As a result, the proposed methodology is associated with significant environmental benefits by providing a closed-looped recycling system for wastes from wind turbine blades. Despite the low cost of virgin glass fibers, which in fact demonstrate the increasing utilization of GFRPs, the viable and economical applications for recycled waste composites will become more profitable in near future.

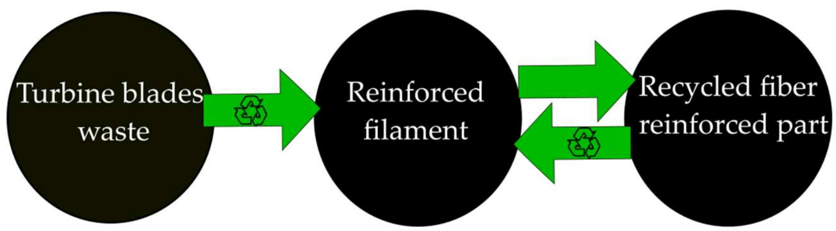

Figure 3-15: The sustainability pattern for the recycled fiber reinforced composites.

The results of this study can serve as the foundation for further work to accurately investigate the entire life cycle of the proposed material. For instance, a study on the recycling and remanufacturing of the 3D printed parts is required. In addition, the mechanical behavior, e.g. strength, of the 3D printed parts should be further studied to bring their performance up in the levels of advanced applications. Other polymers, like ABS can be also considered to explore their interaction and adhesion to recycled fibers. In addition, other types of fibers, e.g. carbon from other end-of-life products can be the subject of future studies.

3.7 Conclusion

The focus of this work is on the recycling of end-of-life wind turbine blades and reusing them in a sustainable 3D printing process. It was shown that the recovered short glass fibers from scrap turbine blades can be effective in enhancing the structural stiffness of FFF 3D printed components. An innovative and economically efficient recycling scheme integrating mechanical grinding and double sieving mechanism was employed to obtain glass fibers from scrap rotor blades. The SEM images from the recycled fibers showed traces of epoxy on the surface of the fibers. Through tensile experiments on 3D printed specimens reinforced with recycled glass fibers, our results have shown that the use of recycled fibers can substantially improve the structural specific modulus of the components. In contrast, the addition of the fibers had an adverse impact on the ductility and ultimate strength of the samples. The cause for this phenomenon was identified through SEM analysis as the development of excessive stress concentration regions due to two main reasons: first, the fiber aggregates, particularly at high fiber weight fractions and second, resin particles with sharp corners remained on the surface of the recycled fibers. A comparative study between specimens out of PLA reinforced with virgin glass fibers and recycled fibers showed that the specific strength and stiffness of the samples made of recycled fibers are higher than those of virgin glass fiber reinforced specimens. The SEM micrographs from the fracture surface of these specimens demonstrated a better impregnation of the ground fibers and PLA as compared to virgin fibers. The reason behind this observation is mainly due to the retention of epoxy particles on the surface of the fibers, which offers the opportunity of potential mechanical and chemical interactions between the molecular network of PLA and epoxy. The mechanical interactions can lead to molecular interlocking and the chemical interactions can form hydrogen bonding between PLA and epoxy resulting in chain extension and further enhancement in the interfacial strength. While the recycling methodology here presented was only applied to glass fiber composite waste from wind energy industry, it can be systematically designed and applied to other glass fiber waste resources, e.g. pipes and boat hulls. This will provide the opportunity to take further steps to meeting the demands of recycling glass fiber reinforced plastics from composite industry.

3.8 Author Contributions

Conceptualization: A.R. and J.K.; Methodology: A.R. and K.F.; Investigation: A.R., J.K. and R.H.; Data curation: A.R. and J.K., Formal analysis: A.R., K.F. and L.L.; Writing - original draft: A.R. and K.F.; Writing - Review & editing: A.R., K.F., and L.L.; Supervision: K.F. and L.L.; Funding acquisition: K.F. and L.L.

3.9 Funding

This work is supported by the Research Center for High Performance Polymer and Composite Systems (CREPEC), Projet Vision and the Natural Sciences and Engineering Research Council of Canada (NSERC), RGPIN-2018-04144.

3.10 Acknowledgement

The authors are thankful to Dr. Ebrahim Jalili and Professor Abdellah Ajji at Ecole Polytechnique de Montreal for fruitful discussions.

3.11 Conflict of Interest

The authors declare no conflict of interest.

3.12 References

[1] Pimenta S, Pinho ST. Recycling carbon fibre reinforced polymers for structural applications: technology review and market outlook. Waste management. 2011;31(2):378-92.

[2] Yang Y, Boom R, Irion B, van Heerden D-J, Kuiper P, de Wit H. Recycling of composite materials. Chemical Engineering and Processing: Process Intensification. 2012;51:53-68.

[3] Cousins DS, Suzuki Y, Murray RE, Samaniuk JR, Stebner AP. Recycling glass fiber thermoplastic composites from wind turbine blades. Journal of Cleaner Production. 2019;209:1252-63.

[4] Patel K, Gupta R, Garg M, Wang B, Dave U. Development of FRC Materials with Recycled Glass Fibers Recovered from Industrial GFRP-Acrylic Waste. Advances in Materials Science and Engineering. 2019;2019, 4149708.

[5] Dell'Anna R, Lionetto F, Montagna F, Maffezzoli A. Lay-Up and Consolidation of a Composite Pipe by In Situ Ultrasonic Welding of a Thermoplastic Matrix Composite Tape. Materials (Basel, Switzerland). 2018;11(5).

[6] Zhang L. The application of composite fiber materials in sports equipment. 2015 International Conference on Education, Management, Information and Medicine: Atlantis Press; 2015.

[7] Pelc R, Fujita RM. Renewable energy from the ocean. Marine Policy. 2002;26(6):471-9.

[8] Albers H, Greiner S, Seifert H, Kühne U. Recycling of wind turbine rotor blades–fact or fiction. DEWI Mag. 2009;34:32-41.

[9] Mishnaevsky L, Branner K, Petersen HN, Beauson J, McGugan M, Sorensen BF. Materials for Wind Turbine Blades: An Overview. Materials (Basel, Switzerland). 2017;10(11).

[10] Chen J, Wang J, Ni A. Recycling and reuse of composite materials for wind turbine blades: An overview. Journal of Reinforced Plastics and Composites. 2019;38(12):567-77.

[11] Jensen JP. Evaluating the environmental impacts of recycling wind turbines. Wind Energy. 2019;22(2):316-26.

[12] Larsen K. Recycling wind turbine blades. Renewable energy focus. 2009;9(7):70-3.

[13] Job S. Recycling glass fibre reinforced composites–history and progress. Reinforced Plastics. 2013;57(5):19-23.

[14] Christian Fischer, Mathias Lehner, McKinnon DL. Overview of the use of landfill taxes in Europe 2012.

[15] Oliveux G, Dandy LO, Leeke GA. Current status of recycling of fibre reinforced polymers: Review of technologies, reuse and resulting properties. Progress in Materials Science. 2015;72:61-99.

[16] Pickering S. Thermal methods for recycling waste composites. Management, recycling and reuse of waste composites: Management, Recycling and Reuse of Waste Composites; 2010. p. 65-101.

[17] Jiang G, Pickering SJ, Lester EH, Turner T, Wong K, Warrior N. Characterisation of carbon fibres recycled from carbon fibre/epoxy resin composites using supercritical n-propanol. Composites Science and Technology. 2009;69(2):192-8.

[18] Palmer J, Ghita O, Savage L, Evans K. Successful closed-loop recycling of thermoset composites. Composites Part A: Applied Science and Manufacturing. 2009;40(4):490-8.

[19] MARTIN SA. Comparison of hammermill and roller mill grinding and the effect of grain particle size on mixing and pelleting.: Master's thesis, Kansas State University; 1981.

[20] Schinner G, Brandt J, Richter H. Recycling carbon-fiber-reinforced thermoplastic composites. Journal of Thermoplastic Composite Materials. 1996;9(3):239-45.

[21] Roux M, Dransfeld C, Eguémann N, Giger L. Processing and recycling of thermoplastic composite fibre/PEEK aerospace part2014.

[22] Palmer J, Ghita OR, Savage L, Evans KE. Successful closed-loop recycling of thermoset composites. Composites Part A: Applied Science and Manufacturing. 2009;40(4):490-8.

[23] Wong KV, Hernandez A. A review of additive manufacturing. ISRN Mechanical Engineering. 2012;2012, 208760.

[24] Huang SH, Liu P, Mokasdar A, Hou L. Additive manufacturing and its societal impact: a literature review. The International Journal of Advanced Manufacturing Technology. 2013;67(5-8):1191-203.

[25] Gardan J. Additive manufacturing technologies: state of the art and trends. International Journal of Production Research. 2016;54(10):3118-32.

[26] Shofner M, Lozano K, Rodríguez-Macías F, Barrera E. Nanofiber-reinforced polymers prepared by fused deposition modeling. Journal of applied polymer science. 2003;89(11):3081-90.

[27] Zhong W, Li F, Zhang Z, Song L, Li Z. Short fiber reinforced composites for fused deposition modeling. Materials Science and Engineering: A. 2001;301(2):125-30.

[28] Stoof D, Pickering K. Sustainable composite fused deposition modelling filament using recycled pre-consumer polypropylene. Composites Part B: Engineering. 2018;135:110-8.

[29] El Magri A, El Mabrouk K, Vaudreuil S, Ebn Touhami M. Mechanical properties of CF-reinforced PLA parts manufactured by fused deposition modeling. Journal of Thermoplastic Composite Materials. 2019:0892705719847244.

[30] Jahangir M, Billah K, Lin Y, Roberson D, Wicker R, Espalin D. Reinforcement of material extrusion 3D printed polycarbonate using continuous carbon fiber. Additive Manufacturing. 2019;28:354-64.

[31] Papon EA, Haque A. Fracture toughness of additively manufactured carbon fiber reinforced composites. Additive Manufacturing. 2019;26:41-52.

[32] Woern A, Byard D, Oakley R, Fiedler M, Snabes S, Pearce J. Fused Particle Fabrication 3-D Printing: Recycled Materials' Optimization and Mechanical Properties. Materials. 2018;11:1413.

[33] Reich M, Woern A, Tanikella N, Pearce J. Mechanical Properties and Applications of Recycled Polycarbonate Particle Material Extrusion-Based Additive Manufacturing. Materials. 2019;12:1642.

[34] Rahimizadeh A, Kalman J, Henri R, Fayazbakhsh K, Lessard L. Recycled glass fiber composites from wind turbine waste for 3D printing feedstock: effects of fiber content and interface on mechanical performance. Submitted to Materials. 2019.

[35] Rahimizadeh A, Kalman J, Fayazbakhsh K, Lessard L. Recycling of fiberglass wind turbine blades into reinforced filaments for use in Additive Manufacturing. Composites Part B: Engineering. 2019;175:107101.

[36] Fayazbakhsh K, Movahedi M, Kalman J. The impact of defects on tensile properties of 3D printed parts manufactured by fused filament fabrication. Materials Today Communications. 2019;18:140-8.

[37] Brydson JA. 26 - Epoxide Resins. In: Brydson JA, editor. Plastics Materials (Seventh Edition). Oxford: Butterworth-Heinemann; 1999. p. 744-77.

[38] Mirkhalaf M, Ashrafi B. A numerical study on improving the specific properties of staggered composites by incorporating voids. Materials Today Communications. 2017;13:144-54.

[39] Fu S-Y, Lauke B, Mai Y-W. 6 - Elastic modulus of short fibre reinforced polymers. In: Fu S-Y, Lauke B, Mai Y-W, editors. Science and Engineering of Short Fibre Reinforced Polymer Composites: Woodhead Publishing: Sawston, UK; Cambridge, UK; 2009. p. 119-63.

[40] Khan BA, Na H, Chevali V, Warner P, Zhu J, Wang H. Glycidyl methacrylate-compatibilized poly(lactic acid)/hemp hurd biocomposites: Processing, crystallization, and thermo-mechanical response. Journal of Materials Science & Technology. 2018;34(2):387-97.

[41] Turner Brian N. A review of melt extrusion additive manufacturing processes: II. Materials, dimensional accuracy, and surface roughness. Rapid Prototyping Journal. 2015;21(3):250-61.

[42] Xiao X, Chevali VS, Song P, He D, Wang H. Polylactide/hemp hurd biocomposites as sustainable 3D printing feedstock. Composites Science and Technology. 2019;184:107887.

[43] Dul S, Pegoretti A. Fused deposition modeling with ABS-graphene nanocomposites. Composites Part A: Applied Science and Manufacturing. 2016;85:181-91.

[44] Ivey M, Melenka GW, Carey JP, Ayranci C. Characterizing short-fiber-reinforced composites produced using additive manufacturing. Advanced Manufacturing: Polymer & Composites Science. 2017;3(3):81-91.

[45] Ning F, Cong W, Qiu J, Wei J, Wang S. Additive manufacturing of carbon fiber reinforced thermoplastic composites using fused deposition modeling. Composites Part B: Engineering. 2015;80:369-78.

[46] Group SM. Recycling of waste glass fiber reinforced plastic with microwave pyrolysis (LIFE07 ENV/S/000904). Stena recycling, Göteborg, Sweden2012.

Link between Chapter 3 and Chapter 4

The effect of recycled fiber content on the mechanical properties of 3D printed composite parts was precisely examined in the previous chapter. Samples containing 5, 10, 15, 20 and 25 wt% recycled fibers from wind turbine waste were successfully fabricated and tested in accordance with ASTM D638. To study the impact of epoxy matrix residue remained on the surface of the recycled fibers on the mechanical properties of 3D printed parts, virgin E-glass fibers featuring identical dimensional properties were used to 3D print tensile test coupons. The results from this comparative study, which was conducted on samples with 10 wt% fiber weight fraction exhibited higher mechanical properties for the recycled samples. While this observation was attributed to the rougher surface of the ground fibers, next chapter will exclusively study the micromechanical properties of the recycled fibers. In particular, singles fibers are extracted from wind turbine waste and evaluated through single fibre tensile and pull-out tests to precisely characterize their tensile and interfacial properties.

Chapter 4

Tensile properties and interfacial shear strength of recycled fibers from wind turbine waste

4 Chapter 4: Tensile properties and interfacial shear strength of recycled fibers from wind turbine waste

Amirmohammad Rahimizadeh a, Mazin Tahir a, Kazem Fayazbakhsh b,*, Larry Lessard a

a Department of Mechanical Engineering, McGill University, Montreal, QC H3A0C3, Canada;

b Department of Aerospace Engineering, Ryerson University, Toronto, Ontario M5B2K3, Canada; kazem@ryerson.ca

*Corresponding author: kazem@ryerson.ca; Tel: (+1) 416-979-5000 ext. 6414; fax: (+1) 416-979-5056

Journal of Composites part A, 12 (23), 3929

4.1 Abstract

The rapid growth of composites combined with imminent recycling legislation have highly increased the interest in recycling and reusing of composite waste. The mechanical properties of recycled fibers such as tensile strength and interfacial shear strength (IFSS) are among the most critical factors contributing to the final properties of recycled products. In this work, we focus on the tensile properties of recycled glass fibers from scrap wind turbine blades and their interface strength with polylactic acid (PLA). The single fiber tensile and pull-out tests are used to characterize the fibers recovered through two recycling systems, namely mechanical and thermal processes. It is shown that while pyrolysis can significantly degrade the recovered fibers, ground fibers with a gage length of 20 mm feature characteristic strength comparable to that of virgin fibers. The effect of the fibers surface coating on the IFSS was also investigated, with results showing an interface between ground fibers and PLA that is 14% and 26% stronger than pyrolyzed and virgin fibers, respectively.

Keywords: A. Wind turbine blade, A. Polylactic acid, D. Single fiber tensile test, D. Single fiber pull-out test.

4.2 Introduction

The load carrying capacity of composites is mainly governed by the mechanical properties of the reinforcement material and the interfacial bonding strength [1]. While the reinforcement material is mainly responsible for resisting against the applied loads, the fiber-matrix interface plays a key role in transferring the load to the fibers. Interfacial bonding is a metric that is determinant to the composite strength and stiffness by increasing the load transferring capacity of the composites. Even though expensive and complex, optimizing the fiber-matrix interface through fiber treatment technologies has shown to be beneficial in enhancing the interfacial bonding [2]. For instance, glass fibers are typically covered with functional agents through the sizing technology [3]. Despite forming a protective layer, the sizing agents can contribute to the binding of the matrix and fibers by providing the opportunity for chemical interactions at microstructural scales [3].

Recent overwhelming use of composites, which raises environmental sustainability concerns, has motivated the reuse of fiber reinforcements from composite waste into new material systems. Wind turbine rotor blades will soon represent one of the major composite waste-generating sources as a tremendous number of turbines are coming to their end-of-life and will be soon decommissioned all around the world [4]. Turbine blades are mainly composed of glass fibers and epoxy or vinyl ester polymers [4]. Thermal, chemical, and mechanical processes are widely proposed to reclaim fiber reinforcements from thermoset scrap blades [5]. However, current recycling routes for scrap rotor blades have only been partially successful because the recycling of rotor blades comes at the expense of fiber strength reduction and interface degradation [6]. The thermal and chemical processes generally result in the inevitable reduction in the fiber properties, which deteriorates the viability and effectiveness of recycling [7, 8]. For instance, Cunliffe et al. [9] have documented a substantial reduction of 40-50 % in the mean tensile strength of E-glass fibers recovered from polyester sheet molding compound (SMC) using the pyrolysis technique. These techniques also require a high amount of waste and a very large plant, which translates into a relatively large investment to motivate such techniques. Another drawback limiting the extensive use of these recycling processes is the degradation of fiber sizing, which in turn necessitates an additional post-treatment process to improve their processability, as well as the interfacial bonding between the recycled fibers and the new resin matrix [10]. The post-treatment process on thermally recycled fibers is typically challenging since they are generally brittle and break during the compounding process generating numerous new untreated surfaces. The sizing removal can also introduce adverse effects on the mechanical performance of the fibers by exposing surface defects and lowering the fiber strength [11]. In an experimental study, Nzioka et al. [8] applied a chemical recycling scheme coupled with ultrasound cavitation to recover E-glass fibers from scrap composite parts. The surface analysis results showed a lower quality non-smooth surface topology for the recovered fibers. However, coating the fibers surface with 1 wt% APS silane agents helped to improve the surface topography.

Unlike the thermal and chemical recycling techniques, mechanical grinding is a straightforward and economically feasible solution for recycling of composites. This technique offers a fast and efficient technique to decrease the size of waste and reclaim fibers with low aspect ratio [12]. The ground fibers differ from thermally or chemically recycled ones by not only preserving the surface sizing, but also the presence of matrix residue on the surface, a phenomenon which highly increases the fiber surface roughness. If used with an appropriate new resin, the presence of the matrix powder on the surface of fibers can allow for mechanical and chemical interactions, where the former results from surface roughness and the latter arises from molecular interactions. Nonetheless, long fibers cannot generally be preserved by mechanical recycling. As a result, mechanically recycled fibers are typically used in composites with short fibers as reinforcement, such as the ones manufactured by bulk molding compound [13]. While the early studies on the mechanical recycling of composites have noticed the different morphology of the recycled fibers, they have mainly focused on the bulk properties of the composites made out of the recycled fibers and they fall short in precisely characterizing the recycled fibers [12].

The authors of this research work used mechanical grinding of wind turbine waste and recently introduced a composite 3D printing filament made of polylactic acid (PLA), a biodegradable thermoplastic used extensively in 3D printing and injection molding, and recycled glass fibers [14]. A systematic mechanical recycling scheme was proposed and applied to a set of scrap turbine blade pieces to reclaim short fibers from end-of-life rotor blades. Using ground E-glass fibers, structurally stiff filaments were manufactured and used to 3D print parts with superior structural properties. A subsequent study confirmed that the ground fibers retaining resin residue have higher structural properties when mixed with PLA compared with those made of virgin glass fibers with silane sizing and PLA [15]. In these early studies, mechanical testing of 3D printed coupons per

ASTM D638-14 was performed, which provides only limited insight into the properties of recycled fibers. Recently, Cousins et al. [4] studied the mechanical properties of fibers recovered from thermoplastic wind turbine blades through a dissolution recycling process. In this study, rovings from the recovered fibers were prepared and tested. The results revealed a reduction of 12 % in the stiffness of the fibers, which was attributed to the possible fiber degradation during the recycling process. Furthermore, the feasibility of reusing ground thermoplastic blades in injection moulding was investigated. However, no micromechanical analysis on the tensile properties and interfacial strength of the ground fibers was carried out. More recently, a two-stage pyrolysis method was used to reclaim E-glass fibers from wind turbine blades [7]. In this study, the tensile strength of the recovered fibers was only characterized and compared with virgin fibers. Consequently, further research work on precisely characterizing the recycled fibers from end-of-life wind turbine blades is crucial to identify proper applications for the use of them.

In this work, the mechanical properties of reclaimed glass fibers from end-of-life scrap turbine blades are characterized and their interfacial strength with PLA is measured. On the first front, the mechanical properties of single recycled fibers extracted thermally and mechanically from scrap blades are characterized for different gage lengths, namely 20, 40, and 60 mm. On the second front, the interfacial strength between the recycled fibers and PLA is assessed using single fiber pull-out test and compared with a baseline, virgin glass fibers and PLA. The test is performed over a wide range of embedded length ranging from 60 – 400 μm. Lastly, the mechanical and interfacial properties of the recycled fibers are used to calculate the critical fiber length required to design recycled composites with effective strength and stiffness.

4.3 Materials and methods

The thermal and mechanical recycling methods are used here to obtain glass fibers from end-of-life wind turbine blades. The mechanical recycling steps are illustrated in Figure 4-1. As depicted, the scrap parts from wind turbine blades are first cut into small 20 cm × 20 cm pieces using a bandsaw. The pieces are then ground using a hammer mill grinder (ECO-WOLF, INC.). To obtain fiber bundles with an appropriate length for single fiber tests, a screen classifier with a hole size of 19 mm is used.

The thermal recycling of the scrap blades is carried out after an initial granulation process, as described above. Following the grinding process, 100 g of the recyclate materials is placed in the pyrolysis furnace (F200 PYRADIA, Quebec, Canada) at 550 °C and retained for a total duration of 45 min. The pyrolysis process is performed in the presence of nitrogen followed by an oxidative stage at 550 °C for 10 min to remove the ash content left on the surface of the recovered fibers, as shown in Figure 4-1D. Subsequently, individual fibers from fiber bundles of both mechanically and thermally recycled compounds are carefully separated and used for single fiber tensile and pull-out tests. For convenience, mechanically recycled fibers before pyrolysis and thermally recycled fibers after pyrolysis are hereafter referred to as ground fibers and pyrolyzed fibers, respectively.

Wind turbine blades are generally made of epoxy and E-glass fibers with a diameter ranging between 3.8 and 20 μm [16]. The average diameter of the recovered fibers in the present study is predicted by measuring the diameter of at least 100 fibers from the recyclate compound using an optical microscope. The average diameter is then used to calculate the cross-sectional area of single fibers. To capture the surface topology of the recycled fibers, scanning electron microscopy (Hitachi UHR Cold-Emission FE-SEM SU8000) is conducted on the recycled fibers and virgin E-glass fibers, a baseline fiber with sized surface finish.

Figure 4-1: The recycling steps to reclaim fibers from scrap turbine blades: (A) Scrap pieces from rotor blades; (B) ECO Wolf hammer mill grinder; (C) mechanically recycled ground fibers; (D) pyrolyzed ground fibers.

4.3.1 Single fiber tensile test

The mechanical properties of the recycled fibers are characterized through the single fiber tensile test. Single fibers are carefully extracted from ground and pyrolyzed fiber bundles at random and glued onto card tabs with a specific gage length (Figure 4-2). To separate off single ground fibers, a ground bundle is first cut into small pieces and then single fibers are separated using a tweezer. The tabs are then gripped by a universal testing machine (Instron Model 3342) equipped with a load cell of 10 N. Enormous care is taken to ensure that the axis of the fibers is aligned with the axis of the cross-head. The test is conducted at a displacement rate of 0.1 mm/min. To study the effect of the gage length on the tensile properties of single fibers, three sets of samples with gage length of 20, 40, and 60 mm are prepared. As suggested by previous works in the literature, a total of at least 10 samples for each gage length are tested [17, 18].

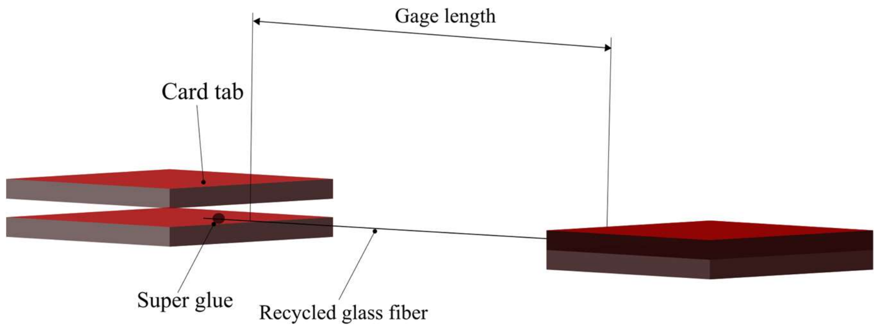

Figure 4-2: Single fiber tensile test set-up.

4.3.2 Single fiber pull-out test

Several micromechanical approaches, including the single fiber pull-out test, the microdroplet test, the push-out test, and the single fiber fragmentation test are proposed in the literature to characterize interfacial shear strength (IFSS) [19, 20]. The single fiber pull-out test has been broadly used for thermoplastic composites, which feature weaker adhesion [21]. According to this method, a single fiber is pulled out of a matrix droplet or block with a specific embedded length. To ensure an interface failure during the test, the length of the embedded fiber has to be less than half of the critical length of the fiber, as explained in [1]:

$$L_e < \frac{\sigma_f d}{4\tau} \tag{4-1}$$

where σ_f, d and τ are, respectively, the tensile strength of the fiber, diameter of the fiber, and the interfacial strength. Controlling the embedded fiber length, especially for thermoplastic polymers, plays an important role in the success and accuracy of this test. Although the single fiber pull-out method has been widely used to determine the apparent interface bonding strength, the reliability and accuracy of IFSS values obtained via this method and other techniques should be regarded with some caution due to several limitations. For instance, in the calculation of IFSS, a constant stress distribution along the fiber interface is assumed, a simplification that is shown to be invalid [22]. In addition, the interfacial failure is associated with some intact regions, which contribute to the peak load through frictional forces [21]. Herein, the interfacial analysis between reclaimed glass fibers from scrap blades and PLA (Ingeo 4043D, Natureworks LLC, Blair, Nebraska) is undertaken using the single fiber pull-out test to carry out a comparison study between the apparent IFSS in three different composite systems including ground fibers/PLA, pyrolyzed fibers/PLA and a baseline, virgin E-glass fibers/PLA.

4.3.2.1 Preparation of samples for single fiber pull-out test

Figure 4-3 illustrates the methodology used to prepare samples for measuring the apparent interfacial strength between either ground or pyrolyzed glass fibers, and PLA using the single fiber pull-out test. Individual fibers are carefully separated and glued onto card tabs. A soldering iron is used to melt PLA pellets and obtain PLA stripes with different width, representing the embedded length. The PLA stripes are then placed on microscope slides, which allow for an accurate measurement of the embedded length. Using a soldering iron, the stripes are first slightly heated to firmly adhere to the slides. Then, the other end of the fibers is placed on the PLA stripes and heated again to slightly embed within PLA. At the end, a total of at least 15 samples are prepared and transferred to an oven with a temperature of 200 °C and maintained for 4 minutes. This heating program will ensure complete melting of the PLA resulting in fibers that are properly embedded within the PLA.

Once the samples are cooled down to ambient temperature, the exact embedded length of the fibers is captured using a Nikon visual microscope. The sample are then vertically placed in the tensile test machine and tested using a 0.1 mm/min displacement rate until interfacial failure.

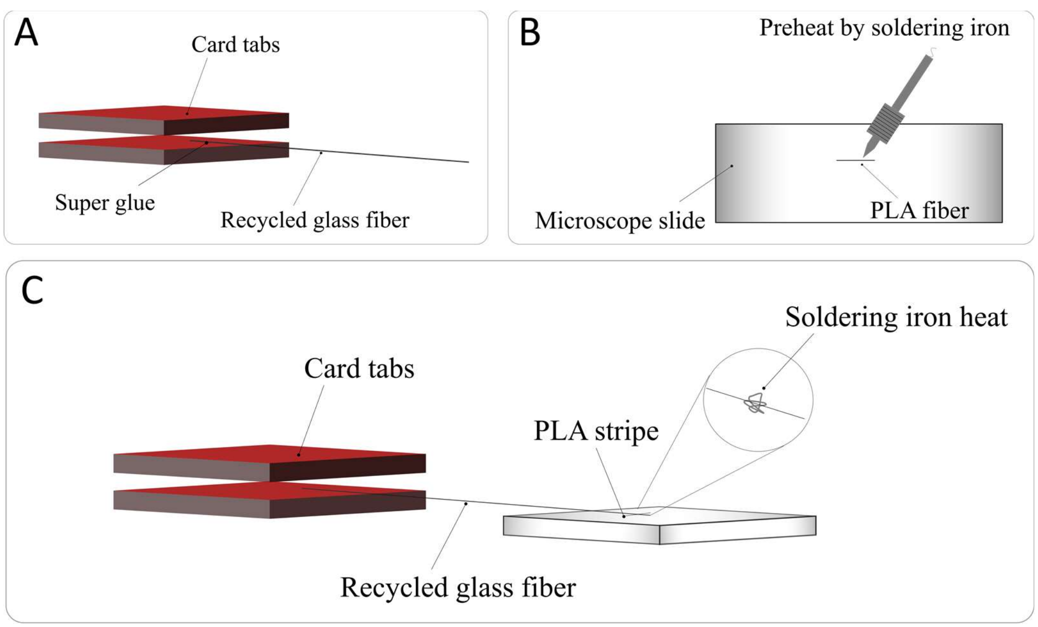

Figure 4-3: Procedure to prepare samples for single fiber pull-out test: (A) single fiber glued onto card tabs; (B) single PLA stripe is placed on a microscope slide and heated by a soldering iron; (C) the other end of the fiber is placed on the PLA stripe and heated again.

One major issue associated with single fiber pull-out test is the formation of a meniscus around the fiber surface. The meniscus does not contribute to the interfacial strength and undergoes a cohesive rupture prior to adhesive debonding at the interface [23]. To minimize the effect of the meniscus in our calculation, each specimen is carefully inspected after the test to accurately capture the trace of the fiber and remeasure the true embedded length (Figure 4-4). Furthermore, this inspection will ensure that unacceptable failure modes such as debonding of the PLA stripe from the glass slide, have not occurred.

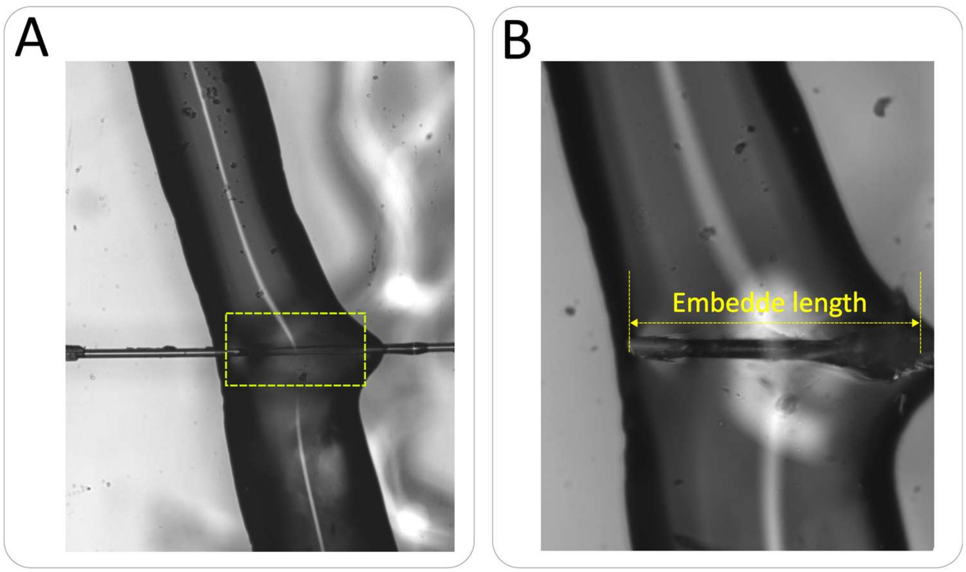

Figure 4-4: The single fiber pull-out test sample: (A) specimen before the test; (B) specimen after the test.

As shown in Figure 4-5, the distribution of the maximum load versus the embedded length for all the samples are then plotted and used to predict the apparent IFSS. Given the non-uniform stress distribution along the fiber interface, the slope of a regression line passing through the data points is used to calculate the interfacial strength, as suggested in [24]:

$$\tau_{d1} = \frac{s}{\pi d} \quad (4\text{-}2)$$

where s and d represent the slope of the regression line and average fiber diameter, respectively. Samples that failed due to PLA stripe debonding or fiber fracture are not considered in the IFSS results. To examine the effect of fiber surface sizing, samples with virgin glass fibers are prepared and tested using the procedure described above. The virgin glass fibers are coated with silane sizing, the most commonly used sizing agent to improve their compatibility with polymers.

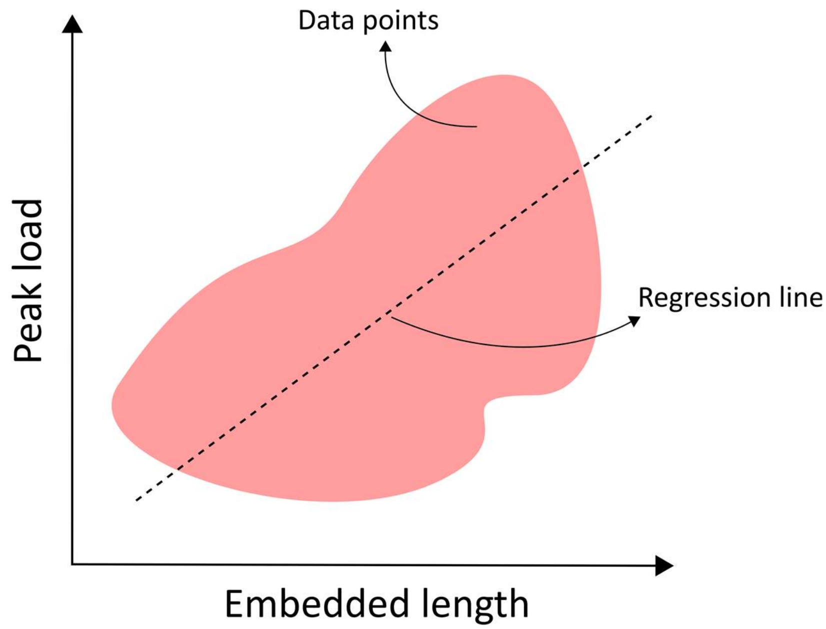

Figure 4-5: Linear interpolation to predict apparent IFSS.

4.4 Results and discussion

This section summarizes two sets of results describing the tensile properties of the recovered and virgin fibers, as well as their surface morphology and interfacial bonding with PLA.

4.4.1 Single fibre tensile test

Figure 4-6 shows the diameter distribution of the recycled glass fibers prior to the pyrolysis process. As seen, the recyclate compound consists of fibers featuring different diameters ranging between 12-21 µm. An average fiber diameter of approximately 17 µm was obtained and used for the strength and IFSS calculations.

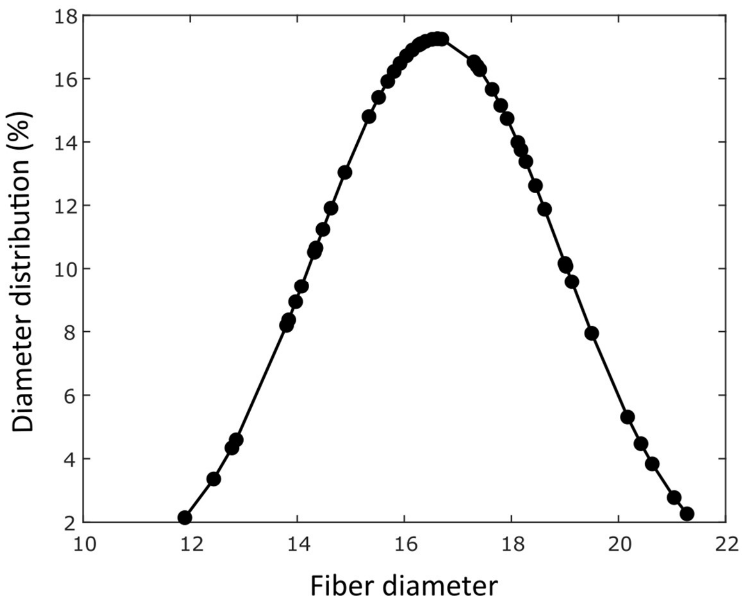

Figure 4-6: Diameter distribution of the recycled fibers.

SEM micrographs from the recycled and virgin fibers are shown in Figure 4-7. These images revealed that the ground fibers feature a higher surface roughness due to the presence of epoxy particles fractured off the adjacent fibers during the grinding process. On the other hand, SEM images from both pyrolyzed and virgin glass fibers showed a smoother surface when compared to the ground fibers. However, some regions with uneven impurities can still be identified on the surface of both fibers, e.g. virgin and pyrolyzed.

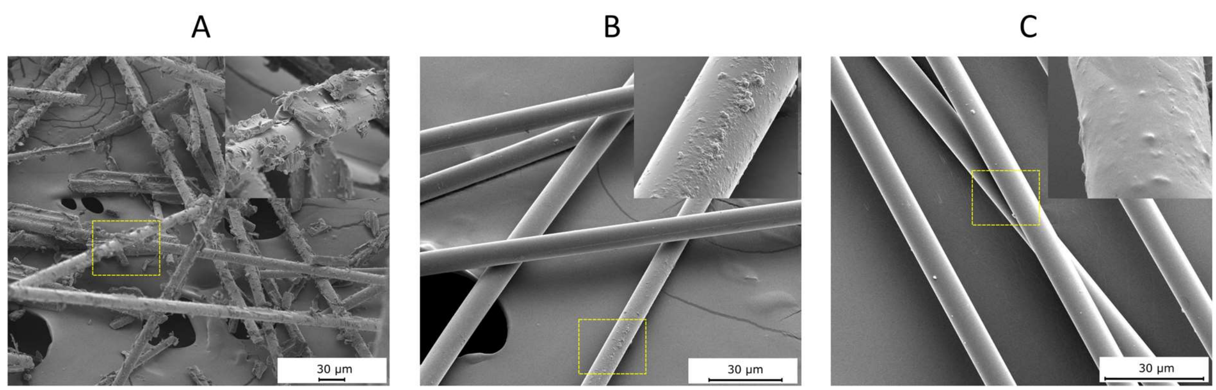

Figure 4-7: Surface morphology of the fibers: (A) ground fibers; (B) pyrolyzed fibers; (C) virgin fibers.

While SEM images clearly showed the rougher surface of the ground fibers compared to the virgin baseline fibers, atomic force microscopy (AFM) was used to accurately capture the surface topology of the recycled fibers and compare to that of virgin fibers. A JPL AFM machine (JPK

Nano-wizard@3 BioScience, Berlin, Germany) was used for surface imaging. Fibers were gently placed and glued to microscope glass slides, such that no movement occurred during the imaging process. The maximum lateral scan was focused on regions with area of 5 µm × 5 µm, and AFM images were obtained at a resolution of 512 × 512 pixels. The surface imaging was completed for 3 regions for a total of 3 samples for each fiber. Figure 4-8 shows representative AFM height images from the surface of the ground, pyrolyzed and virgin fibers. As observed, the surface of the ground fibers is covered with numerous lumps of different sizes caused by residue epoxy particles. The AFM images from the pyrolyzed fibers manifested a surface topology with a rug-like structure, which could be attributed to the removal of the silane coating during the pyrolysis. Further, some regions with large protrusions were detected on the surface of the pyrolyzed fibers. These lumps that were irregularly distributed throughout the surface of the fibers were attributed to the incompletely decomposed polymer resin left on the fibers surface. In contrast, the virgin fibers featured a homogenous and smooth surface topology compared to the pyrolyzed fibers. However, random heterogeneities were also detected at some regions, which could be attributed to the sizing tearing during the extraction process. To capture the roughness of the fibers, JPK data processing software was used to obtain the surface height diagrams along the fiber longitudinal axis. These diagrams were obtained at three different locations and then utilized to measure the average roughness (Ra), as well as the root mean square roughness (Rq). As shown in Table 4-1, the results demonstrated that the ground fibers feature a surface topography with an average roughness that is one order of magnitude larger than that of pyrolyzed and virgin fibers. In addition, the removal of the silane coating, as well as the presence of undecomposed epoxy particles on the surface of the pyrolyzed fibers have contributed to their higher surface roughness compared with the virgin fibers.

Table 4-1: The roughness results for the ground, pyrolyzed and virgin fibers.

	ground fibers			**Pyrolyzed fibers**			**Virgin fibers**		
	Right side	**Middle**	**Left side**	**Right side**	**Middle**	**Left side**	**Right side**	**Middle**	**Left side**
R_a (nm)	88.6	76.1	63.1	16.64	12.66	18.73	8.21	7.05	9.64
R_q (nm)	102.8	92.6	74.4	19.5	14.6	21.1	9.65	10	11.9

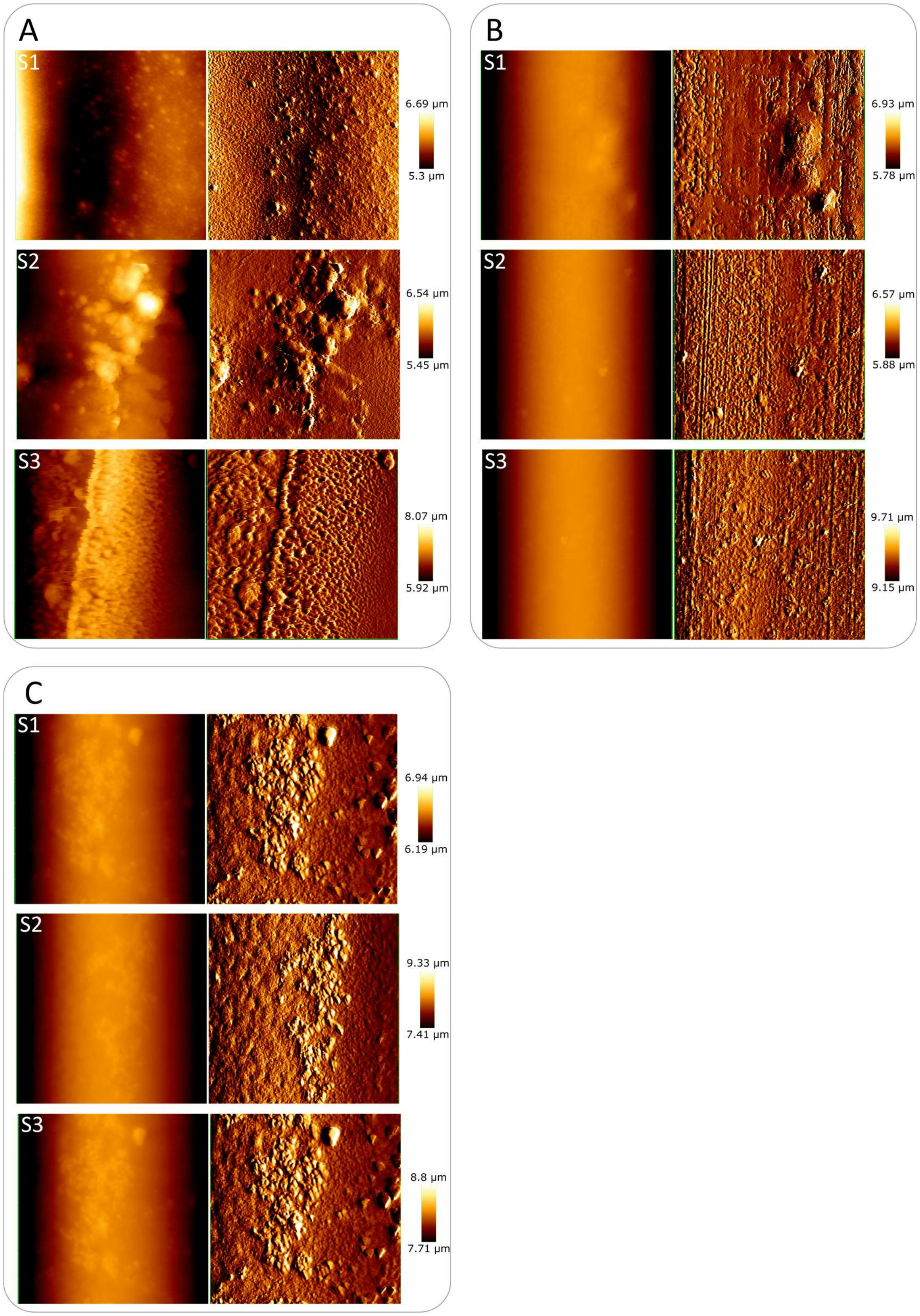

Figure 4-8: AFM height images showing the surface topology of the fibers: (A) ground fibers; (B) pyrolyzed fibers; (C) virgin fibers.

Figure 4-9 displays the tensile properties of the ground, pyrolyzed and virgin fibers versus the gage length. The error bars show the standard deviation (SD) of multiple tests. It should be noted that a smaller number of ground fibers with a gage length of 60 mm were successfully separated and tested owing to the ease of fiber breakage with these longer fibers. Hence, the results for this gage length were only included for completeness.

The mean fiber tensile properties, i.e. strength, stiffness, and strain to failure, along with the SD values are summarized in Table 4-2. As expected, the fibers showed a brittle failure mode with an average strength decreasing with the increase in the gage length. The mechanical behaviour of fibers is mainly governed by the distribution of defects on their surface such that shorter fibers feature lower quantities of surface flaws. On the other hand, fibers with larger surface area incorporate a larger number of extrinsic surface defects, which increases the chance of microcrack formation. Hence, SD values can be mainly attributed to the variation of flaw distribution on the surface of fibers. As shown in Table 4-2, the average strength of the ground fibers reduced by 15 % with an increase in the gage length from 20 mm to 40 mm. As well, increasing the gage length from 20 mm to 60 mm led to a reduction of 30 % in the mean strength of the pyrolyzed fibers. In addition to strength, the ductility of the fibers with a gage length of 60 mm was remarkably lower than that of fibers with a gage length of 20 mm for both ground and pyrolyzed fibers. Compared with ground fibers, it is noticeable that the pyrolyzed fibers showed lower ultimate strength with values decreased by 50 % and 52 % for the 20 and 40 mm gage lengths, respectively. While removing the surface impurities, e.g. epoxy residue, is expected to improve the strength, this reduction can be attributed to the degradation of E-glass fibers at high temperatures used in pyrolysis [25-27]. We also observed that pyrolyzed fibers are much more brittle compared to the ground fibers with failure strain reduced by 47 % and 56 % for the 20 and 40 mm gage lengths, respectively.

Table 4-2: Mechanical properties of the ground, pyrolyzed and virgin fibers.

Properties	**Mean strength (MPa)**			**Mean stiffness (GPa)**			**Mean strain to failure (%)**		
Gage length (mm)	20	40	60	20	40	60	20	40	60
Ground fibers	1990 ± 568	1678 ± 580	876 ± 377*	76 ± 13	74 ± 12	74 ± 11*	2.32 ± 0.6	2.1 ± 0.7	1.1 ± 0.5*
Pyrolyzed fibers	976 ± 260	806 ± 217	679 ± 122	84 ± 12	89 ± 10	91 ± 22	1.23 ± 0.3	0.93 ± 0.17	0.77 ± 0.13
Virgin fibers	2485 ± 508	2073 ± 251	1965 ± 353	71 ± 7	74 ± 9	77 ± 8	3.5 ± 0.6	2.8 ± 0.3	2.7 ± 0.5

*The asterisk symbol shows the results that were obtained with lower number of samples

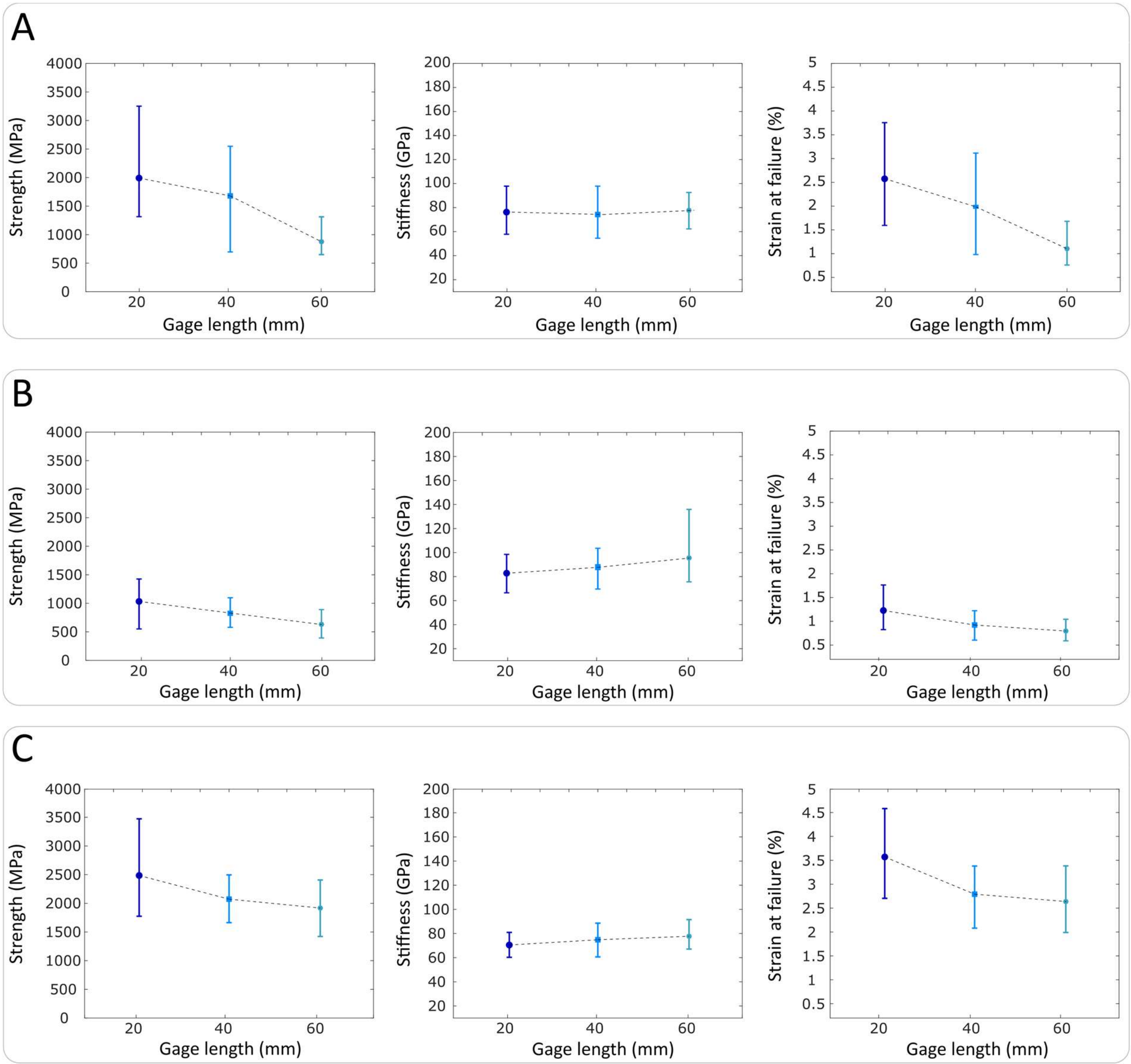

Figure 4-9: Strength, stiffness and failure strain of the fibers: (A) ground fibers; (B) pyrolyzed fibers; (C) virgin fibers.

As a baseline, the tensile properties of the virgin fibers were characterized and summarized in Table 4-2. The average tensile properties reported in the literature align well with those herein measured [28]. As seen, a similar trend appeared in the mechanical properties of the virgin fibers, such that an increase in the gage length was associated with a reduction in the tensile strength and ductility. As expected, virgin fibers exhibited the highest tensile strength with an average value 20 % and 19 % higher than that of ground fibers with gage lengths of 20 mm and 40 mm, respectively.

Compared with the pyrolyzed fibers, virgin fibers showed 60 %, 61 % and 65 % higher values in tensile strength for gage lengths of 20 mm, 40 mm and 60 mm, respectively.

As per the elastic modulus, pyrolyzed fibers showed higher stiffness compared with ground fibers with values improved by 9 % and 17 % for the 20 and 40 mm gage lengths, respectively. The disparity in the stiffness values can be attributed to the molecular network compaction that happens during the pyrolysis process resulting in an increase in the density of the fibers, thereby improving the stiffness [29]. Nevertheless, the mean stiffness of the ground fibers at different gage lengths was comparable with that of virgin fibers, indicating that no degradation in the stiffness of the fibers occurs after mechanical recycling. In contrast to strength, it is demonstrated in the literature that fibers with longer gage length tend to show higher modulus [30]. This behaviour is mainly due to the fact that increasing the gage length is associated with a higher rate of reduction in the ductility of fibers as compared with their ultimate strength. Despite some variations, we observed the same trend in the pyrolyzed and virgin fibers, where the mean stiffness value somewhat increased by increasing the gage length. On the other hand, the ground fibers showed a larger variation in the stiffness results such that the mean stiffness value for different gage lengths remained at the same level.

As shown in Figure 4-10, the non-uniform distribution of the epoxy particles, as well as the surface damage caused by grinding lead to a more dispersed defect distribution on the surface of the ground fibers as compared to virgin and pyrolyzed fibers. The amount of resin residue on the surface of the ground fibers varies from one fiber to another, a variation that influences the tensile performance of the fibers. This irregular defect distribution results in variable surface topographies, particularly for fibers with short gage length. Depending upon the surface flaw distribution, on one hand, the presence of the epoxy residue could be beneficial to the performance of the ground fibers as the surface pitting are filled with epoxy, thus microcracks formed around these spots tend to propagate through the epoxy particles due to their weaker mechanical properties compared to glass fiber. On the other hand, the bulk epoxy protrusions could serve as surface defects by changing the local geometry of the fibers and generating stress concentration. In addition, the presence of epoxy could impact the surface deformation rate of the fibers, when subjected to axial loads. The varying distribution of the epoxy residue could be the major cause for the large variations in the tensile properties of the ground fibers with different gage lengths.

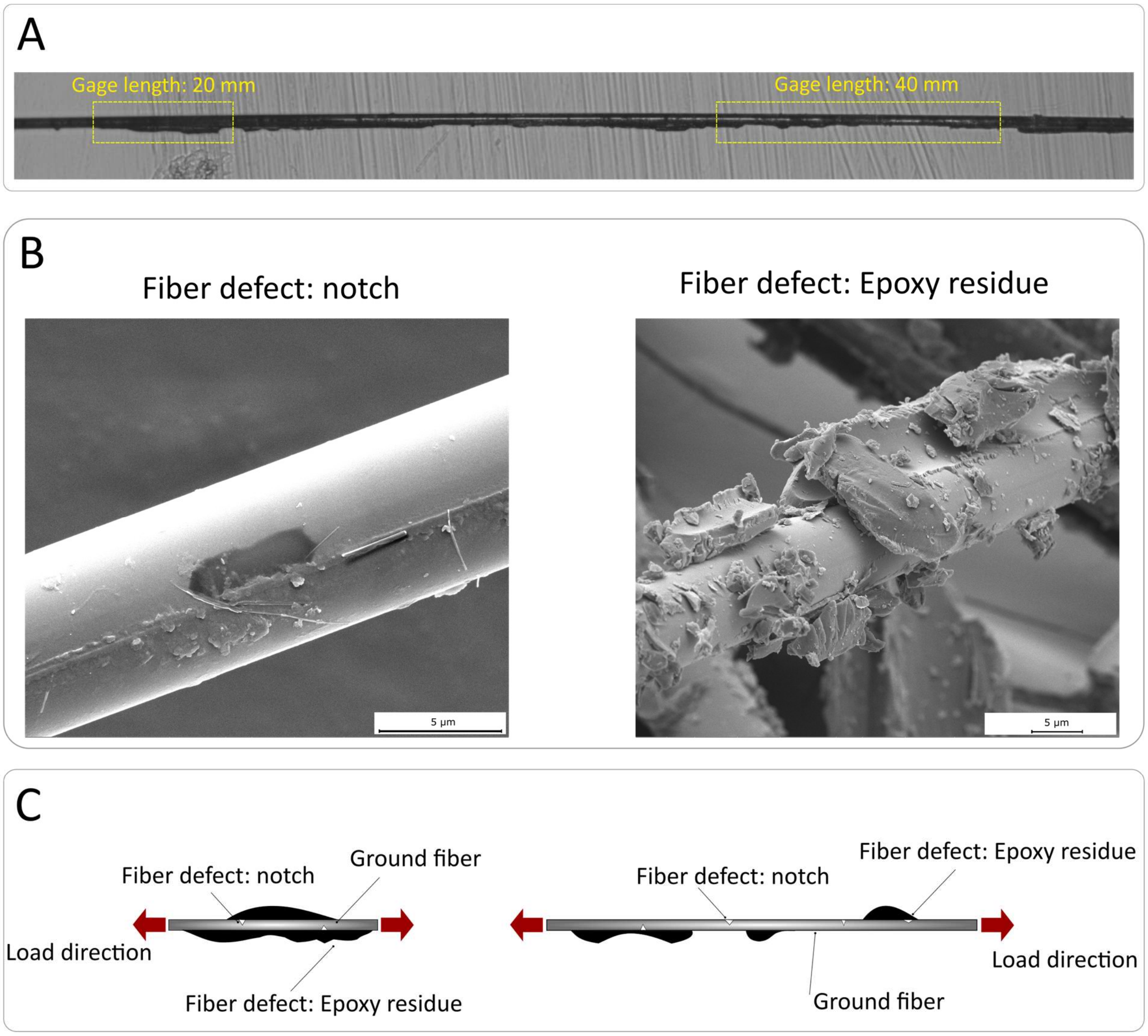

Figure 4-10: Different types of defects present on the surface of ground fibers: (A) microscopic image from a long single ground fiber; (B) defects present on the surface of the ground fiber; (C) schematic showing the distribution of defects on the surface of a 20 mm and 40 mm ground fiber.

To represent the distribution of the strength data obtained for the recycled fibers, a two-parameter Weibull function is used as follows:

$$P_{\sigma_a} = 1 - exp[-(\frac{L}{L_o})(\frac{\sigma_a}{\sigma_o})^w] \tag{4-3}$$

where P_{σ_a} is the cumulative probability of fiber failure for a gage length of L and at a stress level lower than or equal to σ_a , and L_o is the reference length. σ_o and w denote the Weibull scale and shape parameters, respectively. To find the Weibull parameters, the strength data for each gage length is sorted in an ascending order and a probability function is used to identify the probability of fiber failure for the ith strength point, as follows:

$$P_{\sigma_i} = \frac{i - a}{N - b} \tag{4-4}$$

where N represents the total number of strength data points. Also, a and b are statistical parameters with a value of 0.5 and 0, respectively [21]. To obtain the Weibull parameters, Eq. 4-3 is rearranged, and logarithm of both sides is taken to define the following relation:

$$\ln\left[-\ln\left(1 - P_{\sigma_a}\right)\right] = wln(\sigma) - wln(\sigma_o) \tag{4-5}$$

It should be noted that in Eq. 4-3, the scale parameter is defined as fiber strength at a gage length identical to the reference length. Figure 4-11, 4-12 and 4-13 show, respectively, a plot of $\ln\left[-\ln\left(1 - P_{\sigma_a}\right)\right]$ versus $ln(\sigma)$ for the ground, pyrolyzed and virgin fibers, where the slope and the y-intercept are used to determine the Weibull shape and scale parameters, respectively. Due to the low data points for the ground fibers with the gage length of 60 mm, the Weibull plot is not shown. As seen, a satisfactory agreement between the Weibull regression line and the tensile results is observed for all the fiber systems.

The Weibull shape (w) and scale parameter (σ_o) for the ground, pyrolyzed and virgin fibers are summarized in Table 4-3. As observed, the virgin fibers feature the largest scale and shape parameters, indicating the highest properties with the lowest scatter. In addition, the pyrolyzed fibers feature a larger shape parameter compared to the ground fibers, indicating a narrower distribution of the strength data. The difference in the strength distribution is in agreement with the results of previous works [31]. The large variation in the strength results of the ground fibers arises from the random distribution of the epoxy particles, as well as the surface damage caused by grinding. Noticeably, the scale parameter for the ground fibers with a gage length of 20 mm shows that 63% of the ground fibers fractured with an average strength level of above 2190 MPa, a value that is comparable to that of virgin fibers with only 18 % difference. This observation highlights that due to the lower stiffness of epoxy as compared to glass fiber, the role of the resin residue in lowering the strength by generating stress concentration spots is not only negligible, but also critical to the retention of fiber strength by filling up the surface defects. In contrast, the pyrolyzed fibers exhibited lower characteristic strength compared to that reported in the literature [31]. This reduction could be attributed to the excessive damage caused to the fibers during the grinding process.

Table 4-3: The Weibull parameters for the ground, pyrolyzed and virgin fibers with different gage lengths.

	Ground fibers		**Pyrolyzed fibers**			**Virgin fibers**		
Gage length (mm)	20	40	20	40	60	20	40	60
Scale parameter (σ_o)	2190	1892	1073	904	729	2700	2178	2106
Shape parameter (w)	4.22	2.94	4.25	3.78	6.27	5.8	9.87	6.6

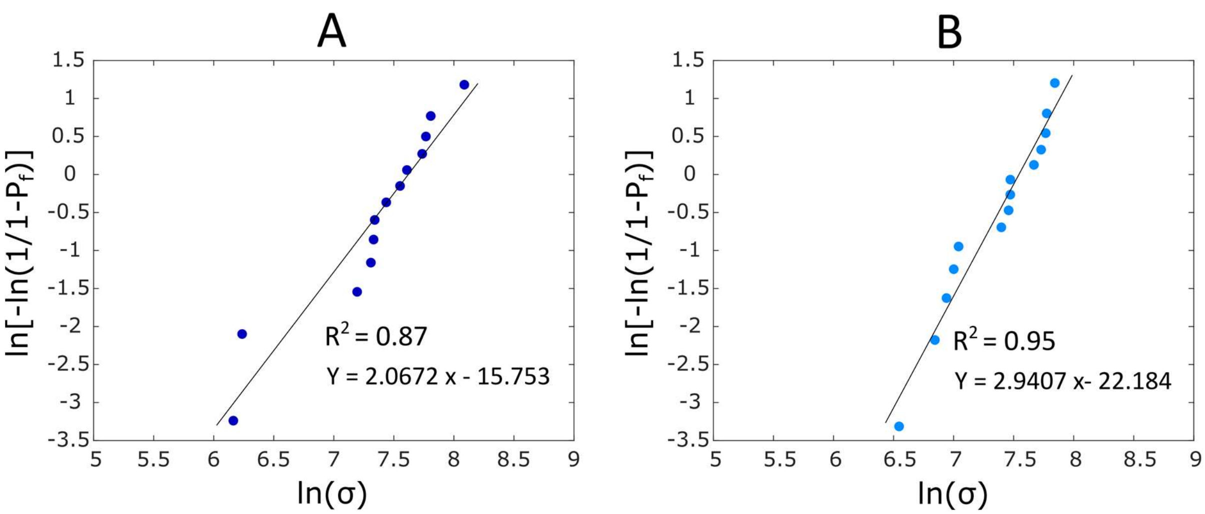

Figure 4-11: Weibull function plot for single ground glass fibers with different gage lengths: (A) 20 mm; (B) 40 mm.

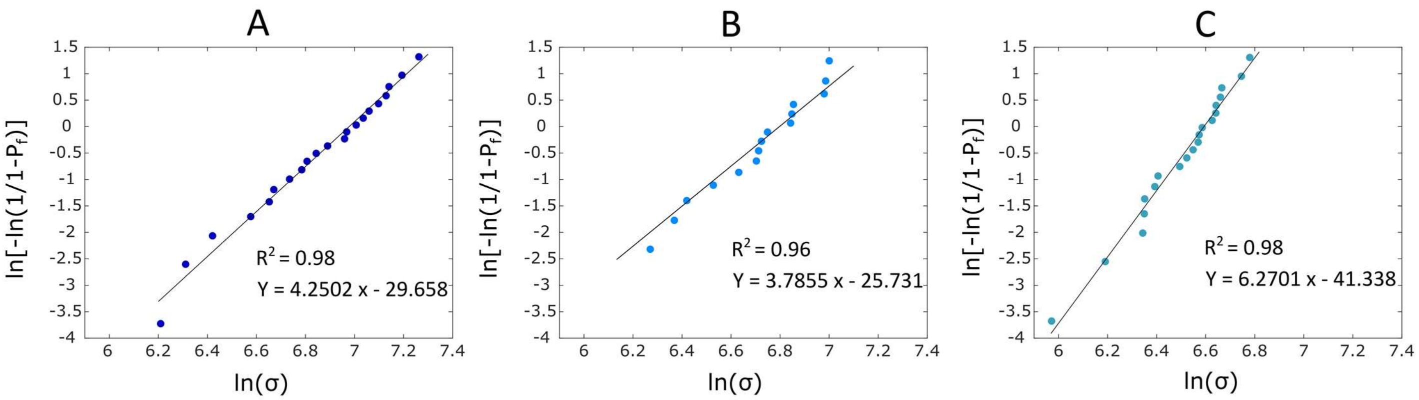

Figure 4-12: Weibull function plot for single pyrolyzed glass fibers with different gage lengths: (A) 20 mm; (B) 40 mm; (C) 60 mm.

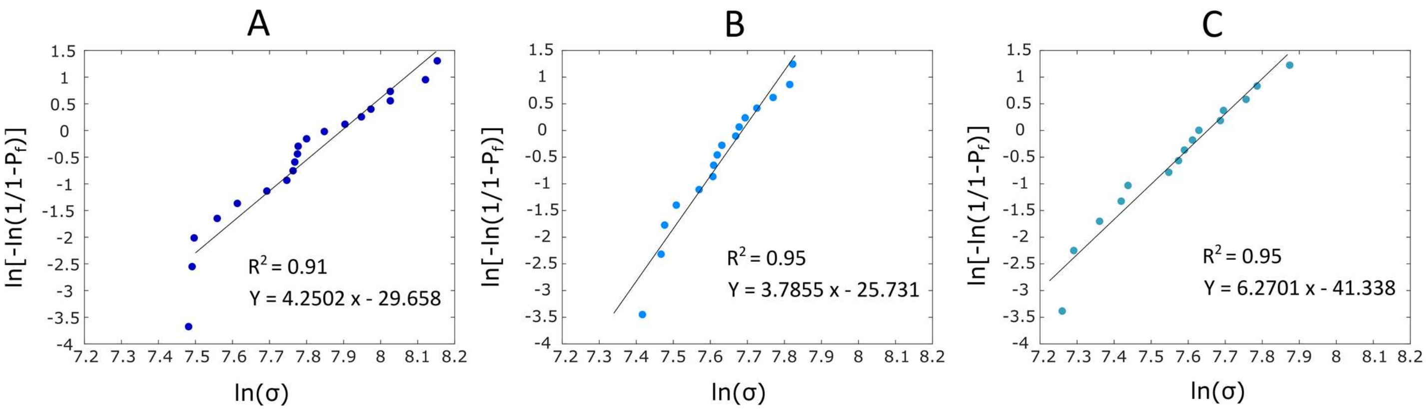

Figure 4-13: Weibull function plot for single virgin glass fibers with different gage lengths: (A) 20 mm; (B) 40 mm; (C) 60 mm.

4.5 Single fiber pull-out test

The maximum load versus embedded length results from the pull-out test of the recycled fibers (ground and pyrolyzed) and the virgin glass fibers are plotted in Figure 4-14. A representative force-displacement curve for each fiber type is presented, as well. The force-displacement curves show a typical behaviour observed in pull-out tests, where the debonding process initiates immediately at peak load and following the interfacial failure, the load drops down to near zero. As shown in Figure 4-14A, continuing the test leads to a minor increase in the load, which corresponds to the frictional force developed at the interface.

Using the slope of the regression lines in Figure 4-14 and Eq. 4-2, the apparent IFSS value for the virgin, ground, and pyrolyzed fibers are calculated (Table 4-4). The results confirmed a stronger interfacial bonding between the ground fibers and PLA, featuring an IFSS higher than the pyrolyzed and virgin glass fibers by 14 % and 26 %, respectively. The larger IFSS for the ground fibers relative to virgin and pyrolyzed fibers stems from the epoxy matrix residues, which increase the fibers surface roughness and allow for better molecular mechanical interactions and interlocking. In addition, epoxy molecules can chemically interact with PLA molecules through the development of hydrogen bonding, which could further improve the apparent IFFS around the ground fibers [32]. The results also showed that the pyrolyzed fibers feature a higher IFSS compared with virgin glass fibers, a result that correlates with the higher surface roughness of the pyrolyzed fibers. The larger IFSS around the pyrolyzed fibers also elucidates the negligible effect of the silane coating on the interfacial bonding. This observation matches well with previous investigations on the effect of silane coating on the properties of composites made of pyrolyzed fibers from wind turbine blades [33]. It is well demonstrated in the literature that sizing coating should be optimized for a specific fiber and resin matrix to improve the interfacial chemical bonding. Herein, the silane sizing present on the surface of virgin E-glass fibers was optimized for epoxy, thus it does not necessarily contribute to any chemical reactions at the interface with PLA.

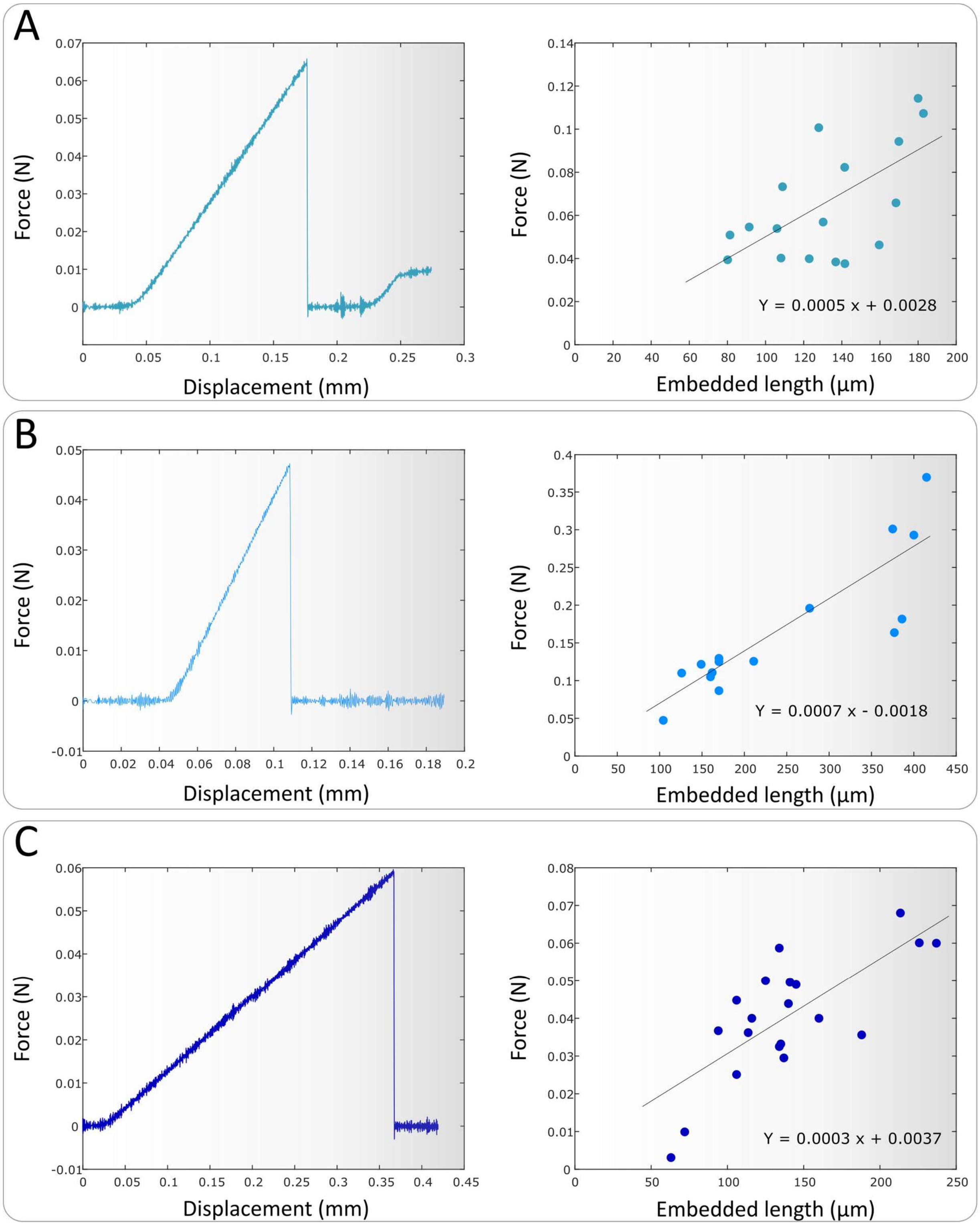

Figure 4-14: Representative force-displacement curve and peak force vs. embedded length plots of single fiber pull out test for PLA and: (A) Pyrolyzed fibers; (B) ground fibers and (C) virgin fibers.

One important factor determining the final properties of short fiber composite structures is the critical length of fiber reinforcements. To efficiently use the maximum fibers strength, the length of the fibers should be larger than the minimum required critical length. Further, it is shown in the literature that fibers shorter than critical length could serve as defects, lowering the strength of the composite relative to pure resin material [34]. The critical length of fibers can be predicted using the fibers strength and interfacial shear strength as:

$$l_c = \frac{\sigma_f d}{2\tau} \tag{4-6}$$

where σ_f, d and τ are the fiber strength, fiber diameter, and the interfacial shear strength, respectively. Considering the large variation observed in the recycled fibers strength, a lower and upper bound critical length can be predicted. Table 4-4 shows the values for the critical length of the recycled fibers. These results can provide insight into the minimum required fiber length to achieve effective strengthening and stiffening using the recycled fibers. As can be seen, the ground fibers feature a wider range with a larger upper bound compared with pyrolyzed ones. This indicates that longer ground fibers should be utilized to obtain composites with efficient mechanical properties.

An extensive amount of literature has investigated the critical role of interface shear strength on the failure mechanism and final properties of composites [35, 36]. Previous works have shown that a strong fiber-matrix interface can enhance the fiber load carrying contribution in the composite, thus increasing the tensile properties of the composite [37]. With tensile properties comparable with virgin fibers, the capability of the ground fibers to form a strong adhesion with PLA enables the fabrication of effective composites out of short fibers extracted from end-of-life scrap blades. In a comparative study between short fiber composites made of ground fibers from end-of-life wind turbine blades and virgin fibers, the mechanical properties of recycled composites have been successfully characterized [15]. The ground and virgin short fibers used in this investigation shared identical dimensional properties, i.e. fiber length distribution and fiber diameter. As a result, the differences between the mechanical properties of the composites were exclusively ascribed to their micro-mechanical properties, namely fiber properties and interface strength. The results from this investigation demonstrated that the recycled composites made of ground fibers feature tensile strength and stiffness that are, respectively, 19% and 18 % higher than those of composites made from virgin fibers. This previous work therefore demonstrates the potential of mechanically recycled fibers from scrap wind turbine blades in manufacturing composites with effective properties.

Table 4-4: The value of IFSS and critical length for the ground and pyrolyzed fibers.

Fiber type	**τ_{d1} (MPa)**	**R^2**	**Critical length, lower bound l_c (mm)**	**Critical Length, upper bound l_c (mm)**
Virgin fibers	9.54	0.57	0.97	1.2
Ground fibers	13.01	0.75	0.57	1.14
Pyrolyzed fibers	11.23	0.51	0.54	0.78

4.6 Conclusion

In this work, we have focused on the tensile and interfacial characterization of recovered fibers from end-of-life wind turbine blades. The single fiber tensile and pull-out tests were employed to characterize the tensile properties of mechanically and thermally reclaimed fibers, as well as the interface strength between the recovered fibers and PLA. The results from the single fiber tensile test revealed that the tensile strength of the pyrolyzed fibers relative to the ground fibers has experienced a significant reduction of 50 % and 52 % for, respectively, 20 mm and 40 mm gage lengths. The stiffness of the pyrolyzed fibers with a gage length of 20 mm and 40mm, on the other hand, were 9 % and 17 % higher than those of the ground fibers, respectively. This observation is mainly attributed to the silica network compaction of the glass fibers, which results in higher density. In terms of the interfacial strength, the ground fibers showed an IFSS, 14 % and 26 % stronger than pyrolyzed and virgin glass fibers, respectively. Differences in the IFSS values result from the irregular lumps from epoxy residue on the surface of the ground fibers, a phenomenon which allows for molecular mechanical and chemical interactions. Using the IFSS and fibers strength values, a critical length rang of 0.57-1.14 mm and 0.54-0.78 mm were calculated for the ground and pyrolyzed fibers, respectively. These ranges can be used to design and analyze short recycled fibrous composites with effective mechanical properties.

Given this work has shown the relative merit of mechanically recycled fibers from scrap turbine blades over the pyrolyzed and virgin fibers, further experimental works are required to account for the effect of thermal and oxidative degradations on the IFSS. Due to inevitable variations in the resin residue on the surface of mechanically recycled fibers, future work on the exact macro-mechanical analysis of composites made of recycled fibers is proposed. The critical fiber length values obtained in this study can be validated by manufacturing and testing polymer composites reinforced with recycled fibers.

4.7 Acknowledgments

A.R gratefully acknowledges Mr. Guangyu Bao and Biomechanics research laboratory for technical assistance with AFM. L.L and K.F acknowledge the funding provided by the Research Center for High Performance Polymer and Composite Systems (CREPEC), Project Vision; and The Natural Sciences and Engineering Research Council of Canada (NSERC), RGPIN- 2018-04144.

4.8 References

[1] Yang L, Thomason JL. Interface strength in glass fibre–polypropylene measured using the fibre pull-out and microbond methods. Composites Part A: Applied Science and Manufacturing. 2010;41(9):1077-83.

[2] Jang J, Yang H. Effect of surface treatment on the performance improvement of carbon fiber/polybenzoxazine composites. Journal of Materials Science. 2000;35:2297-303.

[3] Petersen HN, Kusano Y, Brøndsted P, Almdal K. Preliminary characterization of glass fiber sizing. Proceedings of the Risø International Symposium on Materials Science; 2013. p. 333-40.

[4] Cousins DS, Suzuki Y, Murray RE, Samaniuk JR, Stebner AP. Recycling glass fiber thermoplastic composites from wind turbine blades. Journal of Cleaner Production. 2019;209:1252-63.

[5] Larsen K. Recycling wind turbine blades. Renewable Energy Focus. 2009;9(7):70-3.

[6] Feih S, Manatpon K, Mathys Z, Gibson AG, Mouritz AP. Strength degradation of glass fibers at high temperatures. Journal of Materials Science. 2009;44(2):392-400.

[7] Ginder RS, Ozcan S. Recycling of Commercial E-glass Reinforced Thermoset Composites via Two Temperature Step Pyrolysis to Improve Recovered Fiber Tensile Strength and Failure Strain. Recycling. 2019;4(2):24.

[8] Nzioka AM, Kim YJ. Surface analysis of glass fibres using XPS and AFM: case study of glass fibres recovered from the glass fibre reinforced polymer using chemical recycling. Journal of Physics: Conference Series. 2018;953:012012.

[9] Cunliffe AM, Jones N, Williams PT. Pyrolysis of composite plastic waste. Environ Technol. 2003;24(5):653-63.

[10] Thomason J, Jenkins P, Yang L. Glass Fibre Strength—A Review with Relation to Composite Recycling. Fibers. 2016;4:18.

[11] Guo CC, Zhao Y, Chen D, Zhan MS. Effect of sizing agent on interfacial shear strength of carbon fibre composites. Materials Research Innovations. 2014;18(sup4):S4-997-S4-1002.

[12] Palmer J, Ghita O, Savage L, Evans K. Successful closed-loop recycling of thermoset composites. Composites Part A: Applied Science and Manufacturing. 2009;40(4):490-8.

[13] Chu J, Sullivan J. Recyclability of a continuous e-glass fiber reinforced polycarbonate composite. Polymer composites. 1996;17(4):556-67.

[14] Rahimizadeh A, Kalman J, Fayazbakhsh K, Lessard L. Recycling of fiberglass wind turbine blades into reinforced filaments for use in Additive Manufacturing. Composites Part B: Engineering. 2019;175:107101.

[15] Rahimizadeh A, Kalman J, Henri R, Fayazbakhsh K, Lessard L. Recycled Glass Fiber Composites from Wind Turbine Waste for 3D Printing Feedstock: Effects of Fiber Content and Interface on Mechanical Performance. Materials. 2019;12(23):3929.

[16] Shrivastava A. 4 - Additives for Plastics. In: Shrivastava A, editor. Introduction to Plastics Engineering: William Andrew Publishing; 2018. p. 111-41.

[17] Mallick PK. 13 - Testing the fatigue strength of fibers used in fiber-reinforced composites using fiber bundle tests. In: Guedes RM, editor. Creep and Fatigue in Polymer Matrix Composites: Woodhead Publishing; 2011. p. 409-23.

[18] Ibrahim I, Sarip S, Bani NA, Ibrahim MH, Hassan MZ. The Weibull probabilities analysis on the single kenaf fiber. AIP Conference Proceedings. 2018;1958(1):020009.

[19] Penn LS, Lee SM. Interpretation of the force trace for Kevlar/epoxy single filament pull-out tests. Fibre Science and Technology. 1982;17(2):91-7.

[20] Herrera-Franco PJ, Drzal LT. Comparison of methods for the measurement of fibre/matrix adhesion in composites. Composites. 1992;23(1):2-27.

[21] Burn DT, Harper LT, Johnson M, Warrior NA, Nagel U, Yang L, et al. The usability of recycled carbon fibres in short fibre thermoplastics: interfacial properties. Journal of Materials Science. 2016;51(16):7699-715.

[22] Cox HL. The elasticity and strength of paper and other fibrous materials. British Journal of Applied Physics. 1952;3(3):72-9.

[23] Mäder E, Freitag KH. Interface properties and their influence on short fibre composites. Composites. 1990;21(5):397-402.

[24] Choi N-S, Park J-E. Fiber/matrix interfacial shear strength measured by a quasi-disk microbond specimen. Composites Science and Technology. 2009;69(10):1615-22.

[25] Anane-Fenin K, Akinlabi E. Recycling of Fibre Reinforced Composites: A Review of Current Technologies: 4th International Conference on Development and Investment in Infrastructure - Strategies for Africa; 2017.

[26] Cunliffe AM, Jones N, Williams PT. Pyrolysis of composite plastic waste. Environmental Technology. 2003;24(5):653-63.

[27] Thomason JL, Kao CC, Ure J, Yang L. The strength of glass fibre reinforcement after exposure to elevated composite processing temperatures. Journal of Materials Science. 2014;49(1):153-62.

[28] Kennerley J, Kelly R, Fenwick N, Pickering S, Rudd C. The characterisation and reuse of glass fibres recycled from scrap composites by the action of a fluidised bed process. Composites Part A: Applied Science and Manufacturing. 1998;29(7):839-45.

[29] OTTO WH. Compaction Effects in Glass Fibers. Journal of the American Ceramic Society. 1961;44(2):68-72.

[30] Naik DL, Fronk TH. Weibull distribution analysis of the tensile strength of the kenaf bast fiber. Fibers and Polymers. 2016;17(10):1696-701.

[31] Ginder RS, Ozcan S. Recycling of Commercial E-glass Reinforced Thermoset Composites via Two Temperature Step Pyrolysis to Improve Recovered Fiber Tensile Strength and Failure Strain. Recycling. 2019:Medium: ED; Size: Article No. 24.

[32] Brydson JA. 26 - Epoxide Resins. In: Brydson JA, editor. Plastics Materials (Seventh Edition). Oxford: Butterworth-Heinemann; 1999. p. 744-77.

[33] Group SM. Recycling of waste glass fiber reinforced plastic with microwave pyrolysis (LIFE07 ENV/S/000904). Stena recycling, Göteborg, Sweden2012.

[34] Bolduc S, Jung K, Venkata P, Ashokcline M, Jayasinghe R, Baillie C, et al. Banana fiber/low-density polyethylene recycled composites for third world eco-friendly construction applications – Waste for life project Sri Lanka. Journal of Reinforced Plastics and Composites. 2018;37(21):1322-31.

[35] Unterweger C, Brüggemann O, Fürst C. Effects of different fibers on the properties of short-fiber-reinforced polypropylene composites. Composites Science and Technology. 2014;103:49-55.

[36] Yang QS, Liu X. 13 - Mechanical behavior of extra-strong CNT fibers and their composites. In: Qin Q, Ye J, editors. Toughening Mechanisms in Composite Materials: Woodhead Publishing; 2015. p. 339-72.

[37] Liu BY, Wang XJ, Liu HY, Zhang G, Long SR, Yang J, et al. Effect of silane coupling agent and air plasma treatment on interfacial shear strength of carbon fiber/polyphenylene sulfide composites. In: Ye L, editor. Recent Advances in Structural Integrity Analysis - Proceedings of the International Congress (APCF/SIF-2014). Oxford: Woodhead Publishing; 2014. p. 365-9.

Link between Chapter 4 and Chapter 5

Chapter 4 exclusively investigated single fibers extracted from old wind turbine blades through the two most commonly used composite recycling techniques, namely thermal and mechanical recycling. In addition to showing the merits of mechanical grinding, which leads to recycled fibers featuring higher tensile properties, this chapter characterized the approximate critical length of mechanically recycled fibers, a characteristic that can be incorporated into recycling schemes developed for rotor blades to obtain fibers that can be used to design composites with efficient strength and stiffness. Inspired by this study, next chapter aims to combine all the key elements of recycling and micromechanical techniques to mitigate the knockdown of strength that we observed in Chapter 3 and investigate the feasibility of producing value-added products from second-hand glass fibers out of old rotor blades. Furthermore, a finite element model that enables the prediction of mechanical properties of newly fabricated recycled parts is developed and assessed.

Chapter 5

Mechanical and thermal study of composite filaments from wind turbine waste for 3D printing

5

Chapter 5: Mechanical and thermal study of composite filaments from wind turbine waste for 3D printing

Amirmohammad Rahimizadeh[a], Jordan Kalman[b], Kazem Fayazbakhsh[b,*], Larry Lessard[a]

[a] Department of Mechanical Engineering, McGill University, Montreal, QC H3A0C3, Canada

[b] Department of Aerospace Engineering, Ryerson University, Toronto, Ontario M5B2K3, Canada

[*]Corresponding author: kazem@ryerson.ca; Tel: (+1) 416-979-5000 ext. 6414; fax: (+1) 416-979-5056

Article under review

5.1 Abstract

The wind energy industry has recently confronted the issue of overwhelming numbers of used composite wind turbine blades, which are now being sent to landfills. The subject of composite waste from the rotor blades has become more serious and challenging. This work presents a recycling solution that motivates composite recycling through a step-by-step process, which ends up in structurally stiff and strong recycled parts. Inspired by the recent popularity of the 3D printing industry, we present a novel class of 3D printing feedstock, which offers, respectively, 20% and 28 % enhancement in the tensile strength and stiffness of the currently available pure thermoplastic feedstock materials on the market and can also compete with virgin fiber reinforced filaments. The mechanical performance of the newly introduced recycled parts is assessed through mechanical testing and accurately predicted by a coherent set of finite element simulations.

Keywords: The wind energy industry, wind turbine blades, 3D printing, fiber reinforced filaments.

5.2 Introduction

Wind turbines, which are meant to contribute to a sustainable production of energy, are producing many tonnes of waste [1, 2]. The global pledge of governments and corporations has led to an incredible growth in the wind energy industry, a trend that is predicted to entirely replace conventional fossil fuels with clean energy in less than 30 years [3]. As a carbon-free source of power, 85% of wind turbines are made of recyclable materials, such as steel and copper [4]. Nevertheless, the use of fiberglass composites in the rotor blades with the goal of enhancing their efficiency has brought the wind industry a serious challenge in terms of waste generation. While the problem of composite waste from wind turbines has been virtually ignored for many years, the increasingly growing number of decommissioned blades is now turning into a serious issue, which not only will affect the wind energy industry, but also the entire Ecco-system [5-7].

With blades limited to a lifespan of 20-25 years, Europe is predicted to be dealing with around 3800 blades every year through 2020, and the U.S. will have to dispose of 8000 blades in each of the next four years [3]. Most of these old blades represent installations that date back to more than a decade ago, when the total installed capacity was one fifth of what it is today. Despite the current global concern about the incoming waste from the wind industry, the majority of the end-of-life blades end up in landfills, where leachates from them infiltrate the soil and ground water and pollute the living environment of thousands of creatures [8-10]. Currently, the landfill cost stands at around 150-170 USD per tonne and a sharp increase in the landfill tax is to be expected [11]. Many countries in Europe such as Germany and France have heavily restricted the landfilling of rotor blades with the aim of increasing the recycling rates and reducing the quantity of municipal waste that can go to landfills to 10%. Several routes to reuse the old blades are proposed in the literature, among which cement kiln, incineration, and mechanical recycling to fine filler represent the most commonly used ones [11, 12]. Although extremely promising, the low value of the resulting products coupled with their expensive manufacturing processes has adversely impacted the global interest in reusing the rotor blades. However, the recent environmental legislation has motivated researchers to seek solutions that could gain value from blade recyclates. In parallel, the lack of a mature and viable recycling system for fiberglass composites has steered the wind energy industry towards finding clean solutions to deal with waste blades.

While some researchers and industrial companies have studied the potential of thermal and chemical recycling techniques for blades at pilot or lab scales, they fall short to be considered as profitable solutions due to the high sensitivity of glass fiber to the temperatures used in these processes [13-15]. The property degradation associated with these techniques lowers their viability and commercialization potential for the blade recycling. A recent study has used a microwave assisted chemical technique to recover glass fibers with minimal degradation in properties. This process, however, involves the use of different solvents that can lower its potential at large scale processes [16]. Nonetheless, mechanical grinding still remains a feasible recycling solution, which can be used to simply transform the blade fiberglass waste into short glass fibers [17, 18]. Although short fiber composites exhibit lower mechanical performance when compared with continuous ones, their versatile properties and mass production classify discontinuous composites as an attractive material. New application sectors, such as additive manufacturing, have recently opened-up for them and could be deemed as a potential market for recycled fibers [19-22].

To tackle the blade waste problem, a novel class of fused filament fabrication (FFF) filaments was introduced by the authors, in which short glass fibers recovered from old blades were successfully used to build structurally stiff parts via the 3D printing process [23, 24]. In these previous works, a classification operation was performed to classify the recyclate into different grades featuring different fiber contents and fiber length, and only recovered fibers with an average length below 0.4 mm were utilized. Although enhancement in the stiffness of the 3D printed parts was achieved, the samples lost their original strength due to two main reasons: first, the use of fibers below the critical length; second, due to the presence of old matrix powder inside the recyclate, which generated stress concentration regions. The more recent investigation resorted to micromechanical analysis and experimental testing to characterize the ground fibers and roughly determine the minimum critical fiber length [25]. In the previous studies, the work was also limited to an experimental investigation of the recycled parts. The development of a micromechanical finite element (FE) model of recycled parts can provide a platform for virtual testing, which can facilitate the design process and material assessment.

This study presents a methodology that benefits from micromechanical analysis to use the old wind turbine blades in a systematic recycling system, which aims at producing value-added products. An FE model coupled with a homogenization method is developed to predict the mechanical properties of the 3D printed samples. The developed model comes in handy for a rapid prediction of the properties and selection of an appropriate application accordingly. In addition, an experimental investigation is carried out to study the mechanical performance of the recycled parts and validated the FE model. The experimental observations along with the FE results are then compared with established analytical models for discontinuous composites to further assess the mechanical performance of the newly manufactured recycled composites.

5.3 Methodology

Our recycling methodology is founded on grinding, a conventional mechanical recycling technique. Along this path, we benefit from micromechanical analysis and multiple classification operations to obtain fibers that can be used as reinforcement. This section will first detail our recycling solution and mechanical characterization, and then the modeling of the microstructure of the recycled composite parts using FE and homogenization techniques is described. Eventually, two well-established analytical models that are used for a comparative study are explained.

5.3.1 Recycling of used wind turbine blades

The main focus of this investigation lies in developing a novel recycling methodology to produce value-added products out of used wind turbine blades. To achieve this goal, we have created a new recycling scheme that benefits from mechanical grinding to recover the blade glass fibers with minimum knockdown in the properties. Fibers recovered through mechanical recycling typically retain old matrix residue, a phenomenon that highly increases the surface roughness of the fibers and influences their mechanical properties. In the proposed methodology, micromechanical analysis on the recycled fibers govern the design and manufacturing parameters [25].

The main steps of the recycling process are briefly described in Figure 5-1. As seen, the proposed methodology presents a closed recycling system such that the recycling process can be repeated until a certain degree of degradation in the properties of the fibers is observed. As illustrated, the old blades are first ground using an efficient grinder (ECO-WOLF, INC.) with proper screen size to obtain fibers within the desirable length range. In particular, the grinding process is adjusted to extract fibers at least four times longer than that of the average critical fiber length ($\tilde{l}_f$= 0.85 mm). The main reason for extracting longer fibers is to minimize the possible damages to the fibers, as well as maximally preserve the fiber length following the extrusion process, which is typically associated with fiber breakage. Although wind turbine blades generally contain a core material, the blade pieces used here in the grinding process are made from pure fiberglass with no wood or foam content that could have come from the core. In the next step, once the fibers are extracted, multiple classification operations are performed to separate off the old matrix powder remaining inside the recyclate to a great extent. The classification is conducted using a sieve with a mesh size of 60 µm. The recovered fibers, along with polylactic acid (PLA) are then put into an optimized extrusion process that uses a twin-screw extruder (Leistritz ZSE18HP-40D, Nuremberg, Germany) to produce recycled composite pellets. Details about the parameters used in the extrusion processes are reported in Table 5-1. The pellets can be used in different composite manufacturing processes, namely, compression molding and 3D printing. The focus of this study is on the 3D printing application of the pellets, specifically their use to produce FFF feedstock and fabricate recycled composite parts via 3D printing.

Table 5-1: The extrusion parameters for the single-screw and twin-screw extruders.

Initial extrusion	Screw speed (rpm)	95
	Subzone 1-2 (Temp °C)	190
	Subzone 3 (Temp °C)	185
	Subzone 4 (Temp °C)	180
	Subzone 5 (Temp °C)	175
	Subzone 6-8 (Temp °C)	170
Second extrusion	Screw speed (rpm)	25
	Die temperature (Temp °C)	210
	Winder speed (rpm)	1

Long fibers might cause nozzle clogging during the extrusion process for making recycled composite pellets or 3D printing. Therefore, a nozzle diameter of 10 mm, 3mm, and 1.2 mm is used in the first extrusion, second extrusion and the 3D printing process, respectively.

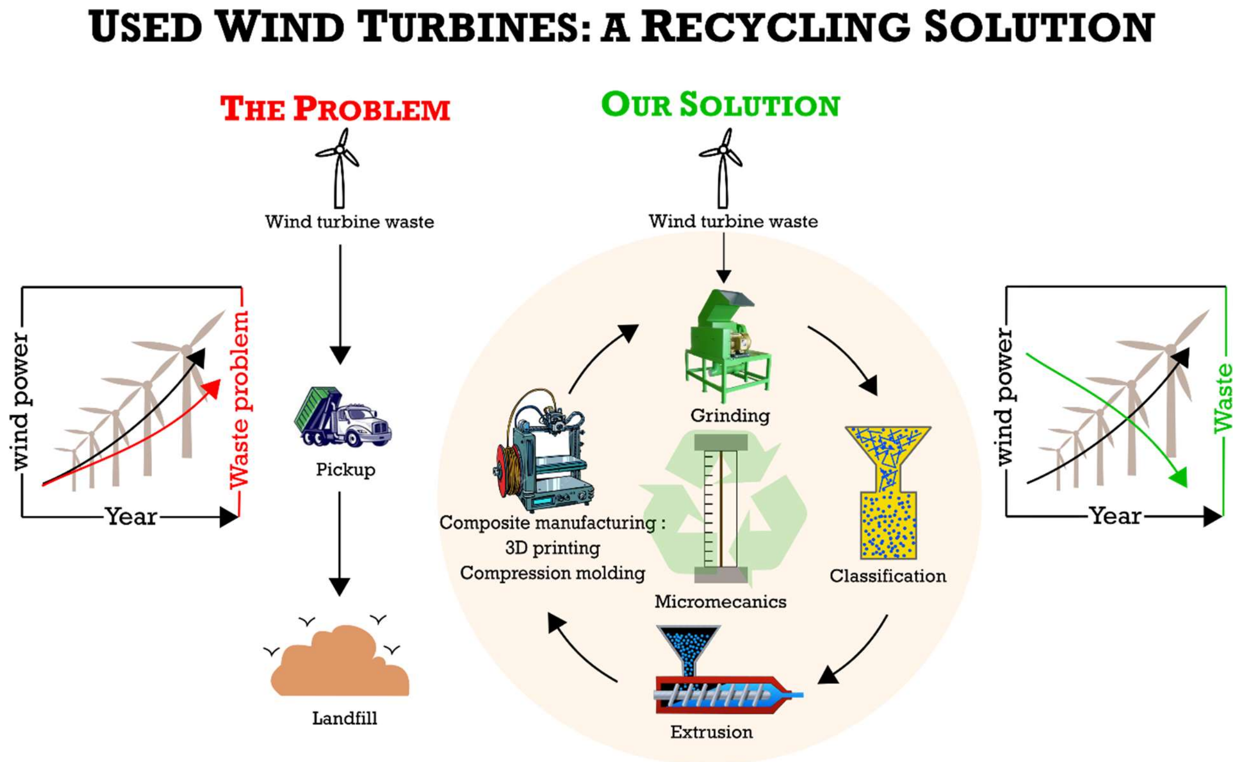

Figure 5-1: Taxonomy of the recycling solution for wind turbine blades.

Thermoplastic composite manufacturing processes are generally associated with an extrusion stage that leads to significant fiber length attrition [26, 27]. In fact, substantial fiber breakage occurs during the compounding due to three main reasons: (i) fiber-fiber interactions, (ii) fiber-screw interactions, and (iii) fiber-polymer interactions. For instance, Bader and Boyer [28] have reported that following the extrusion of fiberglass and nylon 66, only 20% of the fibres featured a length larger than the critical fiber length, even though the initial length was notably larger. While controlling the process parameters, primarily the temperature profile, has shown to be beneficial to fiber length preservation, the fiber fracture inevitably happens in the compression and mixing sections of the extruder. In the present study, the screw speed and temperature profile used during the extrusion processes are adjusted to first minimize the residence time in the melt, and also avoid polymer degradation.

In a previous study, we successfully performed tensile and pull-out tests on single fibers extracted from ground turbine blades [25]. The results from this study identified the critical fiber length for the ground fibers, l_f, to be between 0.57 and 1.14 mm. The fiber length after the double extrusion process is characterized to evaluate the fiber length distribution, as well as the content of fibers longer than the minimum critical fiber length. To do so, samples from the extruded filaments are cut out and incinerated in a thermogravimetric analysis (TGA) system (Q500, TA Instruments, New Castle, DE, USA) to burn off the resin. Using a heating program in the presence of nitrogen and followed by an oxidative stage, the TGA test is performed with a temperature profile ranging from 20-800°C, to obtain clean fibers with no ash content on the surface. The remaining fibers are then randomly spread over a microscope slide. Random sections of the microspore slide are then viewed under a microscope and the length of at least 300 fibers is measured.

The mechanical characterization of the 3D printed parts is undertaken using tensile testing. In this regard, tensile samples following ASTM D638 Type I specimen are manufactured using a Prusa i3 Mk2S printer. The 3D printed samples are composed of 24 layers and feature three different fiber contents including 3 wt%, 5 wt% and 10 wt%. The optimum manufacturing process and design parameters obtained in previous studies are used here in the 3D printing process [23, 24]. These parameters are summarized in Table 5-2. Samples are tested using a 313Q tensile machine from Testresources equipped with a 50 kN load cell. The tests are conducted at 5 mm/min displacement rate and a total of at least 6 samples for each fiber content is tested. The fracture surface of the samples is then imaged using a Hitachi TM3030Plus scanning electron microscopy. Figure 5-2 depicts the macrogeometry of the 3D printed specimen along with its dimensions and microstructure.

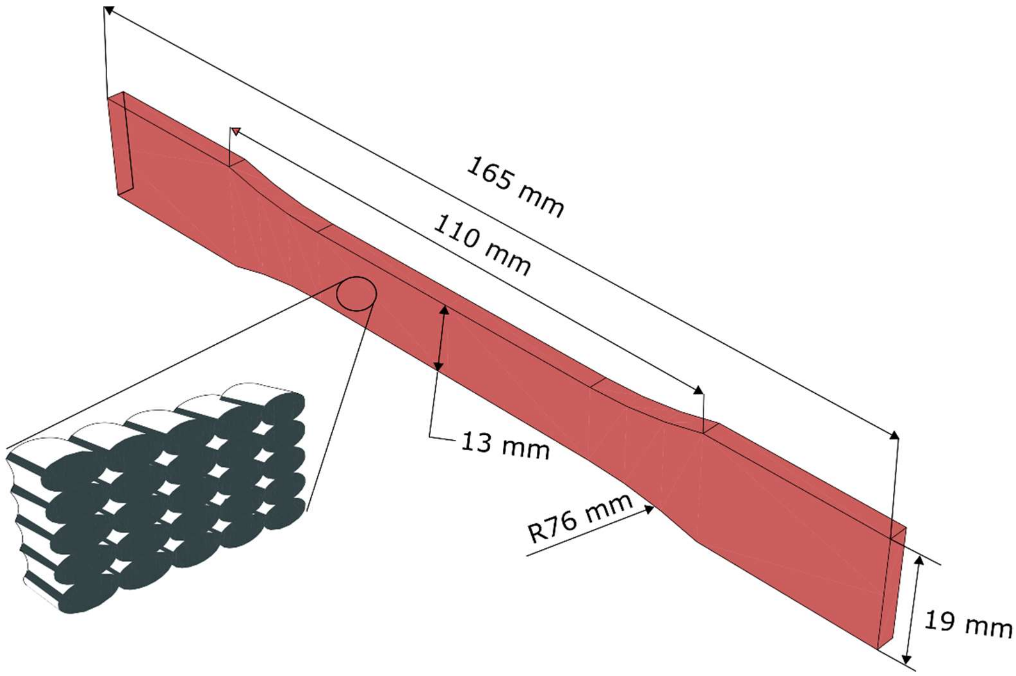

Figure 5-2: The microstructure and dimensions of the 3D printed recycled composite samples.

Table 5-2: Manufacturing and design parameters for specimen 3D printing.

Manufacturing parameter	Value	Manufacturing parameter	Value
Print direction	XYZ	Nozzle diameter (mm)	0.4
Raster angle	0	Nozzle temperature (°C)	215
Layer height (mm)	0.14	Cooling	No fan cooling
Bed temperature (°C)	60	Infill (%)	100
Print speed (mm/min)	2400	Filament diameter (mm)	1.75

5.3.2 Micromechanical FE analysis

Explicit modeling of a 3D printed composite component with all the micromechanical features can be computationally expensive and lengthy. To deal with the problem of elastic prediction for 3D printed parts, methods of mechanical analysis can be beneficial to obtain the effective mechanical properties of the material via analysing a representative volume element (RVE) [29]. The RVE features identical fiber volume fraction and elastic constants to the original composite. As displayed in Figure 5-3, the macrostructure of a 3D printed sample can be represented through three orders of hierarchy: the extrudates, 3D printing building blocks incorporating interlayer voids, and a composite compound unit.

The underlying principal of the homogenization method used here lies in the identical average strain energy stored in the medium RVE and the work executed by the external loads [30]. In this regard, the total strain energy in the RVE can be predicted through the macroscopic stress and strain fields, which are in turn estimated by averaging the local micro stress and strain tensors over the volume of RVE, as

$$\begin{aligned}
\bar{\sigma}_{ij} &= \frac{1}{V}\int \sigma_{ij}(x,y,z)\,dV \\
\bar{\epsilon}_{ij} &= \frac{1}{V}\int \epsilon_{ij}(x,y,z)\,dV \\
\bar{\sigma}_{ij} &= C^{H}_{ijkl}\bar{\epsilon}_{kl}
\end{aligned} \tag{5-1}$$

where, $\bar{\sigma}_{ij}$, $\bar{\epsilon}_{ij}$ and C^{H}_{ijkl} denote the average stress tensor, average strain tensor, and the homogenized stiffness matrix. While taking the average quantities over the RVE volume can be cumbersome, Gauss theorem can be used to obtain the average strain from boundary displacements, as expressed below:

$$\bar{\epsilon}_{ij} = \frac{1}{V}\int(\epsilon_{ij}(x,y,z))\,dV = \frac{1}{2V}\int(u_i n_j + u_j n_i)\,dS \tag{5-2}$$

where V is the volume of the RVE, S is the boundary surface of the RVE, u_i is the *ith* component of displacement and n_j is the *jth* component of the unit normal to S. Since the strain field is continuous within the fibers and matrix, the Gauss theorem can be applied to each constituent separately. Assuming a perfect bonding at the interface between the fibers and matrix, Eq. 5-2 can be defined as:

$$\bar{\epsilon}_{ij} = \frac{1}{V}\int(u_i n_j + u_j n_i)\,dS_2 \tag{5-3}$$

where S_2 denotes the outer boundary of the RVE. Using six independent arbitrary unit macro strains, the average macro stress and thus the elastic constants of the RVE can be determined. One essential factor to the accuracy of the homogenization theory is the periodicity of the strain field, which is ensured by applying periodic boundary conditions on the RVE edges.

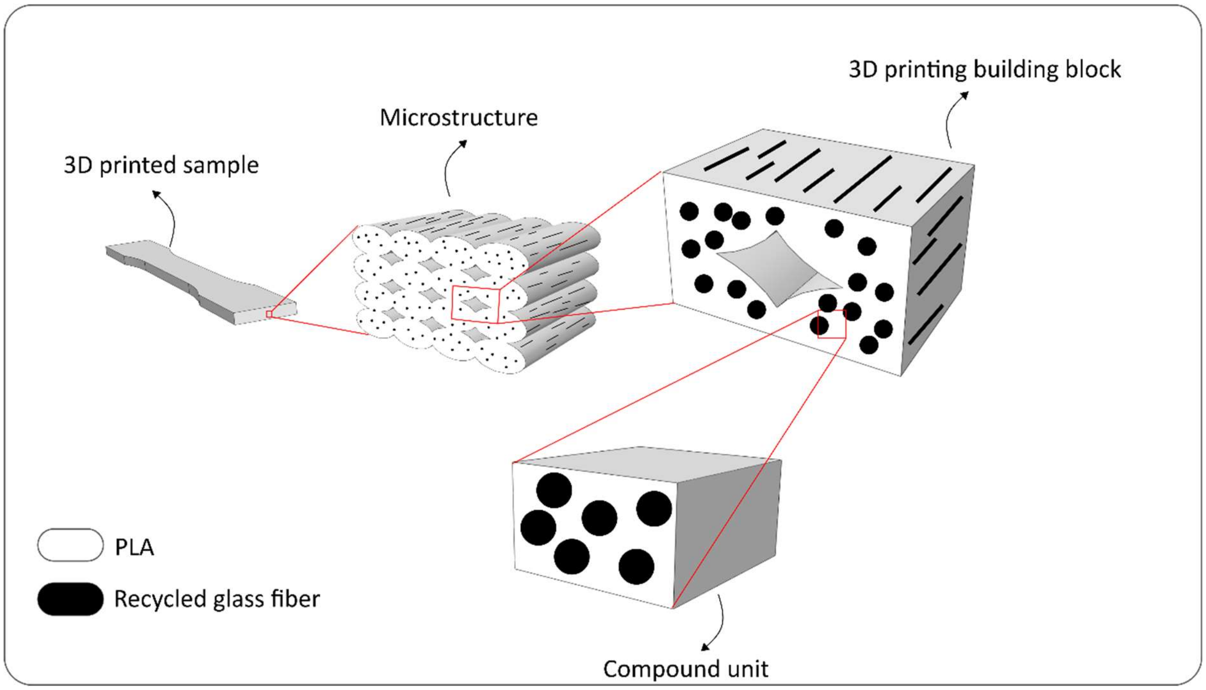

Figure 5-3: Hierarchical structure of 3D printed parts.

To examine the elastic properties of the recycled composite parts, the homogenization method is here applied to sequentially obtain the effective properties of the constructing unit within each hierarchy order. In particular, the effective properties of the main composite compound unit are first predicted and used to replace the heterogenous material of the 3D printing building block with a homogeneous equivalent medium. The homogenization is then used once more to obtain the mechanical properties of the microstructure of the 3D printed sample, which is in turn used to exploit the properties of the 3D printed specimen.

5.3.2.1 Generation of RVEs

At the root of our FE analysis there are three basic notions that enable the prediction of the elastic properties of the recycled 3D printed parts: (i) The creation of distinct hierarchical orders that represent the macrostructure of the 3D printed parts, (ii) the assessment of the structural stiffness of the 3D printed parts via formulating a homogenization problem on the 3D printing building block, and (iii) the evaluation of the elastic properties of randomly distributed fibers within cubic RVE via the homogenization method.

To create the 3D model of randomly distributed fibers, we first start with the RVE cubic volume, which has been assigned a size, dependent on the fiber length distribution and obtained through sensitivity analysis. The fibers are modeled as straight unidirectional cylinders featuring various lengths derived from the measured length range of the fibers present in the extruded filaments. The random position of the fibers is determined via a developed python script. As illustrated in Figure 5-4, while the position of the fibers is conferred by a random function, two main factors control the creation of subsequent fibers: volume fraction, and minimum distance between the neighbouring fibers. Once the coordinates of the first fiber are randomly determined, the length of the fiber is selected from the length range of the recycled fibers. Subsequently, the algorithm will generate the coordinates of the second fiber. To ensure the non-overlapping condition, the distance between the newly generated fiber and the existing fibers is properly checked in XY and ZY planes at each iteration. As well, the periodicity of the RVE geometry is ensured by copying the coordinates that results in fibers cutting the exterior surface of the RVE.

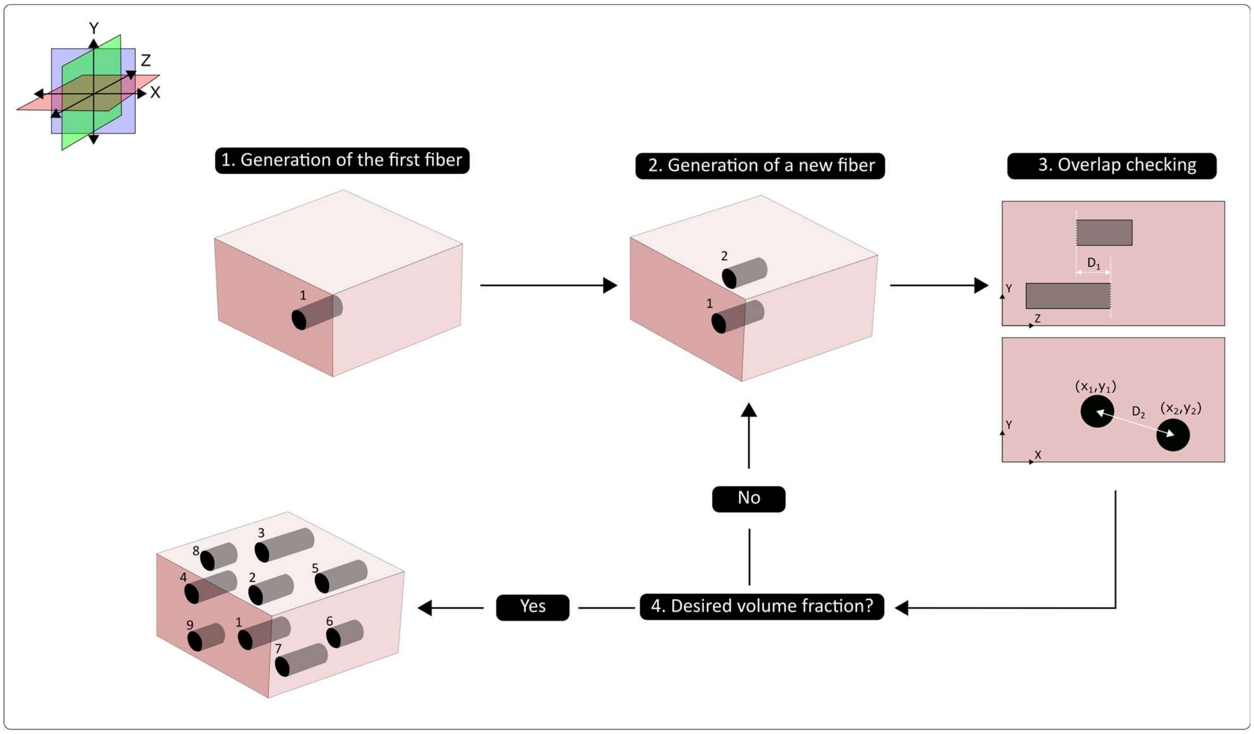

Figure 5-4: Detailed flowchart describing the algorithm used to develop the FE model of the composite compound unit.

Finally, the algorithm will continue until the desired fiber volume fraction is attained. The generated coordinates along with the length array of the fibers are then exported into ABAQUS to build, mesh and solve the 3D problem of randomly distributed unidirectional recycled composites, which is modeled with 10-node quadratic tetrahedron elements (C3D10). To apply the periodic boundary conditions on the RVE planes, an identical mesh pattern was created on the opposite faces of the RVE through a copy mesh scheme. With this technique, the surface of the fibers is first partitioned, and the matrix is precisely meshed on one plane of the RVE. The generated mesh is then copied to the opposite plane followed by a volumetric mesh. Consequently, identical displacement is imposed to the nodes of the opposite sides of the RVE.

As shown in Figure 5-5, the 3D printing building block is reconstructed from SEM images obtained from the cross section of 3D printed parts. The microstructure of FFF parts consists of filaments bonded through sintering and molecular diffusion at the interface. The thermal energy of the filaments at the interface drives a neck growth process, which results in bond formation. The neck growth phenomenon typically affects the cross section of the filaments by forming an elliptical or “ovalized” cross section. In addition, interlayer voids generally appear between the filaments, which influence the part density and mechanical properties.

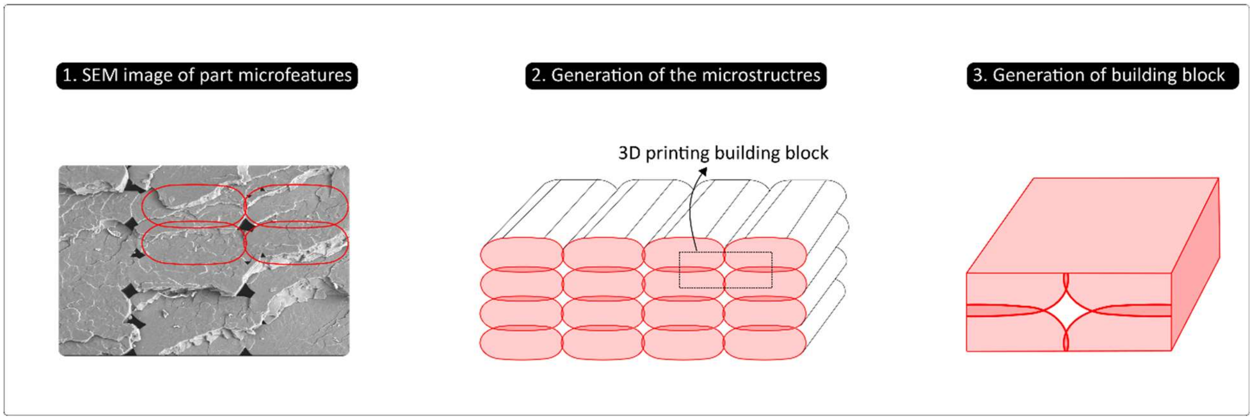

Figure 5-5: Detailed flowchart describing the algorithm used to develop the FE model of the 3D printing building block.

While an infill rate of 100% was used for the 3D printing process, the viscosity of the material at the temperature used in 3D printing can affect the coalesce between the filaments and thus the voids formed between them. Here an asymptotic building block representing the microstructure of the recycled composite parts is regenerated and used to predict the properties of the 3D printed specimens. A representative meshed model from the composite compound unit and 3D printing building block are is shown in Figure 5-6.

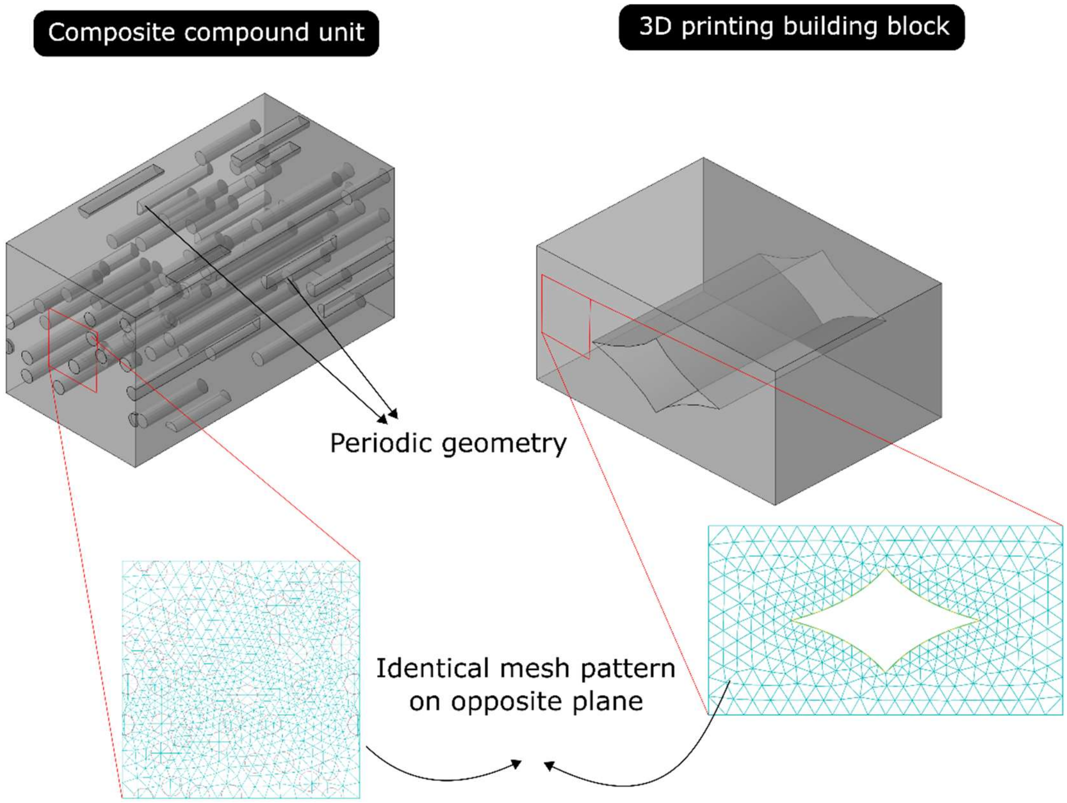

Figure 5-6: Identical mesh pattern generated through mesh copy technique on the opposite faces of the 3D printing building block and composite compound unit.

The procedure above is used for the FE analysis of the 3D printed parts made of PLA and recycled glass fibers. The isotropic linear properties of the fibers here adopted are obtained from single fiber tensile tests on fibers extracted from ground used blades [25]. As a result, the matrix and fibers are assigned a Young's modulus and Poisson's ratio of, respectively, $E_m = 3.6$ GPa, $v_m = 0.33$, $E_f = 75$ GPa and $v_f = 0.21$ [31, 32].

5.3.3 Theoretical modeling of short fiber composites

Several theoretical models have been established and used to obtain the properties of short fiber composites. To provide insight into the theoretical properties of composites made from recycled glass fibers, the well-known Mori-Tanaka and Halpin-Tsai theories are utilized to predict the elastic stiffness of the fabricated composites and to compare with those obtained from tensile testing and micromechanical FE analysis. These short fiber models have shown a high accuracy in predicting the stiffness of perfectly aligned composites at low fiver volume fractions. Since the volume fraction of the 3D printed samples is relatively low, the aforementioned models can be reasonably used to comparatively evaluate the structural performance of the fabricated recycled composites.

The Mori-Tanaka theory assumes elliptical inclusions with perfect interaction between the matrix and the inclusions to predict the elastic stiffness tensor of a composite material [33]:

$$C_c = \langle (C_i - C_m) B_i \rangle [(1 - \lambda_i) I + \lambda_i \langle B_i \rangle]^{-1} + C_m \tag{5-4}$$

where C_c, C_m, and C_i represent the stiffness tensor of the short fiber reinforced composite, matrix and the inclusion, respectively. λ_i is the volume fraction of the inclusion, I is the fourth order unit tensor, and B_i is the dilute mechanical strain concentration which can be expressed as:

$$B_i = [Z(C_m)^{-1}(C_i - C_m) + I]^{-1} \tag{5-5}$$

where Z is the Eshebly tensor. The constants used to compute the Eshebly tensor are detailed in Appendix 1.

Halpin-Tsai represents a semi-empirical approach that can be used to predict the elastic properties of discontinues composites [34]. This theoretical model, which is derived by reducing Hermans' solution to a simple analytical form, predicts the elastic stiffness of unidirectional composites as:

$$\eta_L = \frac{\frac{E_f}{E_m} - 1}{\frac{E_f}{E_m} + 2(l/d)} \tag{5-6}$$

where E_f, E_m, and l/d denote the fiber stiffness, matrix stiffness, and fiber aspect ratio, respectively. This theory indicates that apart from the properties of the constituents, the aspect ratio of the reinforcement plays a crucial role in the elastic stiffness of discontinuous composites.

5.4 Results and discussions

We examined the mechanical performance of a newly developed class of FFF feedstock made from PLA reinforced with recycled glass fibers from old wind turbine blades. Inspired by previous work by the authors, this section aims to summarize the latest results combining the key elements of recycling and micromechanical analysis techniques to 3D print recycled fiber reinforced parts. First, the characterization of the obtained recyclate is discussed by presenting the TGA and SEM imaging results. Subsequently, the mechanical properties of the fabricated parts are described, and their fracture cross section is investigated. Finally, a comparative study further exploiting the experimental measurements versus FE and theoretical results are presented.

5.4.1 Ground recyclate

TGA was performed to precisely capture the fiber weight fraction of the composite filaments. Figure 5-7 (left) shows the TGA results, illustrating the thermal decomposition and weight loss of the filaments with different fiber contents. As seen, the nominal weight composition of the filaments is approximately two times their true fiber content. Besides some simple experimental variations, the main reason for this discrepancy can be attributed to the remaining epoxy in the recyclate, which contributes to the initial weight fraction of the fibers during the filament preparation. This measurement indicates that relatively 50 wt% of the obtained recyclate is still composed of epoxy residue, which are mainly residing on the surface of the long glass fibers used in the extrusion process. In fact, as shown in Figure 5-8, while the small particles of epoxy are considerably removed from the recyclate, the long fibers that are extracted after the grinding process still retain epoxy residues in the form of bulk particles on the surface. Although this substantially lowers the weight fraction of the glass fibers, the presence of these particles could be beneficial to the interfacial strength between the PLA and fiberglass by offering mechanical and chemical bonding [23, 25, 35].

Following the TGA test, the generated fibers were used to estimate the fiber length distribution in each set of the composite filaments. Figure 5-7 (right) shows the probability distribution of the fiber length, elucidating the fact that increasing the recyclate content from 3 to 5, and 10 wt% can adversely affect the fiber length distribution by reducing the mean fiber length from 0.55 to 0.35, and 0.30 mm. This phenomenon arises from the excessive fiber-fiber interactions during the mixing zone of the extrusion process, where the abrasion of the fibers generates stress concentration regions on their surface leading to direct or subsequent fiber breakage. In addition, the high viscosity of PLA, along with the aggregation of long fibers can be other factors contributing to the fiber length attrition through viscous forces and contact with screw surfaces. While the initial fiber length used in the pelletization process was 4 times longer than the estimated average critical length of the ground fibers, these results indicate that only 28%, 18% and 11% of the fibers in the 3, 5, and 10 wt% reinforced filaments exceed the minimum critical length.

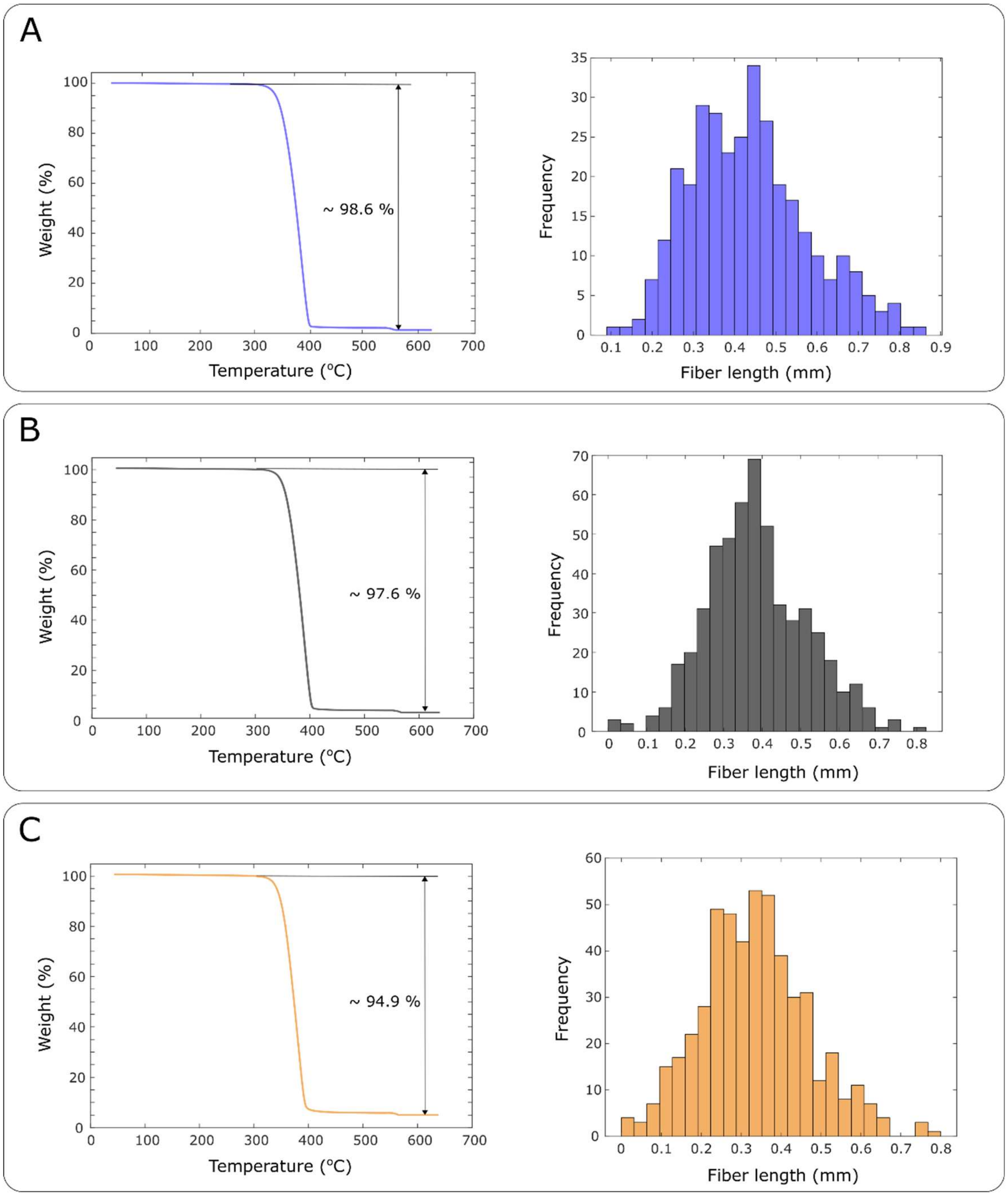

Figure 5-7: TGA (left) and probability distribution of fiber length (right) of the recycled composite filaments: (A) 3 wt% fiber content; (B) 5 wt% fiber content; (C) 10 wt% fiber content.

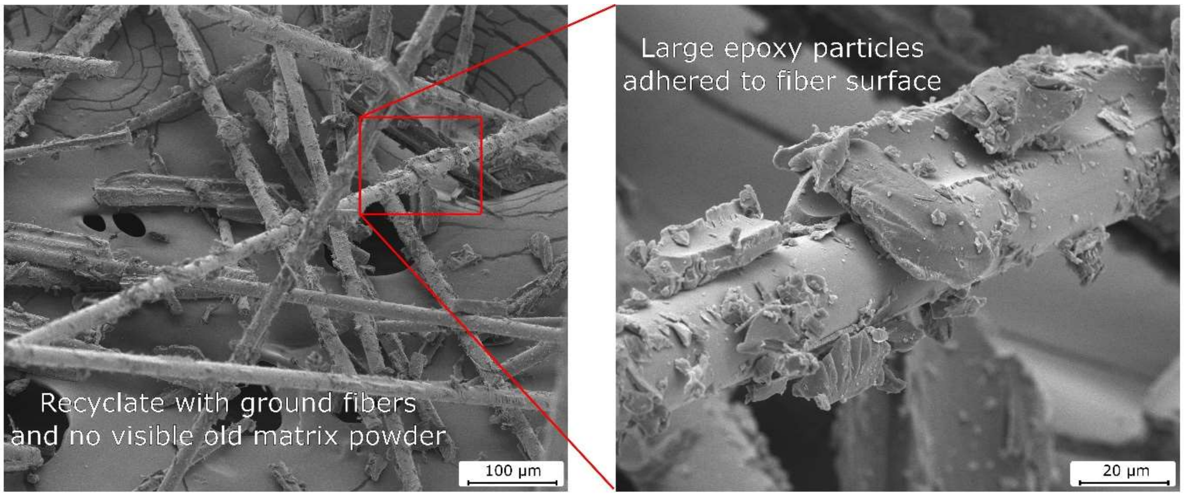

Figure 5-8: The ground recyclate demonstrating the separation of matrix powder while preservation of matrix residue on the fibers surface.

To better explore the microstructure of the recycled 3D printing feedstock, knowledge of the fiber orientation, as a determinant factor to the mechanical behavior of the recycled 3D printed parts, is essential. Micro computed tomography (µCT) is used to capture the orientation of the fibers within the extruded feedstock. Representative samples from the composite filaments were extracted and scanned at a resolution of 3 um. Figure 5-9 shows a transverse and longitudinal cross section of the reinforced filament with 10 wt% recyclate content, along with a 3D visualization. Visual inspection evidently confirms the longitudinal axis of the filament as the main fiber orientation. However, fibers oriented randomly can still be identified, particularly in the core of the filament. These image show that the assumption of unidirectionally oriented fibers can be reasonably used in the micromechanical approaches to predict the mechanical properties of the 3D printed parts.

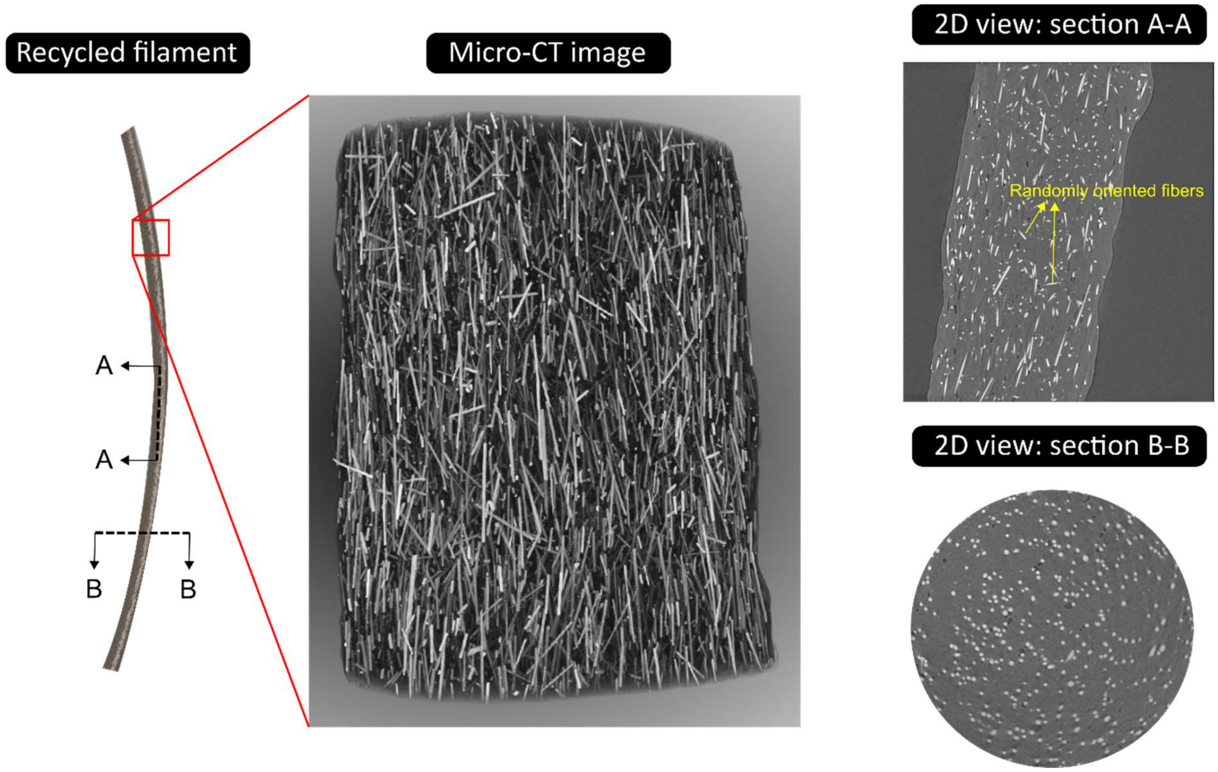

Figure 5-9: Micro CT image from representative reinforced filament with 10 wt% recyclate content.

5.4.2 Mechanical characterization

The representative stress strain curves taken from the tensile testing of 3D printed ASTM D638 specimens are shown in Figure 5-10. Each curve for a recyclate content is selected from the results of 6 samples that best represents the average tensile properties.

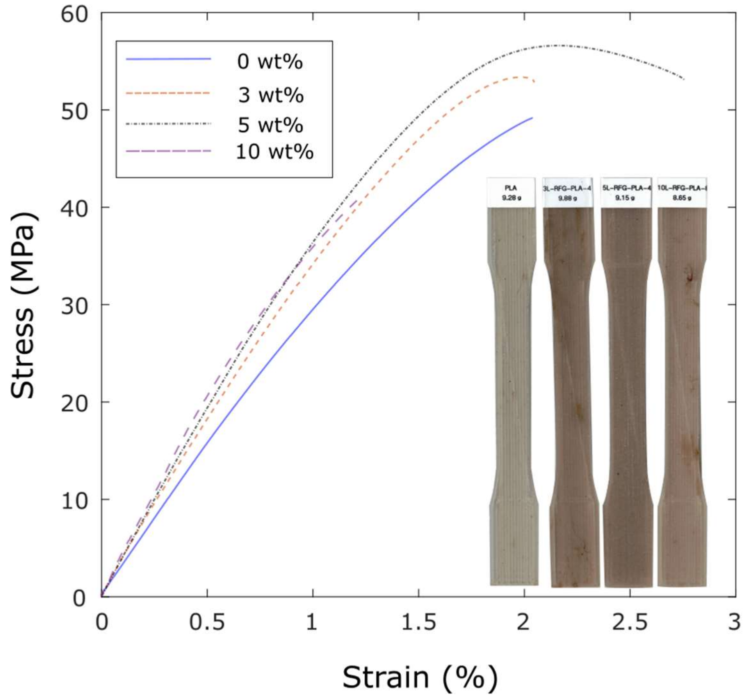

Figure 5-10: Representative stress-strain curves of 3D printed recycled composite specimens.

Figure 5-11 illustrates the tensile properties of the recycled composite parts with error bars representing the standard deviation (SD). In addition, the average tensile properties along with the SD values are summarized in Table 5-3. The presented results interestingly reveal an increasing trend in the strength of the 3D printed parts, in which increasing the recyclate content to 5 wt% was associated with 20% increase in the specific strength of the 3D printed parts compared with pure PLA specimens, the baseline. Further increasing the recyclate content to 10 wt%, however, resulted in a slight reduction in the tensile strength compared with the baseline, a property degradation that can be attributed to the low surface quality of the 3D printed specimens (Figure 5-12). In fact, while the use of a larger nozzle diameter helped to minimize the probability of nozzle clogging and gas evoluted voids, the surface quality of the parts was slightly compromised due to the high viscosity of the compound, a phenomenon that locally generated pores and stress concentration regions. In addition, the high viscosity of the filament reduces the fluidity of the extrudate coming out of the large nozzle resulting in a poorer fiber dispersion and alignment, thus reduction in the mechanical performance. Although increasing the printing temperature could be helpful to increase the part quality at high fiber volume fraction, it can be associated with PLA degradation, which will significantly lower the mechanical properties.

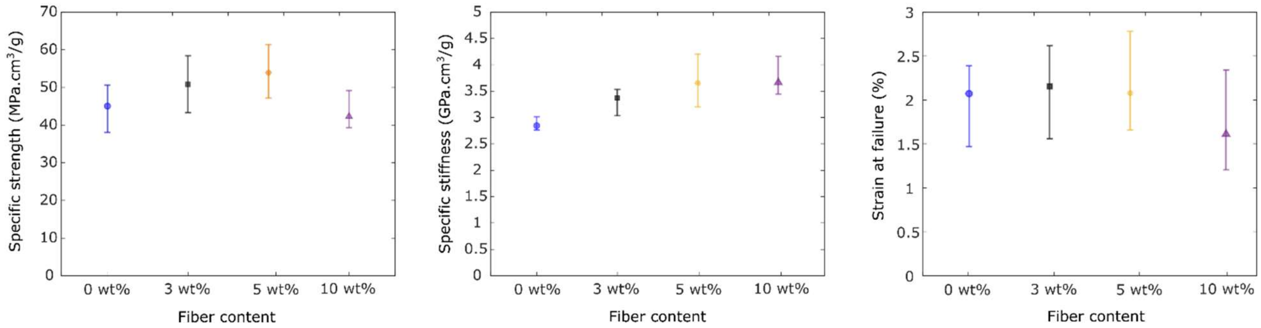

Figure 5-11: Tensile properties of 3D printed samples using the recycled composite filaments.

Figure 5-12: Extrinsic defects on the outer surface of 10 wt% specimens.

As per the elastic modulus, the experiments unveiled an increasing trend in the tensile modulus of the composite samples, an observation that was similarly observed for samples made from short recycled fibers [23, 24]. In particular, the experimental measurements showed an increase in the specific stiffness of 28.9% and 30.3% for reinforced 3D printed specimens with 5 and 10 wt% recylate content, respectively. As discussed in Section 2.4.1, 28% of the fibers exceed the critical length for the 5 wt% reinforced filament, while this is only 11% for 10 wt% reinforced filaments. This will be translated into 3D printing specimens as well and can explain in part the close specific stiffness values of 5 and 10 wt% reinforced specimens. In terms of the ductility, samples featuring recyclate content of up to 5 wt%, interestingly exhibited failure strain comparable to that of pure PLA parts. This is presumably due to the low fiber volume fraction of the recyclate at these contents, as well as the favorable interactions between the fibers and PLA, which are enhanced by hydrogen bonding formed through epoxy. The 10 wt% samples, on the other hand, showed higher brittleness, which stems from their extrinsic printing defects.

Figure 5-13 illustrates the fracture surface of the composite samples after the tensile testing. In all the samples, the majority of the fibers were broken, an observation that further highlights the high load transfer capacity of the 3D printed samples. As displayed in Figure 5-14, while in our previous studies [23, 24], epoxy particles on the fracture cross section of the samples were one of the major sources of failure by creating stress concentration, these SEM images showed no trace of epoxy. This phenomenon can be ascribed to the multiple classification operations performed on the recyclate.

The neck growth between adjacent rods in the microstructure of a 3D printed part results in the formation of intralayer voids, which can impact the ultimate properties. While this process mainly occurs due to viscous flow and molecular diffusion of polymer chains, manufacturing parameters, namely layer thickness and temperature, can be controlled to minimize the internal pores [36]. As opposed to our previously fabricated samples [24], the SEM micrographs from the new long fiber specimens showed a fully solid cross section indicating that the use of a larger nozzle diameter while keeping an identical layer thickness successfully minimized the internal voids and increased interlayer cohesion.

Table 5-3: Mechanical properties and standard deviation of recycled composite samples.

Fiber content	Mean specific strength (MPa.cm^3/g)	Mean specific stiffness (GPa.cm^3/g)	Mean failure strain (%)	Strength SD	Stiffness SD	Failure strain SD
0 wt%	45.04	2.84	2.07	4.06	0.09	0.35
3 wt%	50.80	3.36	2.15	5.15	0.19	0.30
5 wt%	53.91	3.66	2.07	5.47	0.48	0.40
10 wt%	42.27	3.70	1.16	3.68	0.33	0.39

To further study the performance of the reinforced samples, the properties of the newly fabricated specimens with long fibers were compared with those that were previously manufactured using short recycled glass fibers [24]. As depicted in Figure 5-15, the results demonstrate the higher tensile properties of the samples reinforced with long fibers owing to two major reasons: First, the micromechanical characterization of single fibers recovered through mechanical grinding helped us to identify the proper manufacturing and recycling parameters that led to the presence of fibers longer than the critical length in the ultimate parts, a factor that contributed to an effective use of the recycled fibers. Second, multiple classification operations followed by the grinding process allowed to concurrently minimize the epoxy powder particles, which were previously identified as a source of strength degradation, and preserve the epoxy residues adhered to the surface of the recovered long glass fibers. As reports in the literature have demonstrated the capability of PLA molecules to chemically react with epoxy through hydrogen bonding, this preservation of surface epoxy residues could play a critical role in the mechanical performance of the recycled composites by providing an interface 26% stronger than that formed between fibers with smooth surface tomography, namely those recovered through thermal techniques, and PLA [25].

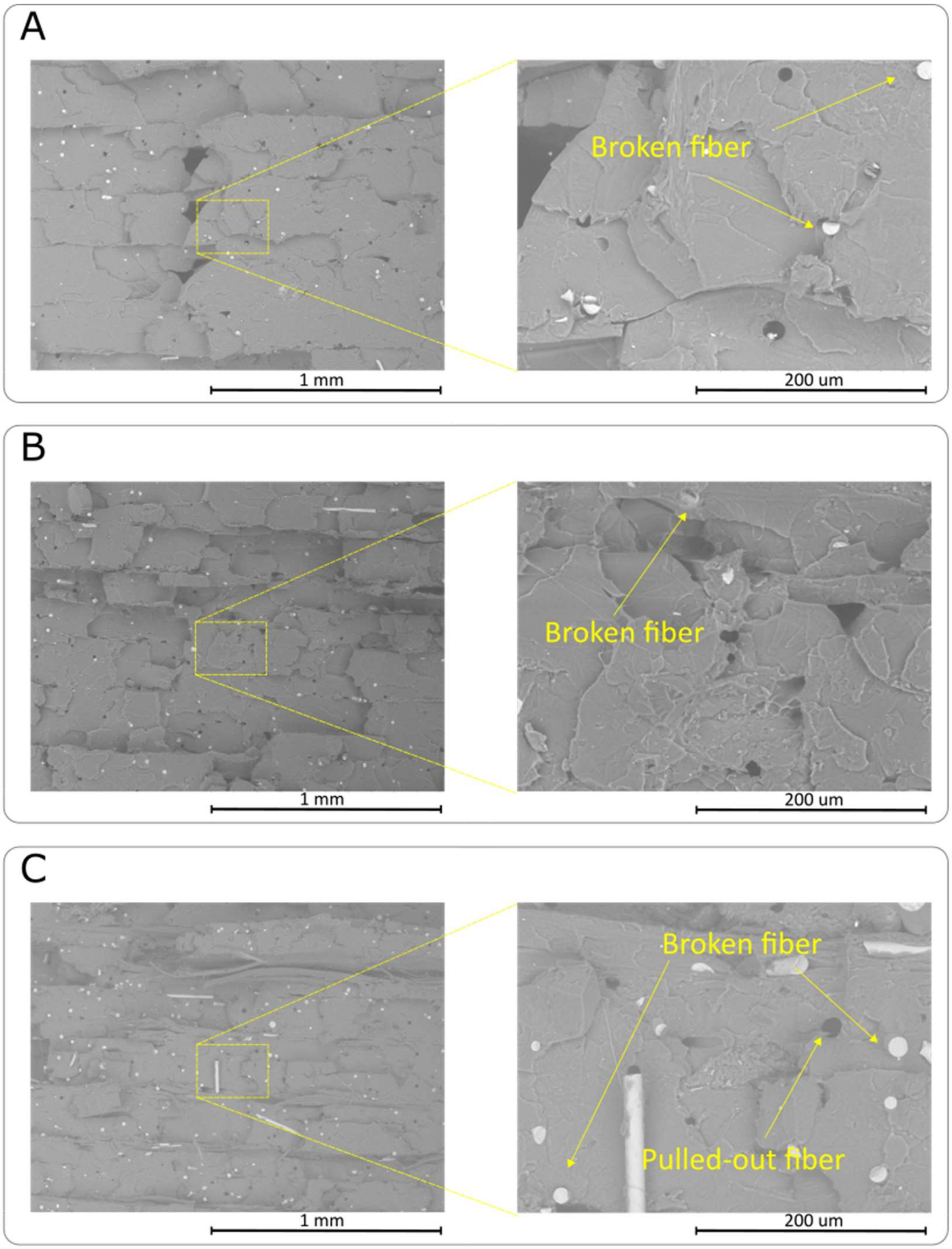

Figure 5-13: SEM images from the fractured surface of the specimens: (A) 3 wt%; (B) 5 wt%; (C) 10 wt%.

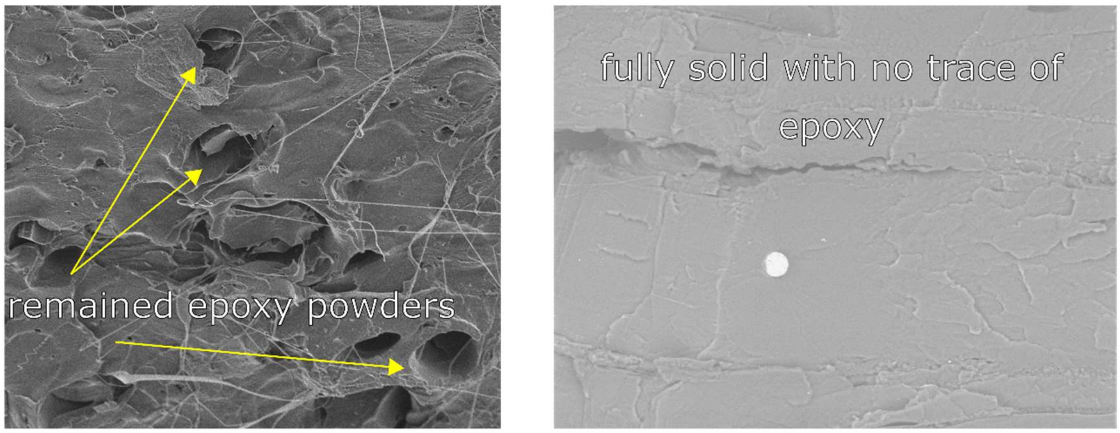

Figure 5-14: Representative SEM micrographs from the cross section of previously fabricated short fibers samples [24], and newly manufactured long fiber specimens.

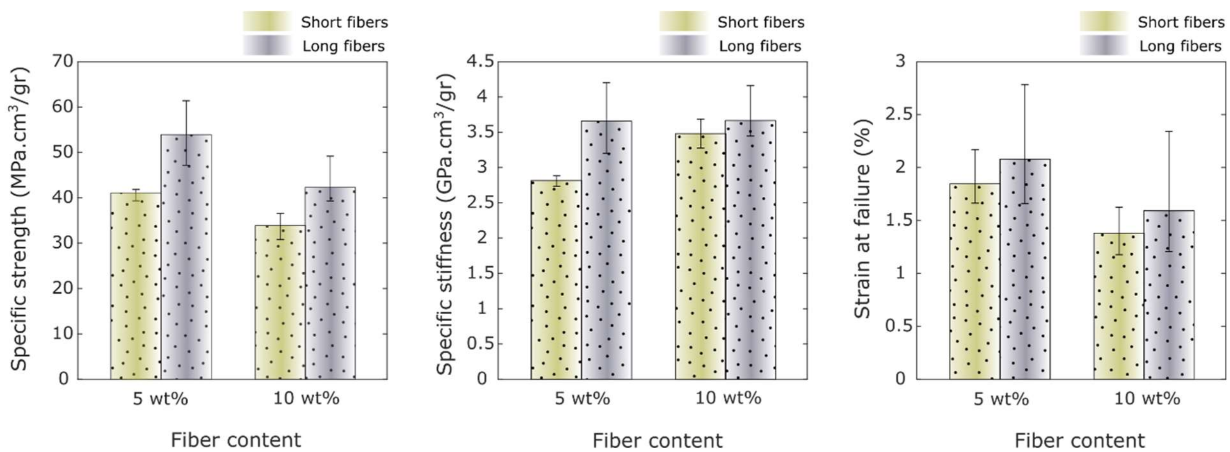

Figure 5-15: Comparison of mechanical properties for samples made from short and long recycled glass fibers.

5.4.3 FE and Micromechanical theories versus experiments

A nonlinear FE analysis was performed to further study the mechanical phenomena observed in the experiments. To conduct a precise comparison, the true fiber content of the filaments obtained via TGA was used to predict the mechanical properties of the parts using FE and mechanical theories of short fiber composites. The numerical results validating the trend of the experimental results are shown in Figure 5-16A. The specific modulus values obtained by the FE model are quantitively in good agreement with the experimental measurements reproducing the key trends observed in the experiments. However, a larger divergence was observed at 10 wt% recyclate content, which could be mainly attributed to the knockdown of stiffness owing to the low surface quality of the samples. Further, while a unidirectional fiber orientation was assumed in the FE modeling, the increased viscosity of the filaments at higher fiber volume fractions can deteriorate the fiber dispersion, as well as the fiber alignment, resulting in larger discrepancy between the experimental measurements and FE results. Another reason for this observation could be due to the variable mechanical properties of the recycled fibers. As demonstrated in our previous study, the recovered fibers tend to show a large range of tensile properties [25]. While the average tensile properties of the recycled fibers were used in the FE and theoretical models, at high fiber volume fractions, the nonlinear modeling would be an overestimation of the properties as it misrepresents the property variation of the fibers.

On the other hand, the theoretical models overestimated the properties of the samples at all the fiber contents. One reason could be due to the unrealistic particle dispersion and assuming prolate spheroidal shaped inclusions instead of the real shape of the fibers. Furthermore, since the average fiber length was used in Mori-Tanaka and Halphin Tsai, another reason for this offset can be ascribed to the variable length of the recycled fibers present in the samples. In contrast, the random selection of the fiber length in the 3D RVE model showed to be beneficial to reproduce a further realistic fiber length distribution. Furthermore, the short fiber composite theories did not account for the interlaminar and interlayer voids present in the 3D printed parts, leading to an overestimation of the properties.

Similarly, a nonlinear FE analysis is carried out using the average fiber length and the true fiber content for the short fiber parts fabricated previously [24]. The FE analysis along with the theories are used to predict the properties of samples featuring two different fiber contents including 5 wt% and 10 wt%. As can be seen in Figure 5-16B, the results suggest a larger offset between both the theoretical and FE results, as well as the experimental measurements at all the fiber contents. These results are indicative of proper minimization of any intrinsic and extrinsic defects and voids in the samples fabricated here, which are the main cause of property degradation in these short fiber samples.

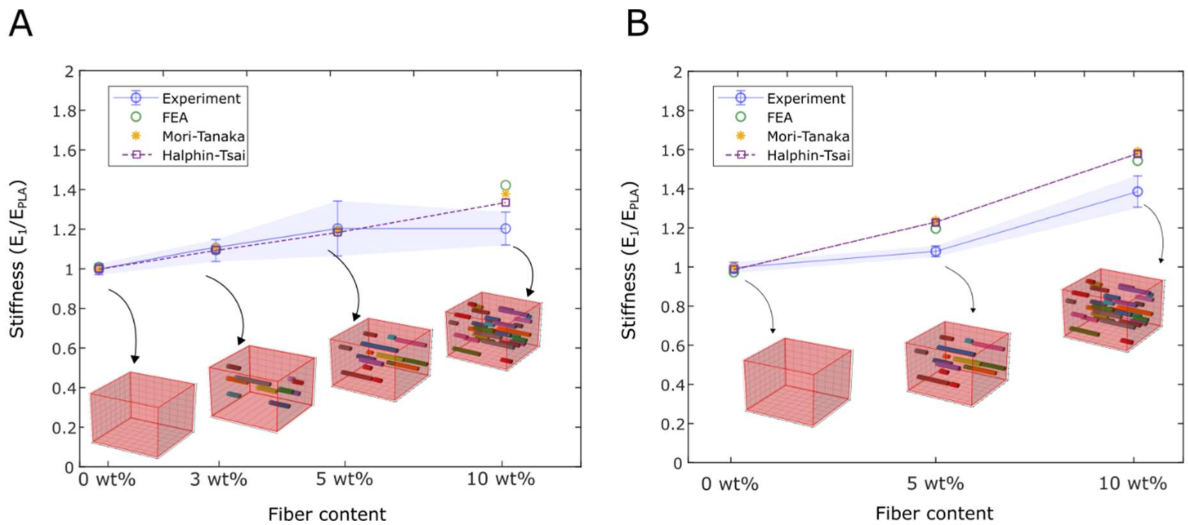

Figure 5-16: Specific stiffness of 3D printed recycled composite samples measured experimentally versus FE and theoretical predictions: (A) long fiber samples; (B) short fiber samples.

5.5 Conclusions

In conclusion, we presented a novel class of recycled FFF feedstock filament exhibiting superior tensile properties compared with pure polymer ones. The enhancement in the tensile strength and modulus of 3D printed parts has been achieved via the use of recyclate from wind turbine blades. Through the proper optimization of the recycling process, which is also integrated with multiple classification operations, recycled fibers are obtained which are longer than the critical fiber length. These fibers are preserved in the reinforced filaments and consequently the 3D printed tensile specimens per ASTM D638. Specimens reinforced with 5 wt% recycled fibers showed an increase of, respectively, 20% and 28% in the tensile strength and modulus. The 3D printed tensile specimens with long fibers exhibited high structural properties, tensile strength, stiffness, and failure strain, compared with the ones reinforced with short fibers. Furthermore, a 3D RVE model correlating well with the experimental results was successfully developed. The proposed micromechanical finite element model can be used to analyze the structural performance of complex composite parts reinforced by recyclate. In addition, it can be used to design parts with optimum structural performance for specific loading and boundary conditions. The developed methodology presents a closed recycling system, which offers high sustainability as the recycled composites can be put back into the same system. However, as each recycling cycle is associated with a certain degree of degradation in the properties of fibers, at some point the use of fibers in 3D printing does not lead to value added products. The fibers, however, can be still used in other low-technology applications such as cement manufacturing. Hence, the landfill of non-biodegradable composites can be delayed for an extended amount of time.

5.6 Appendix 1

The components of the Eshebly tensor can be defined as

$$Z_{11} = \frac{4\vartheta}{3} + RI_3 + 2A^2T$$

$$Z_{22} = Z_{33} = \vartheta + RI_1 + \frac{3T}{4}$$

$$Z_{23} = Z_{32} = \frac{\vartheta}{3} - RI_1 + \frac{4T}{3}$$

$$Z_{21} = Z_{31} = -RI_1 - A^2T \tag{A-1}$$

$$Z_{12} = Z_{13} = -RI_3 - T$$

$$Z_{44} = \frac{\vartheta}{3} - RI_1 + \frac{T}{4}$$

$$Z_{55} = Z_{66} = -2R - R\frac{I_1}{2} + \frac{(1+A^2)T}{4}$$

All other Z_{ij} = 0

The constants in the Eshebly tensor's elements can be obtained as

$$U_1 = \frac{2A}{\sqrt{(A^2-1)^3}}\left(A\sqrt{A^2-1} - cosh^{-1}(A)\right)$$

$$Q = \frac{3}{8(1-v_m)}$$

$$R = \frac{1-2v_m}{8(1-v_m)} \tag{A-2}$$

$$T = Q\frac{4-3U_1}{3(A^2-1)}$$

$$U_3 = 4 - U_1$$

where A and v_m are the inclusion aspect ratio and the Poisson's ratio of the matrix, respectively.

5.7 Acknowledgments

A.R gratefully acknowledges Ms. Sareh Taheri for technical assistance with Micro CT scanning. L.L and K.F acknowledge the funding provided by the Research Center for High Performance Polymer and Composite Systems (CREPEC), Project Vision; and The Natural Sciences and Engineering Research Council of Canada (NSERC), RGPIN- 2018-04144.

5.8 References

[1] Chen J, Wang J, Ni A. Recycling and reuse of composite materials for wind turbine blades: An overview. Journal of Reinforced Plastics and Composites. 2019;38(12):567-77.

[2] Cousins DS, Suzuki Y, Murray RE, Samaniuk JR, Stebner AP. Recycling glass fiber thermoplastic composites from wind turbine blades. Journal of Cleaner Production. 2019;209:1252-63.

[3] Green B. Wind turbine blades can't be recycled, so they're piling up in landfills. Retrieved Feb. 7, 2020 from Bloomberg database 2020.

[4] Mishnaevsky L, Branner K, Petersen HN, Beauson J, McGugan M, Sorensen BF. Materials for Wind Turbine Blades: An Overview. Materials (Basel, Switzerland). 2017;10(11).

[5] Ding A, Wang J, Ni A, Li S. Hygroscopic ageing of nonstandard size sandwich composites with vinylester-based composite faces and PVC foam core. Composite Structures. 2018;206:194-201.

[6] Ding A, Wang J, Ni A, Li S. Ageing of sandwich composites with E-glass fibre/vinylester skins and PVC foam core in synergistic environmental agents. Composite Structures. 2018;202:253-60.

[7] Ding A, Wang J, Ni A, Li S. Assessment on the ageing of sandwich composites with vinylester-based composite faces and PVC foam core in various harsh environments. Composite Structures. 2019;213:71-81.

[8] Jensen JP. Evaluating the environmental impacts of recycling wind turbines. Wind Energy. 2019;22(2):316-26.

[9] Ramirez-Tejeda K, Turcotte DA, Pike S. Unsustainable Wind Turbine Blade Disposal Practices in the United States:A Case for Policy Intervention and Technological Innovation. NEW SOLUTIONS: A Journal of Environmental and Occupational Health Policy. 2017;26(4):581-98.

[10] Larsen K. Recycling wind. Reinforced plastics. 2009;53(1):20-5.

[11] Composites UK Trade Association. End of life options for composite materials.

[12] Job S. Recycling glass fibre reinforced composites–history and progress. Reinforced Plastics. 2013;57(5):19-23.

[13] Ginder RS, Ozcan S. Recycling of Commercial E-glass Reinforced Thermoset Composites via Two Temperature Step Pyrolysis to Improve Recovered Fiber Tensile Strength and Failure Strain. Recycling. 2019;4(2):24.

[14] Nzioka AM, Kim YJ. Surface analysis of glass fibres using XPS and AFM: case study of glass fibres recovered from the glass fibre reinforced polymer using chemical recycling. Journal of Physics: Conference Series. 2018;953:012012.

[15] Cunliffe AM, Jones N, Williams PT. Pyrolysis of composite plastic waste. Environmental Technology. 2003;24(5):653-63.

[16] Zabihi O, Ahmadi M, Liu C, Mahmoodi R, Li Q, Ghandehari Ferdowsi MR, et al. A Sustainable Approach to the Low-Cost Recycling of Waste Glass Fibres Composites towards Circular Economy. Sustainability. 2020;12(2):641.

[17] Chu J, Sullivan J. Recyclability of a continuous e-glass fiber reinforced polycarbonate composite. Polymer composites. 1996;17(4):556-67.

[18] Palmer J, Ghita O, Savage L, Evans K. Successful closed-loop recycling of thermoset composites. Composites Part A: Applied Science and Manufacturing. 2009;40(4):490-8.

[19] Zhong W, Li F, Zhang Z, Song L, Li Z. Short fiber reinforced composites for fused deposition modeling. Materials Science and Engineering: A. 2001;301(2):125-30.

[20] Ning F, Cong W, Qiu J, Wei J, Wang S. Additive manufacturing of carbon fiber reinforced thermoplastic composites using fused deposition modeling. Composites Part B: Engineering. 2015;80:369-78.

[21] Goh GD, Yap YL, Agarwala S, Yeong WY. Recent progress in additive manufacturing of fiber reinforced polymer composite. Advanced Materials Technologies. 2019;4(1):1800271.

[22] Xiao X, Chevali VS, Song P, He D, Wang H. Polylactide/hemp hurd biocomposites as sustainable 3D printing feedstock. Composites Science and Technology. 2019;184:107887.

[23] Rahimizadeh A, Kalman J, Fayazbakhsh K, Lessard L. Recycling of fiberglass wind turbine blades into reinforced filaments for use in Additive Manufacturing. Composites Part B: Engineering. 2019;175:107101.

[24] Rahimizadeh A, Kalman J, Henri R, Fayazbakhsh K, Lessard L. Recycled Glass Fiber Composites from Wind Turbine Waste for 3D Printing Feedstock: Effects of Fiber Content and Interface on Mechanical Performance. Materials. 2019;12(23):3929.

[25] Rahimizadeh A, Tahir M, Fayazbakhsh K, Lessard L. Tensile properties and interfacial shear strength of recycled fibers from wind turbine waste. Composites Part A: Applied Science and Manufacturing. 2020;131:105786.

[26] Mittal RK, Gupta VB, Sharma PK. Theoretical and experimental study of fibre attrition during extrusion of glass-fibre-reinforced polypropylene. Composites Science and Technology. 1988;31(4):295-313.

[27] Schweizer RA. Glass Fiber Length Degradation in Thermoplastics Rocessing. Polymer-Plastics Technology and Engineering. 1982;18(1):81-91.

[28] Bader MG, Bowyer WH. An improved method of production for high strength fibre-reinforced thermoplastics. Composites. 1973;4(4):150-6.

[29] Arabnejad S, Pasini D. Mechanical properties of lattice materials via asymptotic homogenization and comparison with alternative homogenization methods. International Journal of Mechanical Sciences. 2013;77:249-62.

[30] Sun CT, Vaidya RS. Prediction of composite properties from a representative volume element. Composites Science and Technology. 1996;56(2):171-9.

[31] AZoM.com. E-Glass Fibre. AZO Materials. 2001.

[32] NatureWorks. Ingeo™ Biopolymer 4043D Technical Data Sheet, 3D Printing Monofilament – General Purpose Grade.

[33] Bahmani A, Comeau PA, Montesano J, Willett TL. Extrudable hydroxyapatite/plant oil-based biopolymer nanocomposites for biomedical applications: Mechanical testing and modeling. Materials & Design. 2019;174:107790.

[34] Fu S-y, Lauke B, Mai Y-w. Chapter 6 - Elastic modulus of short fibre-reinforced polymers. In: Fu S-y, Lauke B, Mai Y-w, editors. Science and Engineering of Short Fibre-Reinforced Polymer Composites (Second Edition): Woodhead Publishing; 2019. p. 139-88.

[35] Brydson JA. 26 - Epoxide Resins. In: Brydson JA, editor. Plastics Materials (Seventh Edition). Oxford: Butterworth-Heinemann; 1999. p. 744-77.

[36] Brian NT, Strong R, Scott AG. A review of melt extrusion additive manufacturing processes: I. Process design and modeling. Rapid Prototyping Journal. 2014;20(3):192-204.

Chapter 6

Conclusions and future work

6 Chapter 6: Conclusions and future work

6.1 Summary of the main results

The rapid global development of wind energy has significantly increased the environmental concerns of composite waste produced by this industry. Limited to a 20-25 year lifespan, almost 1/3 of all wind turbines installed around the world need to be decommissioned in less than 3 years, a phenomenon that raises disposal issues and pollution. As recent imminent environmental legislation is prohibiting the current unsustainable disposal methods for wind turbine blades, the wind industry is striving to be more sustainable. Despite the low cost of glass fibers, the major reinforcement material used in rotor blades, a mature recycling scheme with high commercialization potential and viability can ideally pave the way towards a more sustainable use of wind energy. In this context, this thesis has provided the following insights on the recycling of wind turbine rotor blades:

In chapter 2, a mechanical recycling methodology integrated with a classification operation has been proposed and successfully used to extract short glass fibers from old wind turbine blades. Statistical analysis on the recycled fibers has been instrumental to unveil the fiber length distribution, obtained following each set of classification operations. Microscopic imaging from the surface of the ground fibers has shown traces of old matrix material, which can influence the final properties of composites made from them. Through an optimum double melt extrusion process, thermoplastic based composite filaments with 5 wt% fiber content have been produced out of recycled fibers for use in fused filament fabrication 3D printing. Mechanical tests on the developed recycled filaments, as well as fabricated parts have shown an increase of, respectively, 16% and 8% in the elastic modulus.

One factor limiting the development of composite reinforced feedstocks for 3D printing is the high viscosity of the composites. Towards this problem, we have focused in Chapter 2 on the characterization of viscosity for the newly developed filaments. The results from these experiments have evidently revealed the occurrence of shear thinning at shear rates used in 3D printing, an incidence that lowers the viscosity and enhances the filament processability, even at higher fiber contents. The feasibility of tuning the operation temperature of 3D printed parts through the addition of glass fibers has been also studied with results showing the trivial effect of short fibers on the glass transition temperature of 3D printed parts. In contrast, the addition of recycled fibers has shown a propensity to increase the crystalline content formed in the composite parts, which can be beneficial to their mechanical properties.

The low mechanical properties of general 3D printed components can be problematic in real world end user applications. In Chapter 3, we have reported the mechanical properties that can be achieved via addition of mechanically recycled fibers. In particular, parts featuring various fiber contents from 5-25 wt% have been manufactured and characterized through tensile testing. The results have shown that while an increase in the fiber content can lead to a structurally stiff material, the final part compromises on the strength. Demonstrations on the mechanical properties of recycled components also include a theoretical study, where mechanics of short fiber composites have been used to predict the properties of the recycled parts. The results showed a good agreement between the theoretical and experimental observations at low fiber contents. However, at higher fiber contents, the discrepancy between the predicted values and actual properties of the samples increased. This observation was attributed to the higher porosity of the samples with high fiber contents, a fact that was further clarified via the SEM micrographs from the fractured surface of the samples following the tensile testing.

In the context of recycling, the relative performance of recycled composite versus original material plays a crucial role in determining the viability and commercialization potential of the proposed recycling technique. One aspect that has been thoroughly studied in Chapter 3 is the mechanical properties of the recycled parts as comparted to those of virgin components. In this regard, virgin fibers with identical dimensional properties e.g. average fiber length and dimeter, to recycled fibers were used to fabricate 3D printed parts. The results from tensile tests on both samples interestingly revealed higher properties for the recycled parts, an observation that was exclusively ascribed to strong interface formed between the recycled fibers and the thermoplastic polymer.

Chapter 4 has experimentally investigated the micromechanical properties of the recycled fibers from used rotor blades. To demonstrate the reason behind the high mechanical properties observed in Chapter 3 for 3D printed recycled parts, Chapter 4 has presented the mechanical and interfacial properties of single fibers extracted from thermally and mechanically recycled old blades. Through a novel and systematic methodology, single fiber tensile test results have proven the merit of mechanical recycling over thermal recycling technique by preserving maximum stiffness and strength of the recovered glass fibers. Atomic Force Microscope (AFM) imaging from the surface of thermally and mechanically recycled glass fibers has precisely quantified the surface roughness of the ground, pyrolyzed and virgin fibers. While theoretically the high surface roughness of the ground fibers can be beneficial to interfacial bonding, single fiber pull-out test results validated the stronger bonding formed between the ground fibers and PLA. This phenomenon results from the combination of chemical and mechanical interactions at the fiber-matrix interface. Although the low price and properties of recycled glass fibers typically lower the recycling profitability of these materials, the micromechanical results presented in this chapter were utilized to measure the critical length of ground fibers. This measurement can be helpful to design and manufacture recycled composites with superior mechanical performance, a fact that can motivate the recycling of rotor blades at industrial scales.

Inspired by Chapter 4, Chapter 5 has combined the micromechanical analysis conducted on single ground fibers with the key elements of recycling and extrusions processes to overcome the issue of strength degradation reported in Chapter 2 and 3. In particular, the recycling process, as well as the manufacturing parameters are adjusted to preserve fibers longer than the critical length in the final part. Through Thermogravimetry Analysis (TGA) the fiber length distribution in the feedstock material is then obtained to evaluate the fiber length retention occurred throughout the entire recycling process. Although the TGA results demonstrated that the extrusion process is associated with fiber breakage, the tensile test results showed favorable enhancement in both the strength and stiffness of the parts featuring a recyclate content of 5 wt%. To enable the prediction of the mechanical properties of parts made from the recycled feedstock material, a finite element (FE) model has been also developed and successfully validated using the experimental measurements. The geometric defects extracted from the fabricated parts are introduced into the numerical models to precisely capture the stiffness through a homogenization technique. The developed FE model can be effective to evaluate the mechanical response of parts with complex geometries and arbitrary composite properties.

In summary, we proposed a complete recycling methodology that can be used as a recycling solution for end-of life wind turbine blades. Firstly, micromechanical analysis determines the optimum design and recycling parameters, which are subsequently incorporated into a mechanical grinding and classification process to recover glass fibers with desirable length range. Then, the fibers along with an identified proper thermoplastic polymer are put into an optimized extrusion process to produce recycled composite pellets, which can be used in different composite manufacturing processes, i.e. 3D printing, compression molding and injection molding. Finally, as an exemplification of the scheme, we used the pellets to 3D print parts with superior structural stiffness and strength.

6.2 Original contribution

The following list summarizes the main findings achieved during the present study:

- An efficient and viable recycling methodology has been created to produce value-added products from wind turbine blades waste. 3D printing feedstock reinforced with recycled glass fibers, for the first time, has been developed and assessed in terms of mechanical and thermal properties.
- A statistical analysis on classified recycled fibers has unveiled the average fiber length achieved following every single classification operation. Thermogravimetry analysis at each stage of classification has revealed the exact amount of reinforcement remained inside the recyclate. Differential scanning calorimetry along with viscosity tests have been used to capture the physical properties of the newly developed filaments. In addition, mechanical tests have demonstrated an increase in the mechanical properties of recycled filaments, an increase that also appears in 3D printed parts.
- 3D printing feedstock filaments reinforced with short recycled glass fibers featuring a variety of fiber contents have been developed to shed light into the relationship between the mechanical properties, namely strength and stiffness, of recycled fibers and the reinforcement weight ratio. Results have demonstrated that increasing fiber content can adversely affect the strength of the parts. Filaments from virgin glass fibers have been developed and compared with the newly introduced recycled filament. The results have shown that the recycled filaments are stronger and stiffer owing to the strong bonding between the recycled fibers and the new thermoplastic resin.
- Micromecahnical analysis on recycled fibers from wind turbine waste, for the first time, was conducted and optimum design parameters to attain effective properties from recycled fibers were obtained. Results from these analyses unveiled the higher properties of fibers recycled through mechanical grinding versus those recovered via thermal recycling. In

addition, it was demonstrated that old matrix particles remained on the surface of ground fibers can contribute to interfacial strength leading to higher properties when used in thermoplastic composites.

- Filaments containing recycled glass fibers longer than their critical length were manufactured at three different fiber contents. Mechanical tests on the parts made from these filaments have shown an improvement in both the strength and stiffness of the parts relative to pure plastic components.
- A numerical model capable of predicting the mechanical stiffness of the recycled parts was developed and validated. The model can be used to find the best application sectors for the proposed recycled feedstock by evaluating the mechanical response of a part featuring a complex geometry and any arbitrary composite properties, i.e. number of layers and fiber orientation.

6.3 Future work

In this work, recycled composite pellets from wind turbine composite waste have been produced to address the critical issue of overwhelming composite waste form the wind industry. The contributions of this thesis provide a platform to further explore the re-use of wind turbine waste in composite manufacturing. The following is proposed as a future continuation to this work:

- While the composite pellets here developed have the potential to be used in different composite manufacturing processes namely, compression molding and injection molding, the present thesis was mainly focused on 3D printing. The proper optimization of manufacturing parameters that allow the use of composite pellets in other processes can highly broaden the application sector for recycled composites and can be the subject of future work.
- In addition to wind turbine waste, the presented strategy can be extended to accommodate composite waste from other industries. To customize the properties of 3D printed parts, future work can focus on other recycled reinforcements and resin materials that can be used in the same recycling system to attain a wider range of properties (fiberglass boat hulls, composite pipe, bathtubs, aerospace waste, etc).
- The results presented in Chapter 3 have shown the high brittleness of composite components versus pure thermoplastic parts. While PLA features high brittleness, the

addition of glass fibers has also further reduced the ductility of the samples leading to small strain at failure. Nevertheless, increasing the ductility of samples through the addition of plasticizers can assist in increasing the ductility of the composite filaments, which will in turn increase their processability even with high fiber contents.

- The effect of fiber content on the mechanical properties of recycled parts has been thoroughly studied in Chapter 3 and 5. While the presence of old matrix powder has shown an adverse effect on the strength of the parts by generating stress concentration regions and voids, and its separation has shown to be beneficial to achieve higher properties, future work might focus on the separation of the remained matrix power through more efficient technologies such as air separation method.
- Though the investigation carried out in Chapter 5 evidently revealed that the preservation of fibers longer than the critical length can lead to an improvement in all tensile properties of the 3D printed compos nets, the extrusion process associated with thermoplastic composite manufacturing generally results in fiber breakage. Hence, future work can investigate the optimum design and extrusion parameters to maximally preserve the critical fiber length following the extrusion and pelletization processes. The intertwine between the 3D printing parameters and recycled feedstock properties can be also studied to enable the 3D printing of high fiber content filaments without the surface issues reported in Chapter 5.
- While this thesis was mainly focused on basic tensile properties, other mechanical properties of 3D printed recycled composites including fatigue life, impact resistance, bending strength and creep should be characterized to provide a deeper insight into their performance under harsh environmental and mechanical conditions.
- Another aspect that can be the subject of future studies is the life cycle assessment of the 3D printed recycled parts. In fact, while our results have shown that the properties of the recycled composites can be comparable to those of virgin parts, a thorough study on the maximum number of recycling cycles that does not lead to excessive property degradation should be performed. This will help to properly identify the potential future applications for the recycled parts based on their actual properties.

6.4 Publications

6.4.1 Refereed journals

- **Rahimizadeh A**, Kalman J, Fayazbakhsh K, Lessard L. Mechanical and thermal study of composite filaments from wind turbine waste for 3D printing. Article under review.
- **Rahimizadeh A**, Tahir M, Fayazbakhsh K, Lessard L. Tensile properties and interfacial shear strength of recycled fibers from wind turbine waste. Composites Part A: Applied Science and Manufacturing. 2020; 131:105786.
- **Rahimizadeh A**, Kalman J, Fayazbakhsh K, Lessard L. Recycling of fiberglass wind turbine blades into reinforced filaments for use in Additive Manufacturing. Composites Part B: Engineering. 2019; 175:107101.
- **Rahimizadeh A**, Kalman J, Henri R, Fayazbakhsh K, Lessard L. Recycled Glass Fiber Composites from Wind Turbine Waste for 3D Printing Feedstock: Effects of Fiber Content and Interface on Mechanical Performance. Materials. 2019; 12(23):3929.

6.4.2 Conference presentations

- **Rahimizadeh A**, Fayazbakhsh K, and Lessard L, 3D printing filament feedstock from end-of life wind turbine blades, The 19th European Conference on Composite Materials (ECCM19), 22-26 June 2020, Nantes, France.
- **Rahimizadeh A**, Wind turbine waste: A recycling solution. JEC World PhD composite challenge, 3-5 March 2020, Paris, France.
- **Rahimizadeh A,** Henri R, Fayazbakhsh K, and Lessard L, Recycling of wind turbine blades for fused filament fabrication feedstock, The 22nd International Conference on Composite Materials (ICCM 22), 11-16 August 2019, Melbourne, Australia.

6.4.3 Awards

- 3D Hubs Manufacturing Company, 2019: 3D Hubs Student Grant
- Selected as finalist at 2020 JEC Composite PhD Challenge